QUANTITATIVE ASSESSMENT OF MYOCARDIAL ISCHAEMIA WITH THALLIUM-201 MYOCARDIAL PERFUSION IMAGING

By

HARDIAL SINGH BSc, MBChB, MRCP

A thesis presented for the degree of

DOCTOR OF MEDICINE

University of Edinburgh, 1986

TO

Vicki

Rebecca

Jai

Nicholas

Rhiannon

ACKNOWLEDGEMENTS

To Dr. J. Pilcher without whose enthusiasm and encouragement this work would not have been started.

To Mr. A. McIntosh who found time in his busy department for the work to be carried out.

To Dr. D.A. Causer for his patience, advice and support. In particular, I acknowledge his assistance in the study on the optimal window width for Tl-201 scanning. The method of quantification of myocardial ischaemia in this thesis was the result of many fruitful discussions with Dr. Causer.

To Dr. R.G. Newcombe for his help in statistical analysis.

The work of this thesis was performed at Walsgrave Hospital, Coventry, while the author was the recipient of a Sheldon Research Fellowship from the University of Birmingham.

I hereby declare that except for the assistance gratefully acknowledged above, this thesis is the result of my own work.

ABSTRACT

Myocardial ischaemia represents the imbalance between myocardial energy supply and demand. Stress tests are used to increase myocardial energy requirements to the point at which ischaemia develops, so allowing an estimate of reserve capacity. Despite the development of many stress tests, an ideal method for the non-invasive, quantitative assessment of myocardial perfusion reserve is not currently available. Such a method has important clinical and research applications, as in studies on the effects of intervention on abnormalities of myocardial perfusion.

Thallium-201 myocardial perfusion scanning has many of the attributes of an ideal method. Reported quantitative methods of analysis of thallium scans were evaluated critically to devise a new method which would allow accurate, reproducible assessment of myocardial ischaemia. To this end, a perfusion variation index (PVI) was devised, based on a comparison of regional count density on post-exercise and resting scans.

Post-exercise, redistribution and resting thallium scans were recorded and then analysed. A correction was made for the different total myocardial uptake of thallium-201 at rest and on exercise. Exercise and rest scans were corrected for background activity. Redistribution scan counts were subtracted from rest scans. Myocardial images were divided into regions of interest determined by the operator. An index, F(n), was calculated from the change in counts in each of five

regions of interest per projection on paired exercise and rest scans. The standard deviation of F(n), SF(n), was determined and the ratio $\frac{F(n)}{SF(n)}$ obtained. The root mean square of $\frac{F(n)}{SF(n)}$, which was termed PVI, gave an index of overall change in count distribution from exercise to rest.

Sixty patients with coronary artery disease and 15 normal subjects had thallium studies from which the PVI was determined. The PVI was 92% sensitive and 93% specific for the diagnosis of coronary artery disease, determined by the presence of at least one significant stenosis ($\geqslant$ 75% reduction in luminal diameter) in the large coronary arteries at angiography. The reproducibility of the PVI as an index of the presence and severity of myocardial ischaemia was tested in 20 patients with coronary artery disease who had repeat studies. Mean values for the PVI did not change significantly from the initial to the repeat studies. In individual patients, however, there was wide fluctuation in the PVI in the two tests.

These results suggest that the PVI is a good indicator for the presence but not the severity of myocardial ischaemia. The reasons for the lack of reproducibility of the PVI in individual patients are discussed. It is concluded that the physical limitations of thallium-201 as a myocardial imaging agent introduce systematic errors which preclude reproducible, quantitative assessment of myocardial ischaemia.

Further developments in radiopharmaceuticals and computer technology are required to overcome the limitations of thallium-201. Studies of myocardial metabolism using positron emission tomography offer the best prospect for the development of an ideal method for the quantitative assessment of myocardial perfusion reserve.

PUBLICATIONS

Publications which have included some aspects of the work in this thesis are listed below.

Singh H, Causer DA. Thallium-201 myocardial perfusion scintigrams in the evaluation of aortocoronary saphenous bypass surgery.
J Nucl Med 1979, 20 : 576.

Singh H, Causer DA, Pilcher J, Gray IR. Thallium-201 myocardial scanning in triple vessel coronary disease.
Br Heart J 1980, 43 : 111-112.

Causer DA, Singh H. The effect of window width on thallium-201 scintigraphy of myocardium.
Br J Radiol 1980, 53 : 142-146.

Singh H, Causer DA. The effect of photon absorption by breast tissue in myocardial imaging with thallium-201.
Br J Radiol 1981, 54 : 966-968.

INDEX

Chapter 1 INTRODUCTION

1.1 Myocardial ischaemia

The contracting heart consumes energy at a high rate. It is therefore heavily dependent on the more efficient process of oxidative metabolism to meet its energy requirements. As a consequence, it is susceptible to hypoxia (a reduction in oxygen supply despite adequate perfusion) and to ischaemia (a reduction in oxygen supply as a result of reduced perfusion, together with reduced washout of metabolites). Neither hypoxia nor ischaemia can be defined in absolute terms as both depend on the heart's energy requirements which, in turn, depend on the physiological conditions pertaining. Thus myocardial ischaemia represents the temporary imbalance between myocardial energy supply and demand, and is defined in relative rather than in absolute terms. Stress tests are used to increase myocardial energy requirements to the point at which ischaemia develops, so allowing an estimate of reserve capacity. A number of different stress tests have been developed.

In general, stress tests are designed to increase myocardial energy requirements in a controlled and reproducible manner : formal protocols are utilised so that the stress can be quantified. The physiological consequences of differing types of stress (e.g. exercise, atrial pacing, hand grip) increase myocardial energy needs in different ways. Ischaemia induced by stress tests may be recognised in various ways (e.g. subjective complaint of angina, deviation of the ST segment on the electrocardiogram,

relative reduction in thallium-201 activity on myocardial scans).

The main clinical expression of myocardial ischaemia is angina pectoris i.e. a characteristic discomfort in the chest or adjacent areas, which is associated with a temporary disturbance of myocardial function. Angina is usually induced by an increase in myocardial oxygen demand, as for instance with exercise or emotion; this is the case in so-called classical angina[1], which is usually due to fixed atherosclerotic stenosis of the epicardial coronary arteries. More recently it has been established that increases in heart rate and/or blood pressure do not always precede the development of spontaneous angina[2], from which it is inferred that the demand is in these cases constant but the coronary blood supply becomes diminished. These episodes of spontaneously occurring angina have been referred to as "variant angina". They may occur in the absence of classical angina or much more commonly on a background of classical angina as "unstable angina pectoris". They are attributable to transient narrowing or occlusion of either atheromatous or angiographically normal coronary arteries[3]. Variant angina, especially in the absence of atheromatous coronary obstruction, is rare and unpredictable. Chronic, classical, effort-induced angina is common and reproducible.

Transient reduction in myocardial blood flow relative to requirements produces myocardial ischaemia. Prolonged ischaemia, in experimental studies lasting longer than about 30 min, produces irreversible myocardial necrosis. The clinical consequences of myocardial necrosis or infarction

are generally different from those of ischaemia. Long-term prognosis after myocardial infarction is inversely correlated with the extent of infarction; a small, uncomplicated, completed infarction may well have no sequelae. Ischaemia, on the other hand, is often recurrent and each episode can potentially cause mycardial infarction or life-threatening arrhythmias. Thus it is important to differentiate between ischaemia, which is reversible, and infarction, which is not.

Assessment of myocardial ischaemia

A reliable method for assessing the severity of myocardial ischaemia in serial studies has both clinical and research applications. It would allow objective assessment of the effect of interventions such as pharmacological treatment, coronary angioplasty and coronary artery bypass grafting. The natural history of clinical subsets of coronary disease e.g. unstable angina, subendocardial myocardial infarction, could be more clearly defined. A correlation of the severity of ischaemia and prognosis might identify high-risk patients e.g. after myocardial infarction who could benefit from an aggressive therapeutic approach.

"Severity" of ischaemia implies an assessment of the relative regional reduction in myocardial blood flow and the mass of vulnerable myocardium. Traditionally, severity has been judged from the anatomical distribution of coronary atherosclerosis, either from coronary angiography or pathological examination[4]. Relevant factors with these techniques include the percentage reduction of luminal diameter by coronary stenosis; the length of stenosis and

the contribution of multiple stenoses in series in the same coronary artery; the number of coronary arteries with stenoses[5]; the contribution of coronary vasomotor tone[6]; and the presence of collateral vessels[7,8]. Under physiological conditions, collaterals appear to have little or no functional role. When myocardial perfusion is compromised by large vessel narrowing or obstruction, perfusion via collaterals may equal or even exceed perfusion via the narrowed or obstructed vessel. Coronary angiography and pathological studies define the extent of atheromatous disease but do not provide a functional assessment of coronary stenoses.

An ideal method for the assessment of myocardial perfusion reserve should be non-invasive so that serial evaluations of ischaemia are feasible. It should estimate severity of ischaemia reliably and reproducibly. It should differentiate myocardial ischaemia from infarction. It should allow regional assessment of coronary flow since coronary atherosclerosis is patchy and often causes regional reduction in coronary perfusion reserve. The ideal method should provide three-dimensional assessment of myocardial perfusion so that severity of ischaemia can be assessed in terms of the mass of vulnerable myocardium. The advantages and limitations of available methods for the assessment of myocardial ischaemia will be reviewed.

Invasive methods of assessing myocardial ischaemia

The drawback of coronary angiography (in providing an anatomical rather than a functional assessment of coronary stenoses) has already been mentioned. A functional

assessment can be made by the thermodilution method measuring coronary blood flow at rest and following interventions[9]. In this technique a catheter is inserted into the coronary sinus. Saline at room temperature is continuously infused from the tip of the catheter and the temperature of the blood-saline mixture downstream in the coronary sinus is monitored by an external thermistor on the catheter. The temperature of the injected saline is monitored by an internal thermistor near the catheter injection orifice. Coronary sinus blood flow can then be calculated from a knowledge of the saline injectate flow rate, body temperature, injectate temperature and temperature of the blood-injectate mixture.

The applicability of this method is limited since it requires invasive cardiac catheterisation under fluoroscopic control. Regional assessment of coronary blood flow is limited (although separate thermistors can assess coronary sinus and great cardiac vein flow individually).

A number of techniques using radionuclides during or after coronary arteriography have been developed to assess the haemodynamic consequences of coronary arterial lesions. Myocardial perfusion can thereby be assessed in the basal state or following an intervention to determine regional myocardial blood flow.

Myocardial perfusion scintigraphy may be performed following intracoronary injection of either macroaggregated albumin or radiolabelled microspheres[10,11]. The main advantages of this approach over non-invasive methods such as intravenous myocardial perfusion scintigraphy are improved

spatial resolution (from the substantially higher target-to-background ratio) and the better physical characteristics of the pharmaceutical (which is labelled with 99m-technetium). The main limitation is the need to inject the tracer directly into the coronary artery, so that serial studies are impractical.

The positron emitter Rubidium-82 can be injected directly into the coronary arteries at the time of coronary angiography[12]. The half-life of 82-Rb is short (75 seconds) so that sequential imaging can be performed e.g. at rest and during pacing-induced angina. However, as with the microsphere method, quantitative measurement of coronary flow is not possible.

The use of a short-lived radionuclide such as Krypton-81m (half life 13 seconds) infused into the coronary arteries at rest and during pacing-induced angina allows continuous imaging and recording of changes in regional myocardial perfusion[14]. A disadvantage of this method is that it requires the use of a cyclotron and is therefore limited to a minority of patients in specialised centres.

The inert gas washout method provides a quantitative measure of myocardial flow, which can be expressed in ml/min/100 gm. The inert gas dissolved in saline is injected directly and rapidly into the coronary artery. Once the tracer has diffused into the tissue, subsequent perfusion is by tracer-free blood, setting up a concentration gradient between tissue and blood. The rate at which the tracer diffuses back into the blood depends on flow rate through the tissue and the solubility partition coefficient between the blood and tissue. The more rapid the flow rate,

the more rapid the clearance or washout from the tissue. Xenon-133 is the isotope most frequently used[13]. The energy of its photon emission is low, so that scattered radiation cannot be easily eliminated; this results in reduced spatial resolution. Xenon-133 can however be used to evaluate regional myocardial perfusion by (1) static imaging of initial distribution and later residual activity and (2) dynamic imaging to record the time course of regional washout.

Non-invasive methods of assessing myocardial ischaemia

Assessment of coronary perfusion reserve by recording the electrocardiographic response to provoked myocardial ischaemia has been well documented[15-18]. The stimulus producing ischaemia is usually exercise (bicycle or treadmill) but hand grip, cold exposure (cold pressor test) and atrial pacing have also been used. The stress produces an imbalance between myocardial energy supply and demand in susceptible patients who develop deviation (usually depression) of the ST segment on the electrocardiogram. ST segment depression is thought to indicate subendocardial ischaemia, of which coronary atherosclerosis is but one, albeit the most common, cause. Poor oxygen delivery from hypoxia, coronary arterial spasm and high left ventricular pressure from any cause may also result in subendocardial ischaemia and displacement of the ST segment[18]. These causes can usually be recognised. Unfortunately, displacement of the ST segment sometimes occurs in the absence of any known cause of ischaemia

and occurs unpredictably in the presence of drugs such as digoxin[19].

The exercise test has been extended to include heart rate, blood pressure and exercise tolerance data (in addition to the changes on the electrocardiogram) in the assessment of coronary perfusion reserve[18]. Patients unable to attain a normal peak level of cardiac work, as reflected in the heart rate-systolic blood pressure product, usually have significant coronary artery obstruction. Patients who develop transient pump failure, as reflected in a fall in blood pressure while exercise is maintained, usually have advanced, widespread coronary disease.

If the applied stress renders the whole left ventricle or a large proportion of it ischaemic, the disturbance in heart function is readily recognised. When ischaemia is regional, affecting only a portion of the left ventricle, other unaffected portions of myocardium may compensate for local deterioration of function. Assessment of heart rate, the blood pressure, the electrocardiogram or exercise tolerance may then not reflect the abnormality.

The exercise test has been used as an assessment of severity of coronary atherosclerosis as well as a diagnostic (disease/no disease) aid. Exercise testing in persons without clinical evidence of coronary artery disease has shown that the level of exercise required to produce ST segment depression reflects the risk of subsequent development of angina or myocardial infarction[20] (the lower the level of exercise at which ST segment depression develops the greater the risk). The prognostic value of the treadmill test applies also

to survivors of myocardial infarction: patients with abnormal treadmill responses had a 30% greater incidence of progression of coronary disease than patients with a normal response. A study in patients with angiographically-defined significant coronary artery disease showed that those with exercise-induced ST segment depression had over three times greater mortality during four years of observation than those without[20]. Goldschlager et al[21] found that ST segment depression which, instead of diminishing immediately after exercise became more pronounced before recovery, was useful in predicting severe coronary artery obstruction.

The correlation between exercise electrocardiography and coronary angiography has been poorer than might be expected from the good agreement between exercise tests and clinical follow-up[15]. Epidemiological concepts have been introduced to explain why the test cannot be as accurate in screening asymptomatic subjects as it has in patients with chest pain. Nevertheless, many patients with significant coronary obstruction do not show electrocardiographic evidence of ischaemia on exercise. These "false negative" results have been attributed to mild coronary disease, severe left ventricular dysfunction or inadequate stress to induce ischaemia[19]. The presence of abnormalities on the resting electrocardiogram reduces the predictive power of any subsequent changes on exercise[19]. Another disadvantage of exercise testing has been suggested by a recent study[22]. During serial testing in stable patients with coronary

obstruction there was considerable variability in (1) exercise time to the onset of angina, (2) the degree of ST segment depression and (3) maximal exercise tolerance. In contrast, the heart rate-systolic blood pressure product at the onset of angina and at maximal exercise was reproducible.

Thus exercise electrocardiography does not satisfy the requirements for an ideal non-invasive method for the assessment of myocardial ischaemia. The electrocardiographic changes on exercise are not specific for ischaemia, false positive and negative results are obtained, three-dimensional assessment of ischaemia is not possible and the reproducibility of serial tests is still debated.

Echocardiography utilises ultrasound to examine the heart and record information in the form of echoes i.e. reflected ultrasound waves. M-mode echocardiography, the original ultrasonic technique developed for examination of the heart, does not allow effective evaluation of the shape of cardiac structures but it is valuable in recording the motion of structures parallel to the ultrasonic beam[23]. The technique of two-dimensional echocardiography, in which the ultrasonic beam is rotated very rapidly, has overcome some of the limitations of M-mode echocardiography in assessing left ventricular shape and size[24]. The principle echocardiographic technique for identifying ischaemic myocardium involves assessment of the motion of the various segments of the left ventricle. The ischaemic segment might be hypokinetic, akinetic or dyskinetic. Frequent serial recordings enable changes in wall motion to be detected as myocardial ischaemia develops and

disappears. If isometric exercise is used to precipitate ischaemia, echocardiograms can be recorded during stress. Technical difficulties resulting from patient movement prevent echocardiograms being recorded during treadmill exercise; this problem may be overcome by recording echocardiograms immediately after such exercise. Abnormal wall motion as a result of exercise-induced ischaemia usually persists long enough to be detected by echocardiography after exercise.

Estimates of left ventricular ejection fraction by standard M-mode echocardiography do not provide reliable information in patients with coronary artery disease. Calculations are based on the assumption that the two sites from which the left ventricular dimensions are measured (the interventricular septum and posterior wall) are representative of the whole ventricle, but in coronary artery disease there are often regional abnormalities of contraction. When the diastolic left ventricular diameter is increased on echocardiography, it can however be assumed that overall left ventricular function is severely impaired[25]. Several studies have suggested that two-dimensional echocardiography provides diagnostic and prognostic information in the early post-infarction period[26,27].

A disadvantage of echocardiography is that in a proportion of patients (10-50%)[28,29], it is not possible to obtain images of diagnostic quality. Subjective analysis of videotape recordings of two-dimensional echocardiograms is open to bias; complex methods of objective analysis have

therefore been developed[30]. Reproducible assessment of myocardial ischaemia is hampered by the difficulty in obtaining exactly comparable views in serial studies.

Radionuclide angiography using technetium-99m is widely used for the assessment of cardiac performance. A first-pass study measures indices of cardiac performance from the initial transit of the radionuclide through the heart. It is limited by the counts acquired during a few cardiac cycles. However, as the radionuclide remains in the intravascular compartment, the heart can also be imaged at equilibrium; a large number of counts can be obtained by constructing an average cardiac cycle as a composite of many cycles. Many indices of the heart's performance can be calculated; in the context of myocardial ischaemia the most important are left ventricular ejection fraction, regional ventricular performance, cardiac output and end-diastolic and end-systolic ventricular volumes.

When radionuclide angiography is carried out during exercise in normal subjects, left ventricular ejection fraction rises significantly compared to levels at rest, and no left ventricular wall motion abnormalities are found. In patients with exercise-induced myocardial ischaemia left ventricular ejection fraction falls and new regional wall motion abnormalities may develop. Criteria for an abnormal left ventricular ejection fraction response to exercise vary considerably between laboratories. Most groups however, require a 5-10% increase in ejection fraction to consider the results normal[31,32]. An abnormal result is not specific for myocardial ischaemia as it may occur in any condition where there is reduced left ventricular reserve e.g. volume or

pressure overload[33,34], decreased left ventricular compliance[35]. The radionuclide angiogram is most useful for the non-invasive diagnosis of the presence of coronary disease if it is combined with clinical information such as the presence of chest pain and ST segment deviation with exercise.

Gamma camera imaging to detect the effects of acute myocardial ischaemia is limited by its inability to show brief, transient changes and its poor spatial resolution for regional wall motion abnormalities. These limitations arise from the low counting statistics inherent in radionuclide angiography; long acquisition times are necessary to obtain images which allow accurate interpretation.

Continuous assessment of left ventricular volume can be made by praecordial counting of the technetium-99m-labelled blood pool using a single scintillation probe[36]. The sensitivity of this instrument is such that sufficient counts can be detected to measure changes in left ventricular volume from beat to beat. It provides a qualitative or semi-quantitative method of assessing changes in left ventricular function in acute myocardial ischaemia. As it measures changes in ventricular volume directly, this method avoids errors associated with derived ventricular volumes, as for instance in echocardiography where a regular ventricular shape is assumed.

Myocardial perfusion scintigraphy using thallium-201[37] has the advantage over methods thus far described in that a direct, functional assessment of myocardial

perfusion reserve can be obtained. The radionuclide is injected intravenously during provoked ischaemia and is taken up by myocardial cells in proportion to regional myocardial perfusion. Thus regions of reduced perfusion appear as defects ("cold spots") on myocardial images. Images of perfusion on exercise are compared with images obtained either after further thallium-201 injection at rest, or 2-4 hours after exercise imaging without further thallium-201 injection (delayed or redistribution images). Ischaemia can be differentiated from infarction. Scans in multiple projections can provide a reliable map of regional abnormalities. Severity of myocardial ischaemia can be assessed from the size of perfusion defects demonstrated. Thallium-201 scanning thus has many of the attributes of an ideal method for the assessment of myocardial perfusion. The physical properties of thallium-201 are, however, not ideally suited for use with conventional gamma cameras. Thallium-201 is the best available isotope of its type and so, despite its inherent drawbacks, it has become widely used for the radionuclide assessment of myocardial perfusion.

Conventional radionuclide studies such as those described above allow assessment of myocardial perfusion and cardiac performance. More recently, radionuclide techniques have been developed which allow assessment of myocardial metabolism. Assessment of uptake and utilisation of energy substrates may provide a direct measure of the severity of myocardial ischaemia, since ischaemia is associated with inadequate blood supply, excessive metabolic demands, or

reduced washout of metabolites.

Studies of myocardial metabolism have become possible with the development of positron emission tomography[38]. Three-dimensional reconstruction using positron emitters is based on coincidence detection. A positron travels a short distance within tissue, giving up its kinetic energy, and then interacts with an electron. The positron and electron are both converted into annihilation photons, each with an energy of 511 keV. The photons leave the site of interaction in opposite directions at an angle of 180 degrees. If two scintillation detectors are placed opposite one another, they will detect the annihilation photons simultaneously (coincidence detection). Scattered photons that reach only one of the detectors are rejected. Coincidence counting with positron emission tomography eliminates the need for mechanical collimation since only the gamma energy arriving simultaneously at the two camera heads positioned at 180 degrees to each other is counted. The information so collected can be subjected to computer manipulation and analysis. Back-projection techniques have been devised to provide a three-dimensional reconstruction of the heart.

Thus positron emission tomography has many advantages over methods using standard gamma camera imaging. It allows, for the first time, non-invasive detection of sequential segmental metabolic alterations that accompany myocardial ischaemia. Nuclear magnetic resonance also promises to provide an in vivo assessment of myocardial metabolic function, but the technique is still at the

experimental stage[39].

Conclusion

Many methods are available for the assessment of myocardial ischaemia. Invasive investigative methods requiring cardiac catheterisation are limited in that serial studies are not feasible. Of the non-invasive methods, electrocardiography during provoked ischaemia is the most widely used but does not provide an objective assessment of the severity of ischaemia. Furthermore, only indirect evidence of ischaemia is obtained. Echocardiography and radionuclide angiography have similar drawbacks to electrocardiography. Myocardial perfusion scanning assesses ischaemia directly but is hindered by the lack of a suitable isotope with physical characteristics suited for conventional gamma cameras. Nuclear magnetic resonance of the heart is still at the experimental stage. Positron emission tomography offers the most potential but it is only available in specialised research centres.

Thus of the currently available methods, myocardial perfusion scintigraphy with thallium-201 appears to be the method most likely to be of use for accurate, reproducible assessment of myocardial ischaemia. The purpose of the work described in this thesis was to determine whether thallum-201 can be used to provide a quantitative measure of myocardial ischaemia.

1.2 Introduction to thallium-201

The possible use of thallium for myocardial perfusion imaging was first suggested in 1970 by Kawana et al[40] who used Tl-199 to demonstrate the relationship of thallium to potassium in biological systems. Production of radioactive thallium was difficult by the methods then available and little progress was made until Belgrave and Lebowitz[41,42] produced Tl-201 of high purity. A natural Tl-203 target was bombarded to produce Pb-201 which decayed to Tl-201; pure Tl-201 was obtained by a two-stage separation where lead was eluted from the target material and then fixed to a second ion exchange column and thallium eluted. The initial evaluation of Tl-201 for myocardial imaging was reported by Bradley-Moore et al[43] who demonstrated in goats that myocardial infarction could be seen on thallium scans. A series of monovalent cations had been used previously as radiopharmaceuticals for myocardial perfusion scanning. These predecessors to Tl-201 (potassium-43, rubidium-81 and caesium-129) all have significant limitations; potassium-43[44] and rubidium-81[45] need special, cumbersome whole-body shielding for use with scintillation cameras[46] and their availability is limited; myocardial uptake of caesium-129 is not rapid enough to detect transient myocardial ischaemia produced by exercise[47].

Tl-201 decays with the emission of gamma rays at 167 and 135 keV which are within the optimal range for detection by currently available scintillation cameras;

unfortunately the gamma-rays are low in abundance so that their use requires undesirably long scanning times. Thallium also decays to mercury with the emission of X-rays at 69-83 keV in 95% of disintegrations; although these photons are of rather low energy, their abundance allows effective imaging with both the rectilinear scanner and scintillation camera.

Following intravenous injection, Tl-201 is distributed throughout the body and extracted in different organs. Thallium concentration in the blood falls exponentially with a half-time of less than 30 seconds and decreases to 2-3% of the injected dose by 8-10 min[48]. The factors which determine initial distribution of Tl-201 in the myocardium are (1) regional myocardial perfusion and (2) cellular factors affecting myocardial uptake of Tl-201.

Several groups have reported a correlation between early Tl-201 distribution and regional myocardial blood flow determined by the microsphere method in canine models[49-51]. In the normal and mildly reduced flow ranges, Tl-201 distribution closely approximates blood flow. In the low-flow range (flow reduction to less than 10% of normal flow) Tl-201 concentration is usually higher than microsphere-determined regional blood flow[49]. Increased cellular extraction of Tl-201 may explain the high Tl-201 concentration relative to perfusion during low-flow conditions.

The thallous ion (Tl+) has many similarities to ionic potassium in biological systems. Mullins and

Moore[52] noted that muscle cell membranes could not differentiate between Tl+ and K+. They suggested that the similarity in crystal radius size of Tl+ and K+ was an explanation for the similarity in passive membrane penetration. Thus previous work on the myocardial uptake of K+ is relevant and has contributed to the current understanding of the kinetics of myocardial thallium uptake.

Studying the plasma-to-interstitium movements of potassium in the myocardium, Conn and Robertson[53] found that the kinetics of distribution followed the compartmental theory and that the limiting factor was rate of blood flow. According to the compartmental theory, isotope distribution is a function of permeability constants; the rate of disappearance of isotope from the circulation is a measure of blood perfusion when transcapillary movement of the isotope is rapid compared with the rate at which it is delivered to the capillaries by the circulation[54].

Renkin[55] studied potassium kinetics in skeletal muscle and found that the distribution was a function of a permeability constant as well as the rate of flow. Sheehan and Renkin[56] attributed 70% of the "non-discriminating" barrier to potassium movements as being in the capillary wall.

The relationship between thallium and potassium uptake in animals was further investigated by Gehring and Hammond[57] who referred to a sodium-potassium active transport system which cannot differentiate between potassium and thallium. They suggested that the

thallium influx into the myocardial cell is ATPase mediated. It was then postulated that reduction of thallium uptake in ischaemic myocardium is primarily due to a decrease in ATPase activity[51]. The existence of such an active transport system correlates with the findings of Gewirtz et al[58] who found that clearance of thallium is independent of flow rate. However, Carlin and Jan[59] in studies in pump perfused dog hearts produced results that indicated that thallium uptake was flow dependent and an active process mediated by ATPase. Some inconsistency in data may be expected because of differences in experimental design and methodology used to study Tl-201 kinetics. Methods used to measure Tl-201 activity have included coronary sinus sampling, myocardial biopsy and implantation of miniature radiation detection devices[60].

The peak myocardial thallium concentration occurs much earlier after intracoronary injection than after intravenous injection. Recirculation, which follows intravenous injection, implies a dynamic exchange between the intracellular and the intravascular compartments. There is a continuous extraction and release of ionic thallium by myocardial cells. Myocardial thallium washout or clearance can be described by a two-compartment model i.e. an initial fast clearance, which may represent the clearance of the unextracted thallium from the interstitial spaces, and a second slower phase representing washout from the intracellular spaces[60].

The use of myocardial uptake of Tl-201 as a measure of myocardial blood flow is based on the fractionation principle of Sapirstein[61] (the fraction of an indicator which is evenly mixed in blood and then distributed with the first circulation to a given organ is proportional to the fraction of the cardiac output perfusing that organ) but only the initial distribution of isotope correlates with myocardial perfusion. Over time, redistribution of thallium activity takes place[62] to produce a scan pattern which is not flow related but is an equilibrium determined by intracellular thallium exchange.

Exercise myocardial perfusion imaging is possible because the extraction of Tl-201 by the myocardium is rapid and initial myocardial deposition of Tl-201 injected during exercise closely parallels regional coronary blood flow at the time of injection. Because coronary flow is preserved at rest in all but the most severe arterial stenoses, exercise is employed to induce or exaggerate regional variations in perfusion; coronary flow in the normal arterial bed will increase several fold whereas that in a bed supplied by a stenotic vessel will not increase appropriately[63].

Although initial distribution of Tl-201 reflects regional flow, subsequent myocardial activity is a dynamic equilibrium between myocardial wash-in and wash-out of Tl-201; immediately after exercise there is a prolonged period of redistribution as coronary perfusion returns to baseline. Delayed or redistribution scans, typically performed 2-4 hr after exercise, provide information

complementary to that obtained on immediate, post-exercise scans (see Section 1.8)

Myocardial perfusion imaging with Tl-201 is limited both by the resolution of scintillation cameras and the imaging characteristics of the isotope. In comparison with other cationic tracers, Tl-201 has a greater heart/blood and heart/liver activity[49]; a greater contrast between the heart and its surrounding structures is therefore obtained. Because its low energy X-rays are used for imaging, Tl-201 is substantially absorbed and scattered by soft tissue or overlapping myocardium. In a dog model, 4-6 g ischaemic ventricular segments (flow reduction 40-60%) were inconsistently detected, although larger ischaemic segments were regularly seen as perfusion defects[64]. Biological factors such as cardiac motion, irregularity of the distribution of myocardial hypoperfusion, superimposition of normal and ischaemic myocardium and background radiation contribute to the limitations in detection of perfusion defects. Scintigraphy of ventricular phantoms eliminates errors arising from many of these biological factors but the degree of insensitivity of phantom scans for the detection of defects suggests that the resolving power of scintillation cameras for Tl-201 is limited[64].

Despite these problems, Tl-201 scanning is widely used in the non-invasive diagnosis and assessment of the severity of coronary artery disease. Although the current reported specificity of exercise Tl-201 imaging

for the detection of coronary artery disease is about 90%[37], the actual figure may be higher. Losse et al[65] found that abnormal exercise thallium images could be obtained in patients who had symptoms of myocardial ischaemia but were found to have angiographically normal coronary arteries and left ventricular function; in many of these patients, a myocardial abnormality was suggested by lactate production and abnormal myocardial biopsies. Opherk et al[66], in a study on a similar group of patients, found that myocardial blood flow reserve was decreased and myocardial biopsies revealed swollen mitochondria. The thallium studies reported by Losse and Opherk would normally be regarded as false positive results because scans are usually compared with the findings on coronary angiography. However, the alternative view is that the scans demonstrated true myocardial ischaemia, though that ischaemia was not associated with demonstrable obstructions in the epicardial coronary arteries. Other situations in which the functional assessment of myocardial ischaemia may be more accurate by thallium scans than from the findings on coronary angiography include left ventricular hypertrophy, hypertrophic cardiomyopathy and coronary artery spasm[37]. There are of course situations when scans may be wrongly interpreted as showing myocardial ischaemia. Apparent perfusion defects on exercise Tl-201 scans can result from soft tissue attenuation from breast tissue or diaphragm[67,68] or normal apical thinning; experience in interpretation of scans should largely eliminate these errors.

The reported sensitivity of rest and exercise Tl-201 scans for the detection of coronary disease is about 80-90%[69]. Sensitivity can be lowered by errors in interpreting the coronary angiograms (for instance when the functional significance of a stenosis is over-estimated), inadequate stress to produce ischaemia or the presence of collateral vessels reducing the effect of obstructive coronary lesions[69].

Initially, Tl-201 myocardial images were assessed visually. A disadvantage of this approach is that visual interpretation of thallium images is frequently difficult and requires considerable expertise. The limitations of subjective visual analysis of analogue images are reflected in considerable intra- and inter-observer variability[70]. Furthermore, visual inspection of analogue images precludes analysis of Tl-201 myocardial kinetics, which are markedly different in ischaemic myocardium as compared to normal myocardium or scar tissue. In normal myocardium or scar tissue, Tl-201 activity gradually decreases after the termination of exercise, whereas ischaemic myocardium is characterised by accumulation, no change or abnormally slow washout of Tl-201 after exercise[71,72]. This diagnostically important information cannot be appreciated from visual interpretation of scans.

The introduction of quantitative analysis of Tl-201 scans has improved not only the overall detection of coronary artery disease but also the accuracy of

predicting the number of diseased vessels[69]. Many methods of quantitative analysis have been reported but none has gained general acceptance. They will be examined critically with a view to arriving at a method which allows an accurate, reproducible measure of the severity of myocardial ischaemia.

1.3 Quantitative thallium scanning

The shortcomings of visual analysis of thallium scans have been well recognised. Quantitative analysis has therefore become increasingly popular in an attempt to improve on the predictive accuracy of thallium scans. The simplest quantitative approach uses conventional imaging hardware and an operator outlining areas of interest to locate and size perfusion defects; such a method might be called visual mapping. With the aid of special software programmes for automatic border recognition and display of isocount densities, more complex analyses can be performed, for example circumferential profile mapping or measurement of regional washout rates of activity. These methods do not provide absolute quantitative measurements of myocardial perfusion and should more accurately be termed computer processing and analysis, or computer mapping, of conventional scanning data. True quantitative imaging is impossible without accurate attenuation corrections, but such corrections cannot be made for low energy isotopes. Attempts have been made to improve quantitative analysis of thallium scans with the use of tomographic techniques e.g. collimator tomography with pin-hole or rotating slant-hole collimators, and single-photon emission tomography with a rotating camera. Although not applicable to thallium scanning, positron-emission tomography, using analogues of compounds involved in metabolism, has been used for quantitative imaging of metabolic processes.

Visual mapping has been used in an attempt to identify disease in specific coronary arteries and improve the predictive power of Tl-201 scanning. Lenaers et al[73], McKillop et al[74] and Massie et al[75] have shown that visual mapping does not accurately localise diseased coronary arteries or differentiate between single or multivessel disease. These findings were confirmed in another study which showed that the sensitivity for demonstrating thallium perfusion defects depended on the severity of coronary stenoses[76]. Sensitivity was lowest with coronary stenoses of 50-70% diameter narrowing, was better with > 70% stenoses and was best with complete occlusion and past myocardial infarction. Even with old myocardial infarction, however, identification of the affected vessels was poor, particularly for left circumflex and right coronary disease. Sensitivity for identifying disease in a specific coronary artery diminished if other arteries were also diseased. These limitations of Tl-201 imaging were said to be related to a basic deficiency in the statistical information of the image i.e. a poor signal-to-noise ratio.

Despite the above deficiencies, visual mapping has been of some clinical benefit. Rozanski et al[77] used this approach to demonstrate that redistribution of thallium activity correlated with myocardial viability. They predicted correctly in 80% of cases that myocardial segments which showed reversible perfusion defects would show reversal of left ventricular asynergy after coronary artery bypass grafting; about 80% of

patients who showed irreversible perfusion defects had no improvement in asynergy after bypass surgery. Visual mapping has also been used in relating infarct size to postinfarction prognosis and in relating the size of the stress defect to the severity of coronary stenosis or the presence of coronary collaterals[78].

Brown et al[79] examined the incidence and causes of abnormal Tl-201 scans in the absence of significant coronary artery disease. A scoring system was used to determine the presence of transient and persistent perfusion defects. They showed a high frequency of Tl-201 defects associated with 21-40% coronary stenoses. These defects would normally be regarded as false-positives but a clinically important alternative view is that such coronary lesions have true haemodynamic significance.

In some studies purporting to show the benefit of computer-enhanced thallium imaging, it is arguable whether visual mapping was the cause of improved results. In a study by Uhl et al[80] Tl-201 scans with computer-enhancement in asymptomatic men produced a 95% sensitivity and 97% specificity for the detection of coronary disease (> 50% diameter narrowing), these figures being a considerable improvement on those generally obtained from simple visual assessment of scans. However it seems likely that the improvement was due not to computer techniques but to the study population which consisted of asymptomatic Air Force crewmen with abnormal exercise electrocardiograms. These men were able to perform vigorous exercise and

were preselected by having an abnormal exercise test; these factors alone would improve the accuracy of scintigraphy compared to studies on unselected populations.

Faris et al[81] also reported increased sensitivity and specificity for diagnosing coronary artery disease from perfusion images analysed with a computer algorithm, but no statistical analysis was provided to indicate the significance of the apparently improved results. The role of computer processing was left unclear as it was said to be useful only in conjunction with visually interpreted analogue images.

The efficacy of coronary artery reperfusion with thrombolysis in acute myocardial infarction has been assessed with Tl-201 scanning. de Coster et al[82] used a semi-quantitative score of myocardial thallium uptake before and after attempted thrombolysis. Their results indicated that serial imaging was an accurate method of assessing changes in myocardial perfusion after acute myocardial infarction. Restoration of thallium uptake was observed after reperfusion of the infarct-related artery.

Computerised mapping of isocount contours or circumferential profiles has been described by a number of investigators. Meade et al[83], Burow et al[84] and Llaurado et al [85] described different versions of producing circumferential activity profiles of Tl-201 images, but with variable improvement in sensitivity and specificity over visual interpretation for identifying coronary artery disease. A quantitative method (based on

differential myocardial washout rates of Tl-201 being related to coronary blood flow[60]) was reported by Watson et al[86] and Berger et al[87] to show only modest increases in sensitivity and specificity (94 and 90% respectively) which were not significantly different from visual interpretation of images (sensitivity 85%, specificity 73%). Becker et al[88] reported that regional measurements of thallium redistribution were not useful in identifying coronary artery disease. A computer-mapping technique that combined circumferential activity profiles and washout rates reported by Garcia et al[89] and Maddahi et al[90], failed to increase overall diagnostic sensitivity and specificity compared with visual interpretation, although the method did demonstrate benefit in identifying diseased coronary arteries, particularly in multivessel disease when localisation can be difficult.

Computer mapping has been of use in clinical investigation, as for instance when a circumferential profile technique was used to show that quantitative Tl-201 redistribution correlated with improved ventricular function in patients successfully reperfused by intracoronary streptokinase thrombolysis in acute myocardial infarction[91]. In general, computer mapping provides a consistent and comparative approach not possible by simple visual interpretation; although automated techniques provide a quantitative and relatively unbiased analysis of images there is little documentation of improved sensitivity and specificity over visual interpretation of perfusion images.

The reasons for these limitations of Tl-201 scanning are readily apparent. Data processing cannot compensate for the basic problems of poor signal-to-noise ratio and statistical count deficiencies. The benefits of data processing or computer mapping are especially limited if non-invasive testing is to be used to avoid proceeding directly from clinical history to coronary angiography. It has been estimated that Tl-201 scanning for this purpose would need a sensitivity of at least 98% for the diagnosis of coronary artery disease[92]. Applying Bayes' theorem in non-invasive testing suggests that sensitivity and specificity of 98% or greater for a given level of coronary stenosis is necessary if Tl-201 computer mapping is to be used as an effective screening procedure for coronary disease[93].

Therefore for routine clinical diagnosis and management, computer mapping may add impartiality and perhaps ease of interpretation to Tl-201 studies but there is no significant improvement in diagnostic accuracy. For research protocols, qualitative or semi-quantitative comparisons of myocardial perfusion and of infarct size are potentially useful. Visual or computer mapping appears to be most appropriate for studying the effect of interventions, with each patient as his own control, in comparison with control groups having comparable disease studied by the same technique. The purpose of the work described in this thesis, then, was to devise a semi-quantitative analysis of Tl-201 scans which would (1) differentiate between normal subjects and patients with coronary disease and (2) provide a

measure of exercise-induced ischaemia with sufficient within-patient reproducibility to detect the effect of interventions. Reported quantitative methods were reviewed critically to decide on the most appropriate study protocol.

1.4 Visual mapping methods

Common to all visual mapping methods is that count density is measured in myocardial regions of interest determined by the operator with a light pen, joystick or other means of cursor control. Fletcher et al[94] defined the left ventricular cavity and myocardial limits on Tl-201 scans and constructed histograms of the total count range of each myocardial image. Matrix elements forming the myocardial wall were divided into five groups according to their counts as a percentage of the maximal value (0-20, 21-40, 41-60, 61-80 and 81-100). The exercise scan histogram differentiated between normal subjects and patients with coronary disease; in the former the histogram showed a unimodal distribution with most matrix elements in the upper half of the frequency distribution, whereas in patients with coronary disease the frequency distribution was shifted from right to left with most of the matrix elements in the lower half of the histogram. The percentage of matrix elements in the upper and lower halves of the histogram in paired resting and exercise images was then compared (Fig. 1(1)). The percentage of elements below 50% of the maximum in each exercise image was divided by the percentage of elements below 50% in the resting image and an average exercise/resting homogeneity index ratio of the three views was calculated. The ratio was categorised as indicating normality (no coronary disease) if it was less than 1.0 and abnormality (coronary disease present) if it was greater than or

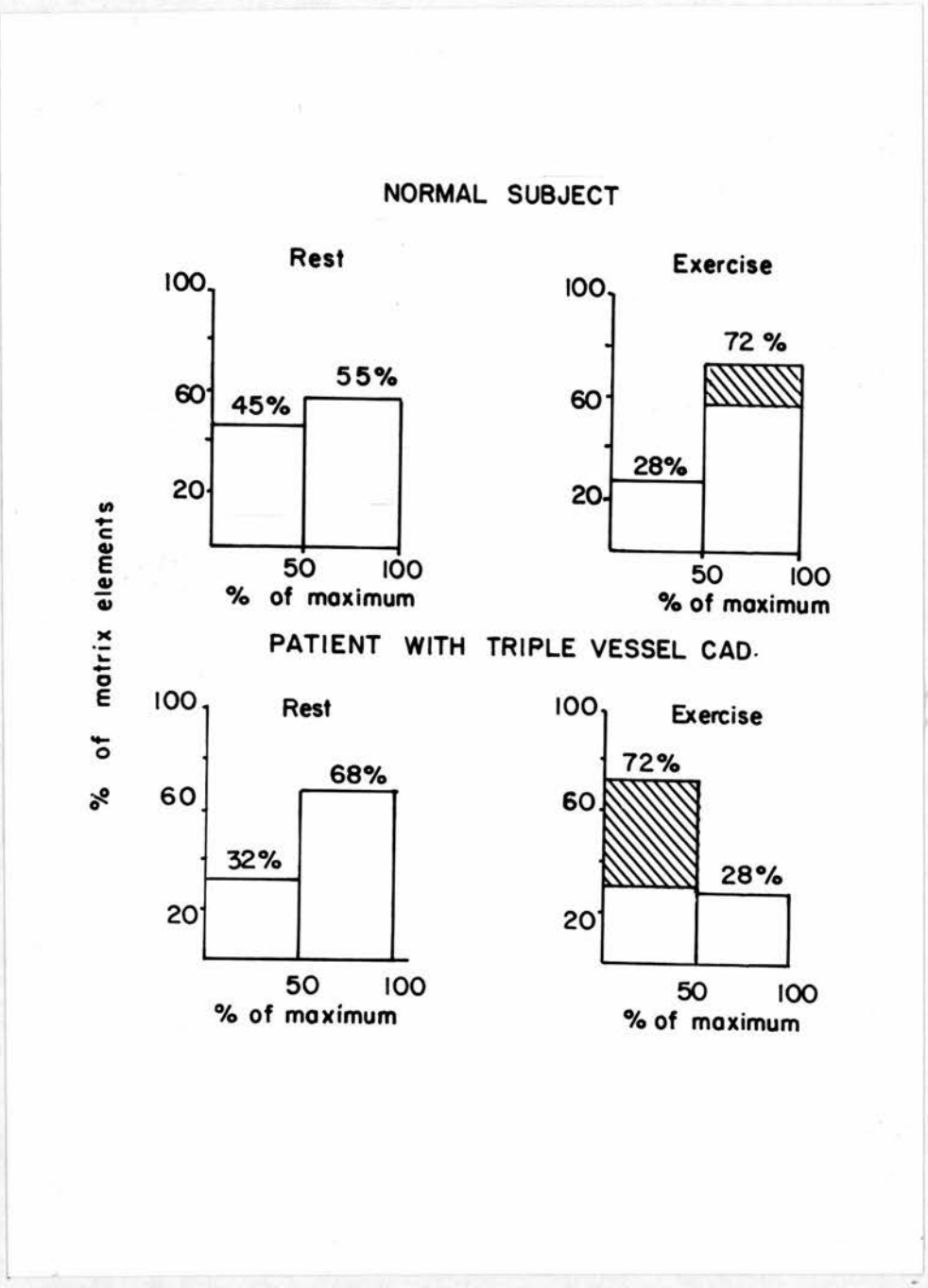

Fig. 1(1) Histograms of thallium-201 myocardial distribution (anterior view) at rest and after exercise in a normal subject and a patient with triple vessel coronary disease. The cross-hatched portion of the vertical bars in the exercise histograms indicates an increase in homogeneity in the normal patient and a right-to-left shift in the patient with coronary disease, the latter reflecting decreased homogeneity of uptake.

equal to 1.0. This visual mapping method did not produce a significant improvement in diagnostic accuracy compared to visual assessment. No mention is made of the time interval between resting and exercise imaging, or which was performed first. Unless resting and exercise images were separated by at least one week, residual counts from one study would affect the other. Also of note is the fact that no background correction factor was used; the authors state in discussion that a correction did increase sensitivity but at the cost of an unacceptably low specificity (50%).

Verani et al[95] used a visual mapping method on exercise and redistribution Tl-201 images to compare normal subjects and patients with coronary artery disease with or without previous myocardial infarction. A count-ratio was obtained by comparing the lowest and highest count densities from the myocardial image divided into five segments (anterior, inferior, septal, apical and posterolateral). No background correction was made.

A similar method was reported in a study of Tl-201 redistribution in dogs with a fixed coronary stenosis[96]. Digitised images were analysed by selecting regions of interest in a perfusion defect area (D), a normal area (N), in the entire left ventricle (LV) and in background areas (BKg). A scan ratio (R_{scan}) was determined from the average counts/pixel in these areas :

$$R_{scan} = \frac{\frac{N-BKg}{LV-BKg}}{\frac{D-BKg}{LV-BKg}}$$

This activity ratio denoted the degree of heterogeneity of Tl-201 distribution and was used to follow Tl-201 redistribution after coronary vasodilatation with an infusion of adenosine. The areas from which activity was measured were traced on subsequent scans to obtain a quantitative measure of the time-course of Tl-201 redistribution. The term (LV-BKg) was used to normalise each region to the total LV activity to facilitate intra- and inter-experimental comparisons.

Faris et al[81] reported improved sensitivity, specificity and predictive accuracy by application of a statistical image analysis algorithm, but as mentioned earlier, the authors do not present a statistical analysis to support their conclusion. Exercise myocardial scans were acquired in routine fashion and a computer system was used to enlarge the myocardial image. An assembly language programme similar to one first described by Laughlin et al[97] located the pixel with the highest counts within the myocardium and placed each pixel count into the appropriate range of a predefined chart. Count ranges were separated from each other by preselected standard deviations and it was assumed that there was no

statistical difference between pixels within any count range. All image pixels were assigned a range value depending on absolute counts and pixels below the three top ranges were excluded from a final bimodal (black and white) computer image which was used for visual comparison with analogue images.

Nishiyama et al[98] studied the effect of coronary blood flow (ischaemia and reactive hyperaemia by occlusion and release of the left circumflex artery) on Tl-201 uptake and washout in dogs. Following myocardial perfusion imaging, technetium - 99m pertechnetate was given as a bolus to define background and anterior and posterior left ventricular walls. Net anterior and posterior wall counts were obtained by normalisation of all counts and subtraction of background counts. As the left anterior descending artery had not been subject to any mechanical intervention, the anterior wall was considered to be the control region in each dog and was compared to the posterior wall. The peak myocardial activity of Tl-201 in the anterior wall was designated as 100% activity and the rest of the activities in the anterior and posterior walls were expressed as a percentage. Time-activity curves were then plotted to show myocardial uptake and washout in the control and experimental areas.

A similar quantitative comparison of Tl-201 activity in anterior and posterior walls was employed by Nichols et al[99] to investigate the relationship between segmental Tl-201 uptake and regional myocardial blood flow in patients with coronary disease. Identical rectangular

regions of interest, each consisting of 96 pixels, were chosen over myocardial segments supplied by the left anterior descending and circumflex arteries on the oblique scan. Counts in each region of interest were summed without background subtraction and the ratio calculated of counts in the anterior and posterior walls. The effect of background correction was determined by deriving the same ratio for each scintigram after subtraction of background activity (defined from an identical region of interest positioned over the left lung field posterior to the left ventricle). A linear correlation was obtained (r=0.84) between regional myocardial blood flow, assessed by regional clearance rates of xenon-133 from the myocardium, and ratios of regional Tl-201 activity in the left anterior descending and circumflex distributions of exercise scintigrams. When the same relationship was plotted after correction for background thallium activity, the linear correlation persisted (r=0.87) but the slope was much greater. This suggested that either an over-correction had been made for background or that depressed uptake of Tl-201 in ischaemic segments had altered the slope and intercept of the graph of Tl-201 activity against actual blood flow.

Okada and Pohost[100] devised a protocol to determine whether Tl-201 imaging was useful for demonstrating short-term changes in regional myocardial perfusion from occlusion and reperfusion of the left anterior descending coronary artery in the dog. Tl-201 was injected 105 min after occlusion of the artery and imaging was completed

by 2 hr when the arterial occlusion was released. 15 min after release, Tl-201 scanning was repeated after a further injection of thallium. A third and fourth series of images were obtained after further injections of Tl-201 at 3 hr and 48 hr. Just before the second, third and fourth thallium injections a myocardial image was recorded as a measure of the residual activity from previous injection(s).

The images of residual activity were then subtracted from the Tl-201 images obtained after the subsequent thallium injection. The initial thallium image and the three subtraction images were analysed by a computer-assisted technique. An ellipse, defined by its width, length and the angle between its long axis and the vertical plane, was positioned by the operator around the left ventricular cavity of the first thallium image. Automatic realignment of the left ventricular cavities of the three subtraction images to fit into the drawn ellipse was achieved by horizontal and vertical movement as well as rotation of the images by computer cross-correlation. A second ellipse was drawn two pixels outside the original and background activity was assumed to be at the perimeter of the second ellipse. Background subtraction was performed for each pixel within the inner ellipse, taking into account the activity and distance of the background point from each pixel. After nine-point smoothing thallium activities in the four serial images were normalised to the pixel of highest activity in the first thallium image. The profile of thallium activity in the left ventricle was

then determined by the peak activity within the myocardium along each of about 200 equally spaced lines drawn perpendicularly from the ellipse perimeter to its centre. Myocardial portions of the ellipse were subdivided into five equal segments along the perimeter and mean normalised regional thallium activities in each of the segments in each image were calculated and plotted. The criterion for a perfusion defect was the reduction in counts to at least 75% in any one segment compared with the most normal segment in the first thallium image; a hyperaemic segment was one with at least a 25% excess in counts compared with the most normal segment in the first thallium image. The ratio of coronary flow to the normal and occlusion myocardial regions at the time of each thallium injection was calculated from the post-mortem activity in relevant myocardial segments of differently labelled microspheres (Sn-113, Ru-103, Nb-95 and Sc-46) which had been injected, one with each injection of thallium. Qualitative and quantitative results of thallium scanning produced virtually identical results. The correlation between perfusion ratios assessed with microspheres and the presence or absence of Tl-201 scan defects was good, indicating the validity, primarily, of the image-subtraction technique. It is noteworthy that defects of perfusion produced by coronary occlusion were severe and large, circumstances which would be expected to produce unequivocal thallium scans whether assessed visually or by visual mapping.

Brown et al[79] studied 100 patients who were evaluated for chest pain and found to have a maximal coronary stenosis of less than 50% diameter narrowing. Tl-201 scans were assessed without knowledge of the clinical or angiographic data. The scans were interpreted from non-background subtracted images, using previously defined average score criteria. Each image was separated into three segments and each segment was given a score of either 2 (normal), 1 (reduced activity) or 0 (absent activity). Scores given for each segment by three independent observers were averaged. A transient defect was present if a segment's score was less than 1.5 and increased by 0.5 or more on delayed images. A persistent defect was present if the average score on the initial image was less than 1.5 and did not increase by 0.5. A segment was judged to be normal if the average score on the initial view was 1.5 or more. The presence of either a transient or persistent defect was considered a positive test response for coronary disease.

A similar analysis was reported by de Coster et al[82] assessing thrombolysis in acute myocardial infarction. Tl-201 imaging was performed before streptokinase infusion, 2-8 hr after attempted thrombolysis (without further Tl-201 injection) and again four days and six weeks later. The four sets of thallium images were read simultaneously and interpreted by two observers without knowledge of the clinical or angiographic findings. Each view was divided into five segments, making 15 segments for each set of scans. Tl-201 uptake in each segment was given a score of 0 (normal), 1 (possibly reduced), 2 (reduced) or 3

(absent). The total score for each set of Tl-201 images was presented as the percentage of a maximal defect score (equal to 45) which would be obtained if no thallium uptake was shown on the three views.

The analyses described by Brown and de Coster are the simplest form of visual mapping. Neither study attempted to compare its analysis against visual assessment only, but the method of Brown et al had previously been shown to have a high sensitivity and specificity for coronary artery disease compared to other scoring systems[101].

The consensus from these and other reports[73-77] of quantitation of Tl-201 scans by visual mapping is that the technique is useful for deciding whether scans are normal or abnormal, although there is often no benefit in terms of clinical decision making. There is argument as to the most appropriate method of background subtraction or indeed whether such a correction should be made at all. In experimental situations, quantitation has been used to give insight into thallium kinetics, particularly with regard to myocardial extraction of thallium and its subsequent redistribution.

With the increasing availability of commercial computer programmes for quantitative Tl-201 scan analysis, visual mapping techniques have been superseded by computer mapping. Since 1982, few original visual mapping methods have been described whereas computer mapping methods have proliferated. The latter have to be assessed critically because of the recognised physical limitations of Tl-201 myocardial perfusion scanning.

1.5 Computer mapping methods

The two main approaches to computer mapping of thallium scans are circumferential profile mapping and determination of myocardial washout rates. Burow et al[84] applied the term "circumferential profiles" to describe their computer method of analysis. Rest and exercise thallium scans were acquired in standard fashion. Each image was smoothed using a nine-point algorithm but no background correction was made. An operator positioned an ellipse around the area of the left ventricle by selecting the centre point and the major and minor axes of the ellipse. An isocount contour within the ellipse, beginning usually at 50% of the maximum count, was determined and then adjusted until the contour best fitted the outer edge of the ventricle as assessed visually. The centre of the isocount contour was then determined and radii constructed to each point on the contour (normally 70-100 points). The distribution of thallium activity was obtained by calculating the average activity per pixel along each radius and normalising the data to the radius with the highest average activity; it was displayed as a circumferential profile curve by plotting normalised thallium activity against angular position. Profiles were generated thus for each view. Normal limits of such profiles were defined from studies in normal volunteers for whom a mean normal profile and curves representing two standard deviations from the mean were calculated by averaging the profiles point by point. Circumferential profiles of images from patients with

coronary disease were then compared with these empirically determined normal limits to determine the percent circumference defect (the percentage of circumference points falling below the normal-limits curve) and a score for the image (percent circumference defect multiplied by the average reduction in thallium activity below the normal-limits curve). A total score for each patient study was obtained by adding the scores of the three individual views. However, when the detection of perfusion defects by visual and computer methods was compared, the computer analysis was less sensitive.

Meade et al[83] described a similar graphical presentation to show relative radionuclide activity as a function of location in the myocardium; the graphical display followed on-line computer enhancement of the scintillation camera image using fast Fourier transform techniques. Radial profiles of counts were presented on a linear graph as a function of angle, the origin of which corresponded to the 12 o'clock position on the myocardial image. Exercise and rest image curves were normalised to an arbitrary constant to facilitate comparisons between curves; comparison between patients was made possible by defining septal, inferior and posterolateral areas of myocardium. A segment was taken to represent myocardial infarction if activity over at least 2 cm of myocardium was at least 40% lower than the average activity around the periphery. Ischaemia was taken to exist when the exercise curve fell below the rest curve by at least 20%

of the mean activity over at least 2 cm of myocardium. Using these criteria, there was a greater than 75% agreement between computer assessment and the presence of ischaemia, infarction or normal coronary arteries.

Watson[86] and Berger[87] described a quantitative method of analysis which took into account both the relative activity in different myocardial segments in the same image and the relative activity of the same segment as a result of thallium redistribution with time. They initially performed background correction using a modification of the interpolative background subtraction method described by Goris et al[102]; quantitation was based on residual myocardial counts above the background. Regional Tl-201 activity was measured on images obtained at 10 min, 1 hr and 2-3 hr after injection. A computer programme[103] was used to obtain identical positioning of the initial and delayed images. The computer then generated four profile slices across each myocardial image, and quantitation in each image was based on the peaks of the four profile slices as they passed across the myocardial rim in selected myocardial segments (inferior and anterolateral wall on the anterior projection, anteroseptal, posterolateral and infero-apical walls on the oblique projection). Measurements of activity from the initial anterior and oblique images were used to assess the initial distribution of thallium and sequential images were used to produce time-activity curves for each region of the heart. Each time-activity curve was defined by three points, from which lines of best fit were determined by linear least-square regression analysis.

The half-time ($t_{1/2}$) for Tl-201 activity and the fractional washout coefficient (k) were calculated from the slopes and Y-axis intercepts of the linear regression lines using the following equations :

$$K = \frac{\text{slope}}{\text{intercept}} \quad ; \quad t_{1/2} = \frac{1}{2K}$$

An abnormal myocardial segment was identified by a focal defect on the initial image, relative redistribution on the delayed images or abnormal washout. Quantitative analysis was applied to 140 patients with chest pain[87] but failed to increase the sensitivity and specificity for detection of coronary disease above that of visual assessment of scans. The same group of investigators applied the quantitative method to try and predict the extent and location of coronary disease in the early post infarction period[104] but they did not compare the method with visual assessment.

Garcia et al[89] employed a method which involved (1) circumferential profiles to measure relative Tl-201 activity and (2) washout circumferential profiles to quantify redistribution. Background subtraction was by the modified interpolative method used by Watson et al[86]. Circumferential maximal-count profiles (CP) of the myocardial distribution were obtained with a method similar to that of Vogel et al[105] and Meade et al[83]. In addition to these distribution profiles, washout circumferential profiles (WCP) were calculated as percent

washout from the exercise image after 40 min, 4 and 24 hr :

$$WCP\ (\theta,t) = \frac{CP(\theta,s) - CP\ (\theta,t)}{CP\ (\theta,s)} \times 100\%$$

where WCP (θ,t) is the washout from a myocardial segment, θ, at time t and s represents the time of immediate post-exercise imaging. The redistribution circumferential profiles and washout circumferential profiles were interpolated to exactly 4 hr. Of the various parameters assessed to separate normals from patients with coronary disease, the following gave the best results : (1) an initial defect on the exercise scans; (2) slow washout (4 hr washout profile falling below the normal limit); and (3) at least two abnormal segments in the combined distribution and washout profiles. Despite the fact that Garcia's method represented a synthesis of what were thought to be the best components of previously described techniques, with the addition of unique features relating to washout analysis, it did not result in an overall improvement over visual assessment for sensitivity and specificity in the detection of coronary artery disease. The application of the quantitative technique to both seven-pinhole tomographic and planar thallium images failed to show any advantage of tomography[106].

The quantitative method of Watson et al[86] was used for the prospective assessment of regional myocardial perfusion before and after coronary artery bypass surgery[107]. Myocardial thallium time-activity curves were constructed from the peak profile counts from

multiple segments in serial images to determine the quantitative patterns of initial distribution and washout of the isotope. Each image was divided into six segments and each segment was scored on a scale 1 to 5 : 1 = normal uptake and washout; 2 = initial defect with complete redistribution; 3 = initial defect with partial redistribution; 4 = persistent defect, activity reduced by 25-50%; 5 = persistent defect, activity reduced by > 50%. The study confirmed the improvement of regional myocardial perfusion after successful coronary bypass surgery. The more severe the perfusion defects pre-operatively, the less likelihood there was of restoring myocardial blood flow toward normal by operation. The authors emphasised the lack of a precise definition of complete or partial redistribution. Another methodological difficulty was in deciding the optimal timing for delayed or redistribution imaging, bearing in mind the limitations due to Poisson statistics as well as systematic errors such as non-uniformity or instability of the gamma camera response and the changing contribution of background activity.

Patients with extensive coronary artery disease may have the extent of disease underestimated by thallium scans, or worse still, the scans may appear normal on conventional interpretation[75,76]. The main reason for this limitation is that scintigraphic interpretation normally depends on detecting relative perfusion defects. Thus uniform global hypoperfusion cannot be

distinguished from normal perfusion, and a region of marked hypoperfusion may mask lesser abnormalities in adjoining regions. Bateman et al[108], using the computer processing method of Garcia et al[89], reported diffuse slow washout of myocardial Tl-201 as a new indicator of extensive coronary artery disease. However, only 4% (46 of 1,265) of patients had a slow, diffuse washout pattern with either no perfusion defect or a defect limited to the distribution of a single coronary artery. Of these 46 patients, 32 underwent coronary angiography and 23 (72%) were found to have either three vessel or left coronary disease. Thus the addition of washout analysis was of benefit in only a small number of patients; even in those patients, the predictive accuracy was far from perfect. There was, however, no loss in predictive accuracy when patients achieved less than 75% of predicted maximal heart rate on exercise. False positive diffuse slow washout occurs with for instance tissue infiltration at the injection site. Isolated diffuse slow washout should therefore be interpreted with caution.

A further approach to the quantitation of Tl-201 scanning has been reported by Lim et al[109]. They describe a computer method to analyse and compare myocardial distribution of Tl-201 before and after percutaneous transluminal coronary angioplasty.

An ellipse is placed by the operator around the left ventricular activity in one of three serial images. Automatic realignment of the left ventricular activities

on the other two serial images is performed by horizontal and vertical translation as well as rotation by computer cross correlation. Background subtraction (B_p) for each pixel within the ellipse is computed from the equation :

$$B_p = [\text{Sum } (A_i)\ (W_{ip})]/K_p,$$

where A_i is the counts activity in one pixel along the perimeter of the background ellipse at point i, and W_{ip} is the weighting factor for the pixel measured according to the distance d between pixels i and p and the angle 0 subtended by the two adjacent pixels to i from p. The weighting factor W_{ip} is inversely proportional to the distance d between two pixels i and p but directly to the angle θ. K_p is a constant defined as the sum of all weighting factors on the perimeter of the background ellipse.

$$\text{Thus } W_{ip} = [(\theta_{ip})\ (1-d_{ip})]/d_{max}$$

$$\text{and } K_p = \text{Sum } W_{ip}$$

Profile curves of activity along radii perpendicular to the tangent of the elliptical circumference are then compared from serial Tl-201 images. The difference in normalised Tl-201 activity in each of five segments per image (delayed scan minus initial scan) is taken to represent regional redistribution. The clearance rate of the isotope in each left ventricular segment was also quantitated.

The authors claim several advantages over previously reported computer approaches : (1) the use of an ellipse rather than a circle to plot activity; (2) the assessement of transmural rather than peak pixel

activity; (3) a more comprehensive interpolative background subtraction method; and (4) the generation of a functional colour-coded image to depict regions of redistribution, normal perfusion and persistent defects.

A comparison was performed between qualitative and quantitative analysis of Tl-201 scans in 20 patients who had coronary angioplasty. No difference was found between visual and quantitative analysis. No correlation was found between the degree of improvement in regional Tl-201 uptake and the changes in the percentage of luminal stenosis and/or pressure gradient across the stenosis.

A further study by Okada et al[110] is of interest because it reports on a computer method to subtract a rest scan from an exercise scan. The study was designed to determine the feasibility of assessing two sets of scans performed within about 30 min, each set of scans being preceded by an intravenous dose of Tl-201. Clinical situations where two perfusion studies close together would be desirable include coronary angioplasty and thrombolysis in acute myocardial infarction.

Left ventricular activities on the first and second images are aligned by an automatic computer programme. The alignment took about 30 sec and required about 16,000 words of memory. The memory requirements are within the capacity of portable cardiac computers. The realigned first image (acquired after injection of Tl-201 at rest) was subtracted from the second (exercise) image to produce an image representing exercise perfusion.

The image subtraction technique was validated by correlating the subtraction studies with the presence of coronary artery disease (specificity and sensitivity about 90%). The results are comparable with those in studies using the conventional single dose technique.

Automatic computer realignment of left ventricular activities was again reported in another study by Okada et al[111] which used the same quantitative analysis as the study of Lim et al[109]. Computer realignment allowed the quantification of Tl-201 distribution, redistribution and clearance rate from myocardial zones assessed before and after coronary angioplasty.

Madeira et al[112] reported a study which was at variance with studies showing the value of Tl-201 washout analysis after stress testing. They performed immediate post-exercise and delayed Tl-201 imaging in 19 patients each with a single obstructive coronary lesion. Quantitative washout analysis showed that counts decreased in myocardial zones supplied by the obstructed coronary artery. In the corresponding normal zones, counts were similarly reduced. It was concluded that washout curves were limited in their ability to detect haemodynamically significant coronary disease. These findings are at variance with suggestions that washout curves can be used to detect coronary disease independent of visual comparison with another normal zone[86,89]. An important difference between the studies of Madeira[112] and Watson[86] and Garcia[89] is that Madeira did not use an interpolative background subtraction method. There is considerable debate as to the most appropriate method of

correction for background activity (see section 1.7).

Abdulla et al[113] followed up their previous studies[89,90] to reaffirm the importance of Tl-201 washout analysis. Quantitative analysis of Tl-201 perfusion defects and washout rate was performed on scans of 116 patients. Additional analysis of slow washout rate improved sensitivity for detection of disease in the left anterior descending (from 74 to 82%), left circumflex (from 40 to 61%) and right coronary arteries (from 78 to 90%) without significant loss of specificity. The results of this study are in accordance with experimental studies of myocardial thallium kinetics[71,72] which have demonstrated a slower than normal washout rate of Tl-201 in ischaemic regions. Abdulla's group used absolute rather than relative washout rates to define abnormal regional washout : each patient's observed regional percent washout values were compared with previously determined normal limits rather than with findings from other regions in the same patient. Once again, however, the diagnostic accuracy of this technique for overall detection of disease was no better than with conventional visual analysis. As previously reported[90], the analysis of washout rates increased the sensitivity for detection of individual coronary artery stenoses when compared with visual analysis.

The prognostic significance of normal quantitative Tl-201 stress scintigraphy in patients with chest pain has been examined. Pamelia et al[114] reported on 345 patients with normal Tl-201 scans who were followed up

from 8 to 45 months (mean 34 months). Quantitative analysis was performed using the technique described by Watson et al[86], measuring washout rates and the activity along horizontal profiles across the myocardial rim. Lung Tl-201 uptake, graded qualitatively, was also taken into consideration. During follow-up, there were five cardiac deaths (0.51% per year) and six non-fatal myocardial infarctions (0.61% per year). These event rates are comparable to those reported for patients with chest pain and angiographically normal coronary arteries.

Wackers et al[115], reporting on 95 patients with normal quantitative Tl-201 scans, found a similar small incidence of cardiac events (infarction rate 1% per year). Computer processing and analysis involved interpolative background correction and segmental mapping with 36 segments, and the generation of circumferential count and washout profiles. In this study cardiac events occurred in patients with a moderate to high pre-test likelihood of coronary artery disease whereas in the larger study of Pamelia et al[114] patients with low and high pre-test probabilities of coronary disease had similar event rates. Both studies nevertheless suggest a good prognosis for patients with normal Tl-201 scans, and in such patients coronary angiography may reasonably be delayed unless symptoms are disabling.

Wackers et al[69] have presented a critical evaluation of quantitative planar Tl-201 scintigraphy. The computer algorithm used in their laboratory involves the following steps : (1) interpolative background

subtraction; (2) segmental mapping; (3) circumferential profiles; (4) distribution profiles and (5) washout profiles. They have defined lower limits of normal for Tl-201 distribution and washout; these are displayed with the patient's circumferential profiles as an aid to image interpretation. Compared to visual analysis, quantitative analysis markedly improved the sensitivity for detection of coronary disease (from 55 to 84% in single-vessel, from 79 to 94% in double-vessel, and from 80 to 100% in triple-vessel disease). Overall specificity was 95% by quantitative analysis. The benefits of quantitative analysis appear obvious but it is worth noting that the sensitivities for visual analysis are considerably lower than has been reported from other centres.

The principal quantitative techniques used today involve either horizontal[86] or circumferential[89] profile analysis. Progress since these methods were first described has been mainly in the form of refinements rather than in novel approaches. Many studies have been reported using quantitative analysis. The advantages of such analysis over visual interpretation have been accepted but the improvement in the predictive accuracy of Tl-201 scintigraphy has rarely been enough to benefit clinical decision making. The potential limitations of planar Tl-201 scanning, whether interpreted visually or by quantitative methods, have encouraged the application of tomographic techniques to myocardial perfusion imaging.

1.6 Tomographic Tl-201 myocardial scintigraphy

Tomographic images that provide a three-dimensional distribution can be obtained by using either a rotating gamma camera (single photon emission computerised tomography - SPECT), which acquires images over 180° or 360° around the heart, or a restricted-view angle system such as a slant-hole collimator or a seven-pinhole collimator.

Vogel et al[116] first described a method of emission tomography using a seven-pinhole collimator and an Anger scintillation camera. The imaging technique calculated multiple slice reconstructions through an organ from a single multiprojection image. A special collimator containing seven pinholes was attached to a conventional wide-field-of-view scintillation camera and recorded simultaneous, non-overlapping projections of a small organ (such as the heart) over a limited angle of ±26.5°, and at six equally spaced angular intervals about the principal optical axis. The seven-view raw data, along with flood and point-source calibrations, were computer processed by the simultaneous iterative reconstruction technique (SIRT) to obtain multiple image planes through the organ of interest. The reconstructed planes are parallel to the pinhole aperture plate. Thus tomographic imaging of the myocardial distribution of Tl-201 in the left anterior oblique view produces reconstructed planes from apex to base, perpendicular to the long axis of the heart.

Williams et al[117] studied seven-pinhole emission

tomography under conditions that simulated clinical myocardial imaging with Tl-201, and compared it with planar imaging of a heart phantom. Tomography produced significantly greater image contrast than planar imaging, even when maximal background subtraction was used to enhance the planar images. Two quantitative limitations of seven-pinhole tomography were noted : (1) a simulated defect's activity was not accurately reconstructed; and (2) the defect's activity was propagated longitudinally into some reconstructed planes that did not contain the defect. A further limitation (as shown in experimental temporary coronary artery occlusion in dogs[118]) is that seven-pinhole tomography does not provide accurate Tl-201 kinetic data. Thus the limited angle range of seven-pinhole tomography results in only modest tomographic power, error propagation in image reconstruction, but considerable contrast enhancement compared to planar imaging.

Clinical studies with seven-pinhole tomography have produced conflicting results. Some have shown improved sensitivity and specificity for detecting coronary disease[119] whereas others have shown no such benefit[120]. More recently, tomographic data has been analysed using circumferential count profiles[121]. However, there was no significant advantage in this analysis as compared to qualitative analysis of planar Tl-201 scans. Massie et al[122] used analysis of both distribution and washout profiles to determine the accuracy of seven-pinhole tomography in detecting coronary disease. The results were significantly better than visual analysis (85% of

significantly obstructed coronary vessels detected compared with 47% by visual analysis) but the tomographic technique was not compared with quantitative analysis of planar Tl-201 data.

The concept of single photon emission computed tomography is similar to that of X-ray computed tomography. Data is collected circumferentially about 180° or 360° around the patient's chest; images are then reconstructed in discrete slices in the transaxial plane by computer techniques. The mathematical methods involved have been discussed in general by Brooks et al[123] and in detail for emission tomography by Budinger et al[124]. A major advantage of transaxial tomography over seven-pinhole collimation is that 360° of data can be gathered. Reconstruction of discrete transaxial slices should help to overcome the problem of overlap of adjacent areas of myocardium and other non-cardiac background structures. The drawback of SPECT, particularly with 360° data collection, is that acquisition time may be over 30 minutes - during which time there will have been a degree of redistribution. With transaxial tomography, the absolute quantification of Tl-201 activity in the myocardium could only be performed if attenuation corrections could be applied to correct for absorption of photons by thoracic structures. For low-energy photons such as Tl-201, an exact attenuation correction cannot currently be made. Therefore, at best, analysis of Tl-201 tomographic studies can only be semi-quantitative.

Recognising the problems of inter- and intra-observer variability in image interpretation, Prigent et al[125] developed criteria for the visual interpretation of Tl-201 stress-redistribution myocardial rotational tomography. Visual criteria were developed from studies of 22 normal subjects and 28 patients with coronary disease. For overall detection of disease, the best criterion for abnormality was > 8 sectors of moderately decreased Tl-201 uptake. With this criterion, the true positive and true negative rates for detection of disease were 96% and 91% respectively. The study provided a reference for the systematic evaluation of tomographic images, but visual analysis was tedious and subject to inter-observer variability. Other disadvantages of the visual analysis approach are the inability to assess myocardial washout, and the inability to quantify a perfusion defect or a washout abnormality.

Garcia et al[126] therefore described a method for the quantification of the relative three-dimensional distribution of myocardial thallium, following stress and subsequent redistribution. The method used maximal-count circumferential profiles of well-defined long- and short-axis tomograms to determine the three-dimensional distribution of Tl-201, which was mapped on to a two-dimensional representation. Abnormal Tl-201 distribution or washout was defined by automatic computer comparison of each patient's profile with the corresponding lower limits of normal profiles. Abnormality could be defined both in extent and

severity.

In this study, 32 projections were acquired using the 180° rather than the 360° collection method to obtain higher image contrast and resolution. Tomograms were reconstructed without correction for scattering or attenuation, recognising the difficulty of correcting for the variable attenuation of 80 keV X-rays through the thorax.

Analysis of myocardial Tl-201 washout did not improve detection or localisation of disease. This could have been predicted from the inability of current tomographic techniques to provide accurate Tl-201 kinetic data[118,127]. Furthermore, the defect size was not related to total left ventricular mass; without this, or corrections for scattering, attenuation, heart motion and myocardial thickness, the error in measuring e.g. infarct size or the size of a perfusion defect could be considerable.

Tamaki et al[128] have reported on visual analysis of Tl-201 emission tomography with a rotating gamma camera. Tomography provided contiguous transaxial, short- and long-axis sections of the myocardium; images were divided into nine segments. Segmental analysis of stress tomographic studies was as sensitive and as specific for the diagnosis of coronary artery disease as planar imaging. Another report[129] using a similar segmental analysis suggested that emission computed tomography was superior to planar imaging for the diagnosis of coronary disease.

Tamaki et al also compared quantitative and qualitative analysis of emission computed tomography with Tl-201[130]. Data collection was over 180°. The initial uptake and percent washout of thallium were assessed by the circumferential profile curves of three short-axis sections and one middle right anterior oblique long-axis section. Abnormal distribution was found in 98% of patients with coronary disease, whereas qualitative analysis showed abnormality in 93%. Localisation of individual vessel involvement was reported to be better with quantitative as compared to qualitative analysis.

The main controversy regarding the application of transaxial SPECT technology to Tl-201 myocardial scintigraphy is the choice between 360° and 180° data sampling techniques. Go et al[131] used the original 360° sampled raw data of 25 patients who had SPECT Tl-201 imaging for back projection reprocessing to perform the 360°/180° comparison. The results showed a high incidence (36%) of false-positive segmental perfusion abnormalities and a high incidence (24%) of moderate to severe image distortion with the 180° data sampled reconstructed images as compared to the 360° data. The authors concluded that although the 180° data sampling method had the advantage of providing improved image contrast and reduction in acquisition time, it was an unreliable technique which should be abandoned.

Tomographic imaging of the heart with Tl-201 has not become routine practice, despite suggestions that it is a significant improvement on planar imaging. There

is little evidence to suggest that collimator tomography provides a clear benefit in any of the major objectives of tomographic imaging (detection of a lesion, determination of the size of a lesion, or measurement of the regional concentration of radionuclide). SPECT with a rotating gamma camera satisfies the data sampling requirements for a reconstruction algorithm. 360° data collection is better than the 180° method because with the latter distortion of normal and hypoperfused myocardium is an inherent problem. Even with SPECT, absolute quantification of regional Tl-201 acivity is not possible because of the difficulties of exact attenuation correction. The clinical benefits of tomographic imaging are not great, although there is probably an improvement in the detection of individual coronary stenoses. Visual or computer mapping of planar scans remain the mainstays of quantitative Tl-201 myocardial imaging.

1.7 Background correction methods

From the foregoing review of quantitative analysis of thallium scans, it can be seen that there is no one method of background correction that is generally accepted. Sometimes no background correction was used[84,94,95], either because when a correction was applied an unacceptable number of false positive defects were identified, or simply because no method of correction was felt to be adequate. In an experimental study by Leppo et al[96] background was assessed from regions outside the myocardial image and subtracted from myocardial counts. A threshold subtraction of this sort has been used in a number of studies[98,99] but has been criticised by Goris[132] because of his belief that background activity is not homogeneously distributed. However, Narahara et al[133] used an experimental model to analyse the true myocardial and background image components. They concluded that simple threshold subtraction, not exceeding 20-30% of the maximal myocardial counts, seemed the most appropriate method if a background correction was felt necessary. They performed resting thallium images in dogs who were then killed, a thoracotomy performed and the heart isolated but left in situ. Thallium imaging was repeated, and again after the heart was replaced by first a water-filled and then an air-filled balloon. Digitised images were analysed by generating profile curves from the centre of the heart in a horizontal and vertical plane. Estimated background was taken as the activity in the area surrounding the heart, whereas "true" background

was obtained from the curve generated from the image with the water-filled balloon in place. Background subtraction was performed on the initial image (the heart in situ) by subtracting the true background image and also by using the interpolative background subtraction method of Goris[102]. In each animal, the estimated background overestimated true myocardial background by 26-151% (mean overestimation 87%). The true background component constituted 15 - 27% of the gross counts recorded as myocardium in the image with the heart in situ. The interpolative method of Goris overestimated background activity, residual myocardial activity after background subtraction being 62-75% (mean 70%) of the true myocardial activity in the four dogs studied.

The conclusions of Narahara et al were challenged by Goris in support of his method of interpolative background subtraction[102] which, as modified by Watson et al[86], has been used in a number of studies[87,89,90]. Goris stated that background activity was non-uniform and could not therefore be treated as a constant, as it is in methods involving a threshold subtraction. Separation of myocardial from background activity in his method utilised a non-uniform background reference plane which enclosed the heart image. All image points outside this boundary were defined as background. Background at any point P inside the reference plane was computed from the counts on the orthogonal boundary points of the reference plane, taking into consideration

the distance of these points from point P. Weighting factors were used in the computation of background activity; Watson's method differed from that of Goris in that the weighting factors were inversely related to the distances between the background point P and the boundary points, and in that a constant K was introduced which caused a more rapid fall-off of the background reference plane as it moved beneath the heart away from a region of intense extracardiac activity.

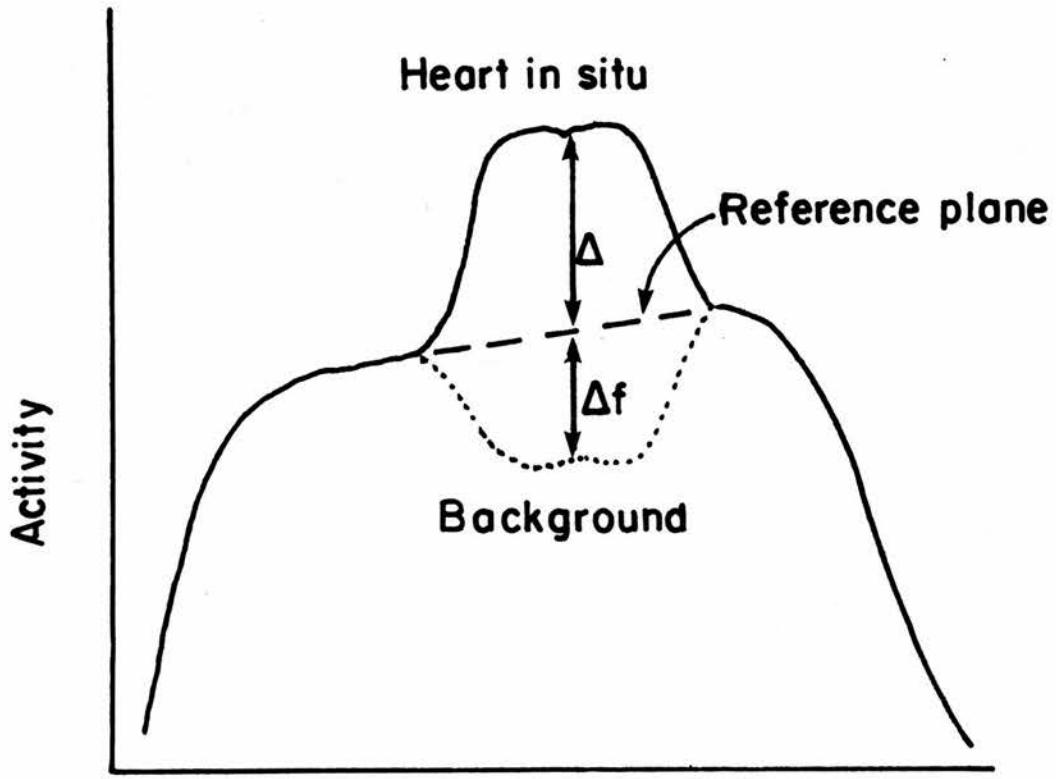

Fig. 1(2). Schematic representation of profiles of average background components, showing the relationship between image data with heart in situ, reference plane and background. (Background = reference plane - Δf).

The study of Beck et al[134] attempted to devise a computer method for background subtraction which, while using interpolative background subtraction, would not lead to an overestimation of background activity (as had been suggested by Narahara et al[133] to occur with the interpolative method).

The method was derived from measurements of background components when hearts of animals injected with Tl-201 were replaced with hearts from non-radioactive animals. A background image construction algorithm was developed. An elliptical region encompassing the heart image was defined on a digitised Tl-201 image; within this region a "reference plane" (Fig. 1(2)), an interpolated set of new pixel values, was generated by using the method of Goris[102]. A final correction to these pixel values was made by subtraction of a fraction, f, of the difference, Δ, between the original image and the reference plane, from the reference plane itself. The background image then had new values inside the heart region and original values outside that region.

In Fig. 1(2), the profile labelled background represents activity within the heart outline after replacement of the radioactive heart with a non-radioactive one. It is clear from the figure that background activity surrounding the heart exceeds that within the heart outline and thus subtraction of a background based on activity surrounding the heart image could result in excessive background subtraction.

Beck et al determined a proportionality constant, f, from experimental data in five dogs by integration of activity within an ellipse enclosing the heart image :

$$f = \frac{\text{reference plane - true background}}{\text{heart in situ - reference plane}}$$

The value for f for anterior views was 0.64 $\pm$ 0.06 (mean $\pm$ SD). The proportionality constant was used to calculate background activity in each dog using images recorded before removal of hearts which had taken up thallium. The computed background was compared with true background (activity behind the heart when radioactive hearts were replaced by nonradioactive ones); the mean difference between the resultant images was 3% (range 1-6%). Goris[132] disputed whether the method of Beck et al was different from his interpolative subtraction. He also argued that the results obtained by Beck et al and Narahara et al might have been quite different if background activity had been measured during injection of Tl-201 on exercise, or if part of the heart had been rendered ischaemic.

Steingart et al[135] reported on the effect of different methods of background correction on the assessment of redistribution in a dog model of sustained regional myocardial ischaemia at rest. Regional activity on sequential scans was assessed using five methods : method (1a) - an analysis of mean Tl-201

activity in the region of a perfusion defect, SDW, in the opposing normal ventricular wall, SNW, in adjacent background and in lung; method (1b) - comparison of SDW and SNW regions minus their respective periventricular backgrounds; method (1c) - comparison of SDW and SNW regions minus lung background; method (2) - comparison of SDW and SNW regions minus interpolated background; method (3) - interpolated background was subtracted from peak ventricular activity determined from one-pixel slices through the defect and normal wall. Time-activity curves were generated with these methods of quantification on sequential scans. They found that without background correction no specific time activity profile would separate SNW from SDW in all dogs. Background periventricular activity remained constant over the experiment whereas activity in the lung started high and decreased with time. Disappointingly, no method of background subtraction or region of interest selection produced unique SDW and SNW patterns of redistribution. While quantification yielded SDW-to-SNW ratios equivalent to those from microsphere injection for the initial Tl-201 images, the calculation of patterns of redistribution showed poor correlation with microsphere-determined regional flow and results were markedly affected by the method of background correction. These results question conclusions on myocardial thallium kinetics and diagnosis based on quantitation of serial resting thallium images.

Because thallium activity from the target (the heart) is higher than from background, the

contribution of background activity can be subtracted by thresholding. If background is included in the scale, the contrast between two parts of the target is also a function of the proportion between background and target activity, instead of only a function of the relative difference in count density in the target. Thresholding will therefore be of particular importance when the background contribution differs between studies.

Thus there are many methods for background correction, but none is ideal. The problem of background can only be solved when accurate three-dimensional reconstruction of emission images becomes possible; until then true background correction will not be possible and available methods will remain approximations.

1.8 Exercise/rest or exercise/redistribution studies?

The initial myocardial uptake of thallium after injection on exercise corresponds with regional myocardial perfusion, but subsequent redistribution of activity takes place. Perfusion defects on exercise scans which disappear on redistribution are said to represent exercise-induced ischaemia in viable myocardium. Defects which are unaltered by redistribution indicate permanent loss of myocardial cells i.e. myocardial scarring[136-138]. Because of its simplicity, the protocol of exercise and redistribution scans has gained favour over two separate thallium injections for exercise and rest scans; it is arguable whether the two protocols are equivalent. Ritchie et al[139] reported a comparison of redistribution and rest images. Exercise, redistribution (4-5 hr after exercise) and resting (one week later) scans were performed on 41 patients with suspected coronary artery disease. The extent or severity of image defects on the redistribution study exceeded that in the rest images in 44% of patients, thus presumably understating the extent of reversible ischaemia and overestimating the extent of myocardial scarring (earlier studies had shown a good correlation between resting image defects and old myocardial infarction assessed from contraction patterns on left ventricular angiography[140]).

The time-course of thallium redistribution and its relation to coronary flow has been reported by Pohost et al[138] and Schwartz et al[62], showing that initial

thallium activity parallels blood flow and that redistribution can begin as little as 5 min later[62]. Experimental studies on the myocardial uptake of Tl-201 during ischaemia and subsequent redistribution usually involve the occlusion and release of a normal coronary artery. In the clinical context, exercise-induced ischaemia is usually associated with fixed, obstructive coronary disease, and the ischaemic territory is variably supplied by collaterals. Therefore experimental data on Tl-201 kinetics may not be directly applicable clinically.

When Tl-201 is injected on exercise or at rest, immediate myocardial activity correlates well with microsphere assessment of regional blood flow[49]. Myocardial Tl-201 activity on redistribution scans, however, consistently overestimates regional blood flow at that time[139]. Therefore, to assess myocardial blood flow accurately some hours after exercise (for instance to differentiate between myocardial ischaemia and infarction), a further injection of Tl-201 appears to be necessary.

If thallium is injected at rest, in the absence of clinical or electrocardiographic evidence of acute ischaemia, perfusion defects are generally thought to represent areas of myocardial scarring[140]. However, Wackers et al[141] suggested that patients with unstable angina who are imaged in a pain-free period may have defects on resting scans which do not represent myocardial infarction. This led to the hypothesis that

analysis of redistribution on serial imaging after thallium injection at rest might differentiate between underperfused but viable myocardium and infarction or scarring. Berger et al[142] assessed the significance of redistribution of resting thallium defects in patients with stable and unstable angina. They confirmed that some defects on initial resting thallium images are not necessarily related to prior myocardial infarction but in such cases, patients have severe and usually multivessel coronary disease. Most of the myocardial segments with an initial defect and subsequent redistribution were associated with normal or hypokinetic wall motion, contraction patterns usually considered to represent viable myocardium[143]. Brown et al[144] found that significantly fewer patients with chronic stable angina showed transient defects on rest scans when compared with patients with unstable angina (12% vs 100%), but Berger et al[142] found no such difference (39% vs 40%). However, despite the fact that perfusion defects on resting scans may not differentiate between ischaemia and infarction, myocardial uptake after thallium injection at rest will initially correlate with regional myocardial perfusion. It is appropriate, therefore, to use exercise and resting scans for quantitative analysis of myocardial perfusion.

Chapter 2 PRELIMINARY STUDIES

The purpose of the work described in this thesis was to use Tl-201 to obtain an objective, reproducible assessment of myocardial ischaemia. Exercise would be used to induce ischaemia and post-exercise scans would be compared with rest scans to obtain an index of variation in perfusion (PVI) from rest to exercise.

The working protocol was that Tl-201 would be injected at rest to obtain resting scans in three standard projections (anterior, left anterior oblique (LAO) and lateral). Repeat imaging to obtain redistribution or residue scans would be performed when the biological decay curve of Tl-201 was flat. A second dose of Tl-201 would be injected at maximal exercise and immediate post-exercise imaging would be performed.

The suitability of such a protocol was tested by preliminary studies which are presented in this chapter, together with consequent changes in the study design.

2.1 The effect of window width on Tl-201 images

Because of the high renal radiation dose (0.104 cGy/MBq or 3.85 rad/mC_i) and the high cost of the radionuclide, Tl-201 is usually administered in quantities of only 37-74 MBq (1-2 mC_i). As such a dose places myocardial counts at a premium, good counting statistics can only be obtained if the gamma camera is made as sensitive as possible without producing serious loss of resolution. Because of their greater abundance, X-ray emissions from the mercury daughter of thallium allow for better imaging compared to the gamma photons at 135 and 167 keV[42]. The X-ray emissions have a photopeak at about 80 keV and window widths varying from 10-25% around this peak have been suggested[42,145]. As the chosen window width might affect the outcome of quantitative studies using Tl-201, a study was undertaken to determine the optimum window width[146].

Methods

Measurements of line spread function (LSF) were made with a 1 mm diameter line source of Tl-201 positioned 10 cm from the face of an Elscint gamma camera with a low energy, medium resolution collimator (CCL4). The source was at the centre of Perspex scattering material (10 cm thick), thereby imitating counting conditions for myocardial scanning. LSF curves were recorded for window widths between 5 and 40 keV; modulation transfer functions (MTF curves) were calculated from them using a fast Fourier transform computer programme.

A plane source for sensitivity measurements was made by placing 20 MBq of Tl-201 in a disc-shaped water filled phantom (internal phantom dimensions : diameter 40 cm, depth 1.75 cm) covered by 5 cm of phantom material. Counts were accumulated for a fixed time for the same range of window widths as for the LSF measurements; the average count per second per unit area of useful camera face was found for each window width. These figures were a measure of camera sensitivity. For both sensitivity and LSF measurements, one observation was made for each window width from 5 to 40 keV.

To test the effect of window width on myocardial scans, two patients were studied, after the injection of 40 MBq of Tl-201 at maximal exercise, in the left anterior oblique view using window widths of 5, 20 and 40 keV. One set of scans were recorded for equal times (300 sec) and a second set to the accumulation of equal counts (500K per frame).

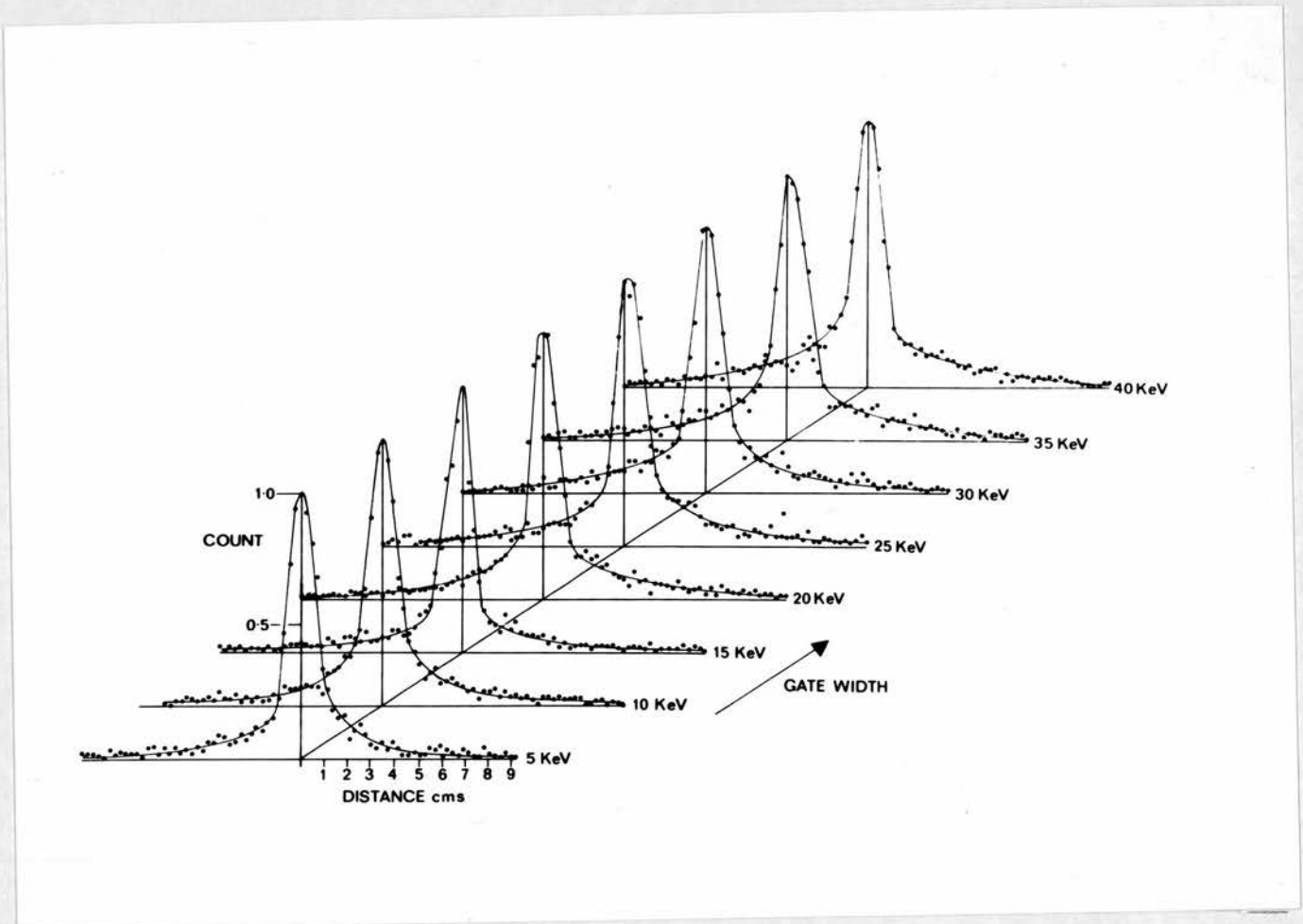

Fig. 2(1) Line spread functions to show the effect of varying gamma camera window width. Curves are normalised to unity at maximum height.

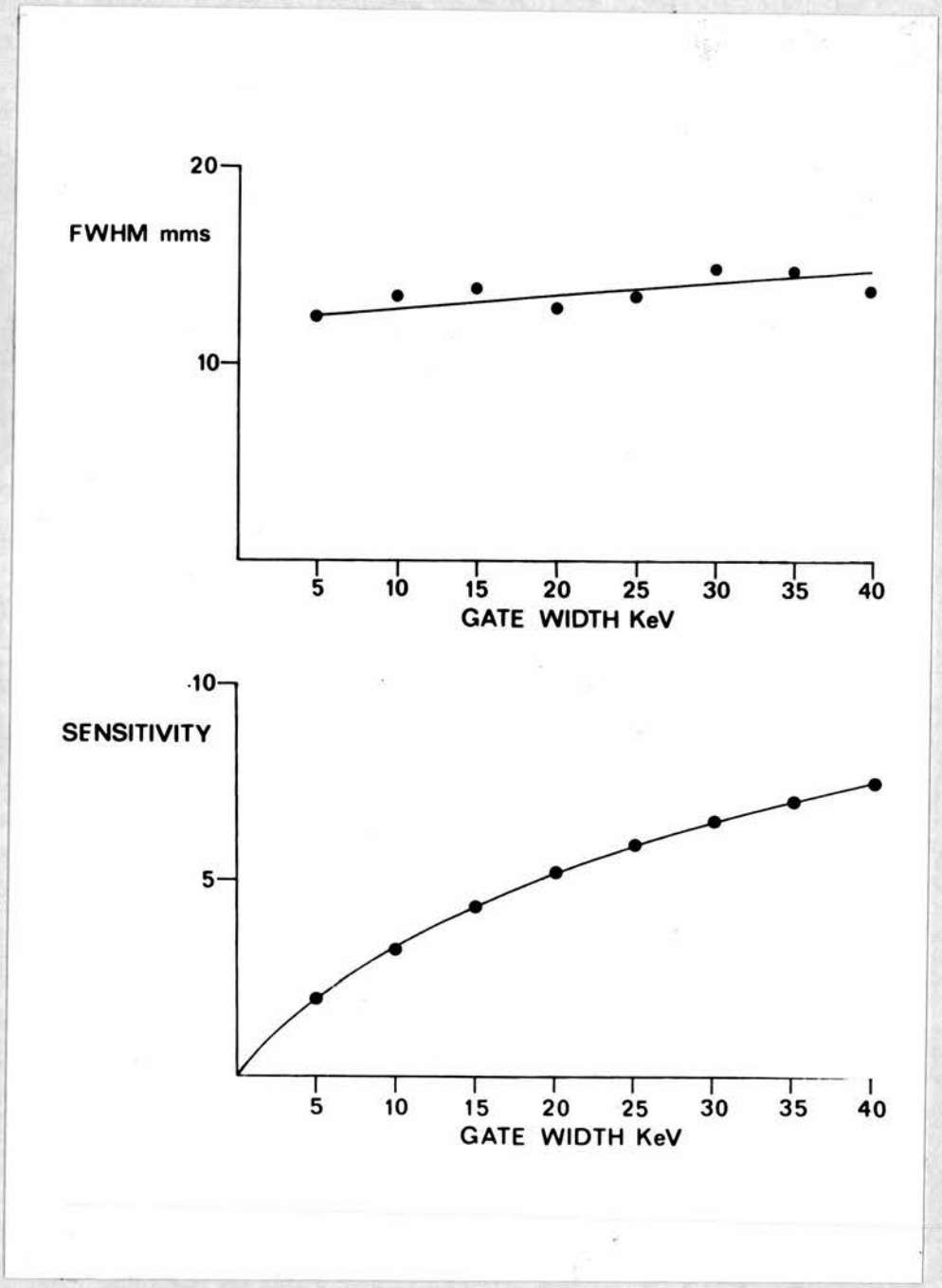

Fig. 2 (2) Resolution index and sensitivity plotted against window width.

FWHM = full width at half maximum

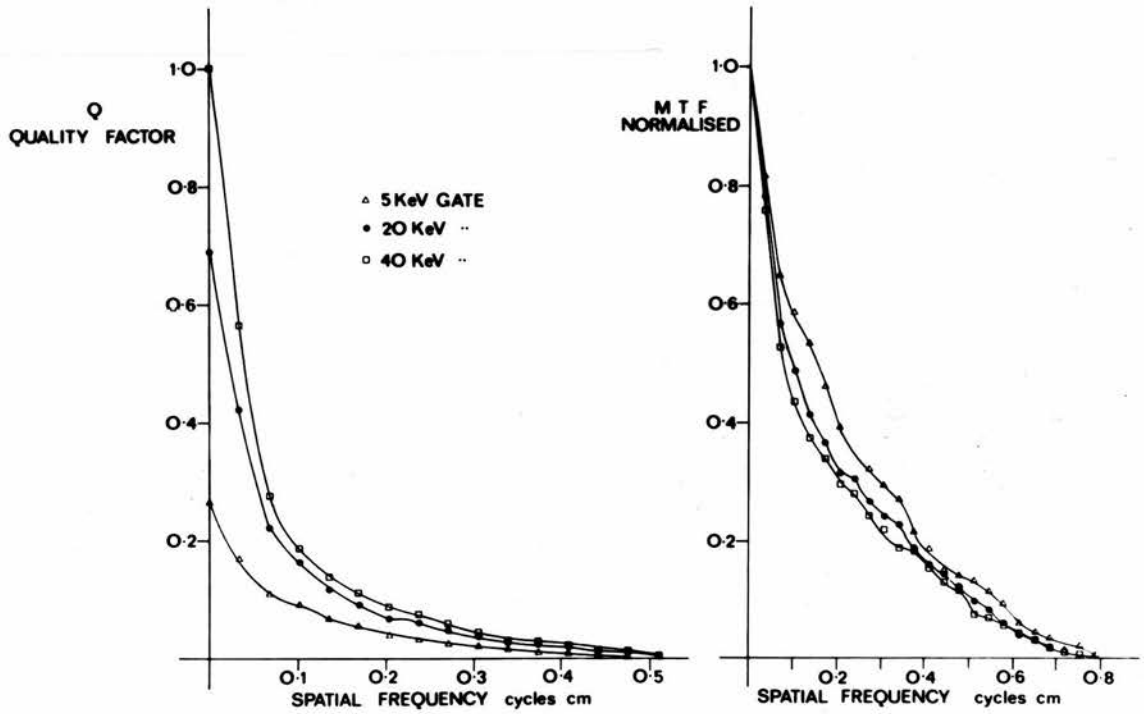

Fig. 2 (3) Quality factor and modulation transfer function plotted against spatial frequency

Results

Figure 2 (1) shows the LSF curves at varying window widths; the shoulders on the curves become more prominent with increasing window width. Resolution indices calculated from a similar set of LSF curves are shown in Fig. 2 (2); these tend to increase only slightly as the window is increased. Fig. 2 (2) also shows plots of plane source sensitivity against window width, demonstrating a considerable increase in sensitivity with increasing window width. Since the resolution index is an incomplete measure of resolving properties MTF curves were calculated and those for 5, 20 and 40 keV windows are shown in Fig. 2 (3). There is little difference between the MTF curves at a 20 keV and 40 keV gate. The curve at 5 keV is better than the other two, as would be expected.

An analysis of scanning systems by Beck and Harper[147] suggests that the performance of an imaging device for a given spatial frequency (f) can be expressed in terms of a figure of merit, Q (f), given by:

$$Q(f) = S\,(MTF(f))^2$$

where S is the plane source sensitivity of the device. Values of Q (f) for 5, 20 and 40 keV window widths are plotted against spatial frequency in Fig. 2 (3). The 40 keV window has a superior figure of merit for all important frequencies.

Studies of patients are shown in Fig 2 (4) and 2(5). The images in Fig 2 (4) demonstrate the change

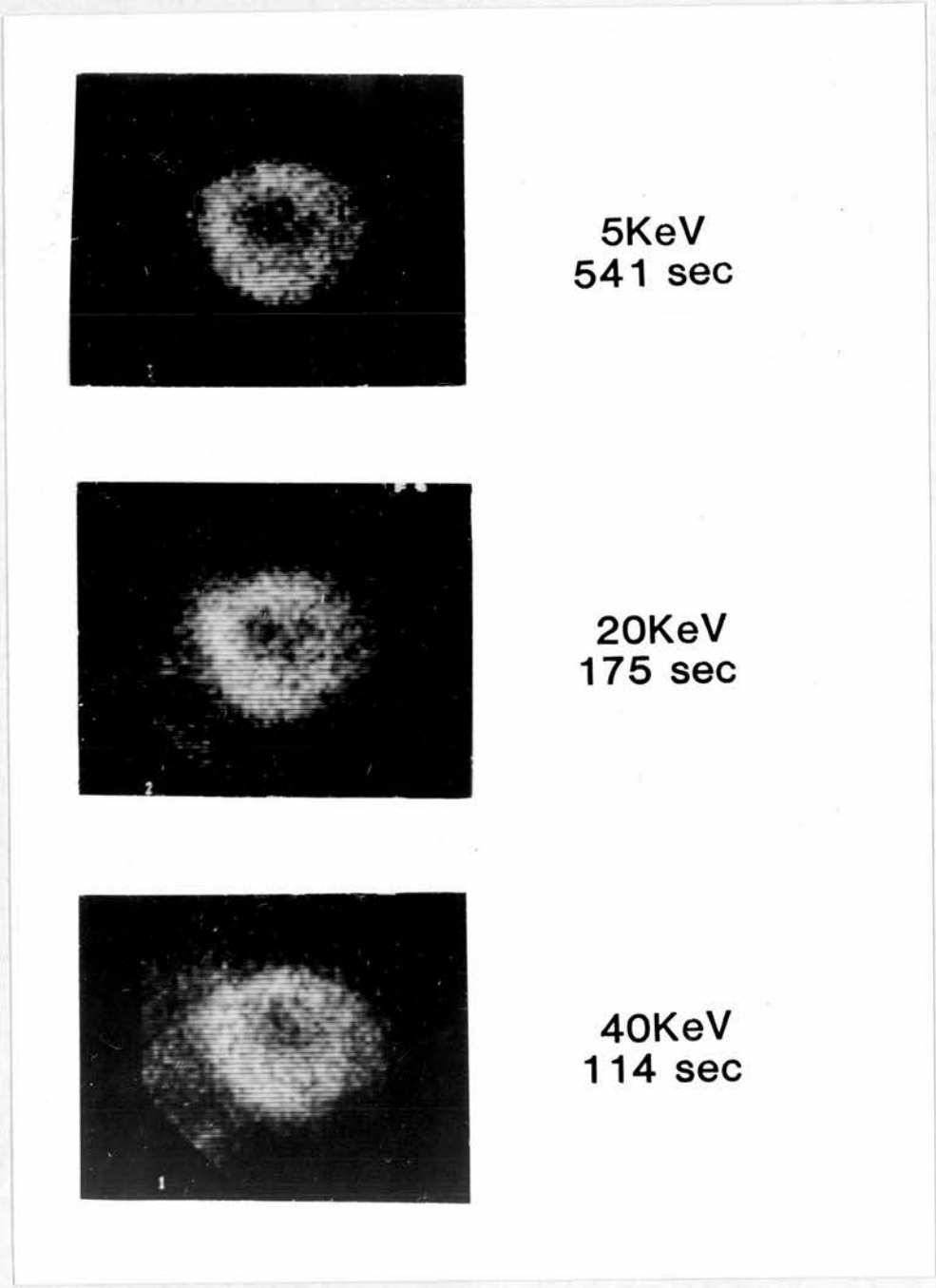

Fig 2(4) Consecutive Tl-201 scans (LAO view) using different window widths but otherwise similar technique. Each scan is recorded to the accumulation of equal counts (500k).

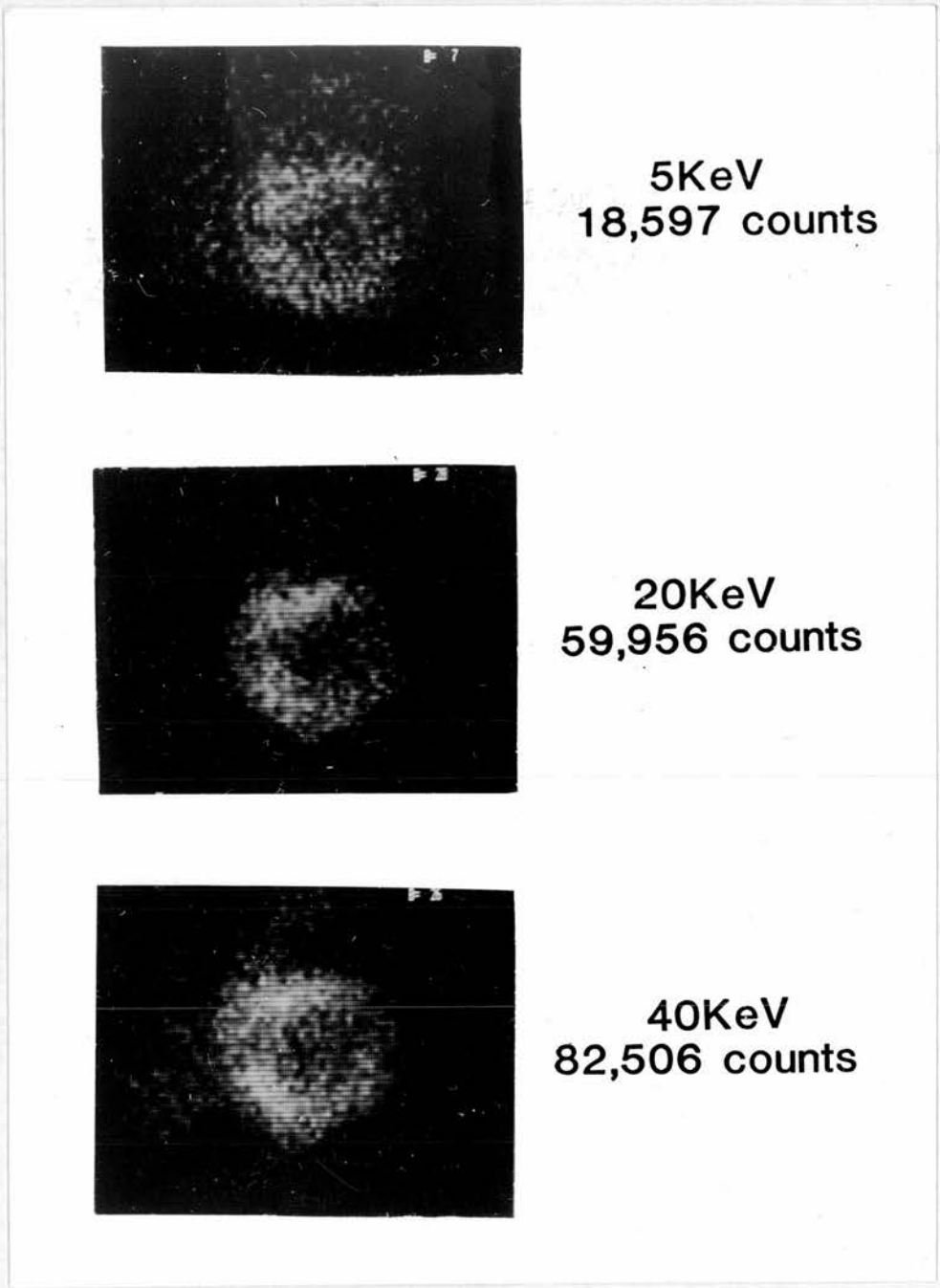

Fig 2(5) Consecutive Tl-201 scans (LAO view) using different window widths but otherwise similar technique. Counts are recorded for the same time (300sec) on each scan.

in resolving properties as the window width is increased. The superior performance at 5 keV is evident, but it must be emphasised that these are images with equal numbers of counts (500k). The times taken to produce the 20 and 5 keV images were in a ratio of 1.5 and 4.7 to that taken for the 40 keV image.

Images for equal times (300 sec) are shown in Fig 2 (5). The advantage in resolution obtained by using a narrow window is greatly offset by the fall in sensitivity. The total counts collected over the heart for the 20 and 5 keV images are in a ratio of 0.7 and 0.22 to the counts collected with a 40 keV window.

The flood field uniformity of the gamma camera is also of importance in quantification studies. With the camera set to less than $\pm$ 10% integral uniformity for $^{99}Tc^{m}$, values of 20, 13.8 and 14.7% were obtained for Tl-201 at window widths of 5, 20 and 40 keV respectively.

In these studies, gamma camera uniformity had been set up for technetium using a 20 keV window. With this setting, the uniformity would not be optimal for Tl-201, but was found to be best (13.8%) at the same 20 keV window. There was no significant difference in uniformity for Tl-201 when the window width was increased to 40 keV. Decreasing the window width to 5 keV produced a large change in uniformity.

Discussion

These results indicate that large window widths can be used for Tl-201 scanning without seriously degrading the image. Presumably this is because the predominant scattering processes (photoelectric and Compton) do not have as large an effect on low energy thallium quanta as they would on quanta of a higher energy. Compton scatter from the high energy contaminant Tl-202, which produces gamma rays at 439 keV, might allow these gamma rays to penetrate the collimator and scatter into the X-ray gate and inevitably lead to a loss of resolution as the window width is increased. However, the high energy gamma rays are in low abundance and the results suggest that the degradation of image quality which they cause is more than offset by the advantage of collecting more X-ray photons as the window width is increased. Lastly, as image resolution will be limited by cardiac motion, sacrificing sensitivity for increased resolution would not have its usual advantage.

Therefore a window width of 40 keV (50%) was decided upon for all subsequent studies, to give good counting statistics without serious loss of resolution (if the dosage of Tl-201 was about 60 MBq and counting time 300 sec per frame). This protocol would ensure that post-exercise scans could be completed within 30 minutes of exercise.

2.2 Effect of exercise on redistribution scans

Tl-201 images are usually recorded after injection of the isotope at rest or on exercise. There are no reports of what effect (if any) exercise has on scans recorded after injection at rest. The study protocol required the recording of rest and redistribution scans followed by a second injection of Tl-201 on exercise. The following experiment was performed to determine whether exercise per se would alter Tl-201 activity on the redistribution scan.

Routine myocardial scans in three views were recorded in a normal subject after injection of Tl-201 (45 MBq) at rest. Following repeat scans 24 hrs later (redistribution scans) the subject exercised maximally on the bicycle ergometer (exercise time 12 min), and scans were repeated at the end of exercise, no further Tl-201 having been given.

Visual inspection of the pre- and post-exercise scans showed that myocardial Tl-201 activity had altered. An analysis of the cause of the change in activity was not undertaken. It could not be concluded that exercise per se was the cause of the change in activity, but it was decided to obviate the possibility by amending the study protocol so that exercise studies preceded redistribution and rest scans.

2.3 Biological decay curve of Tl-201

The planned protocol involved the acquisition of exercise, redistribution and rest scans followed by the subtraction of redistribution counts from rest scans so that regional Tl-201 activity at rest and on exercise could be compared. When redistribution scans are performed and followed by repeat scanning after Tl-201 injection at rest, the accurate subtraction of redistribution counts from the rest scans requires that the former remain constant from the time that redistribution scans are recorded until the completion of rest scans. In order to minimise the effect of biological decay on redistribution counts, redistribution scans should be performed when the decay curve becomes flat. The precise timing of redistribution scanning was therefore determined from the biological decay curve of Tl-201.

Methods

The biological decay curve of Tl-201 was obtained in 8 patients; in four the Tl-201 (45 MBq) was injected at rest and in the other four at maximal exercise. Myocardial imaging in the LAO view was begun 10 min after injection (frame time 300 sec) and scans were repeated at intervals over the next 48 hr. A uniformity correction was applied to all frames.

On the initial scan, a region of interest (ROI) was drawn with the light pen to encompass the myocardial image and counts per unit area within the ROI were recorded. No correction for background activity was

applied. Each subsequent scan was then displayed in turn and myocardial counts per unit area were obtained by superimposing the ROI created on the first scan.

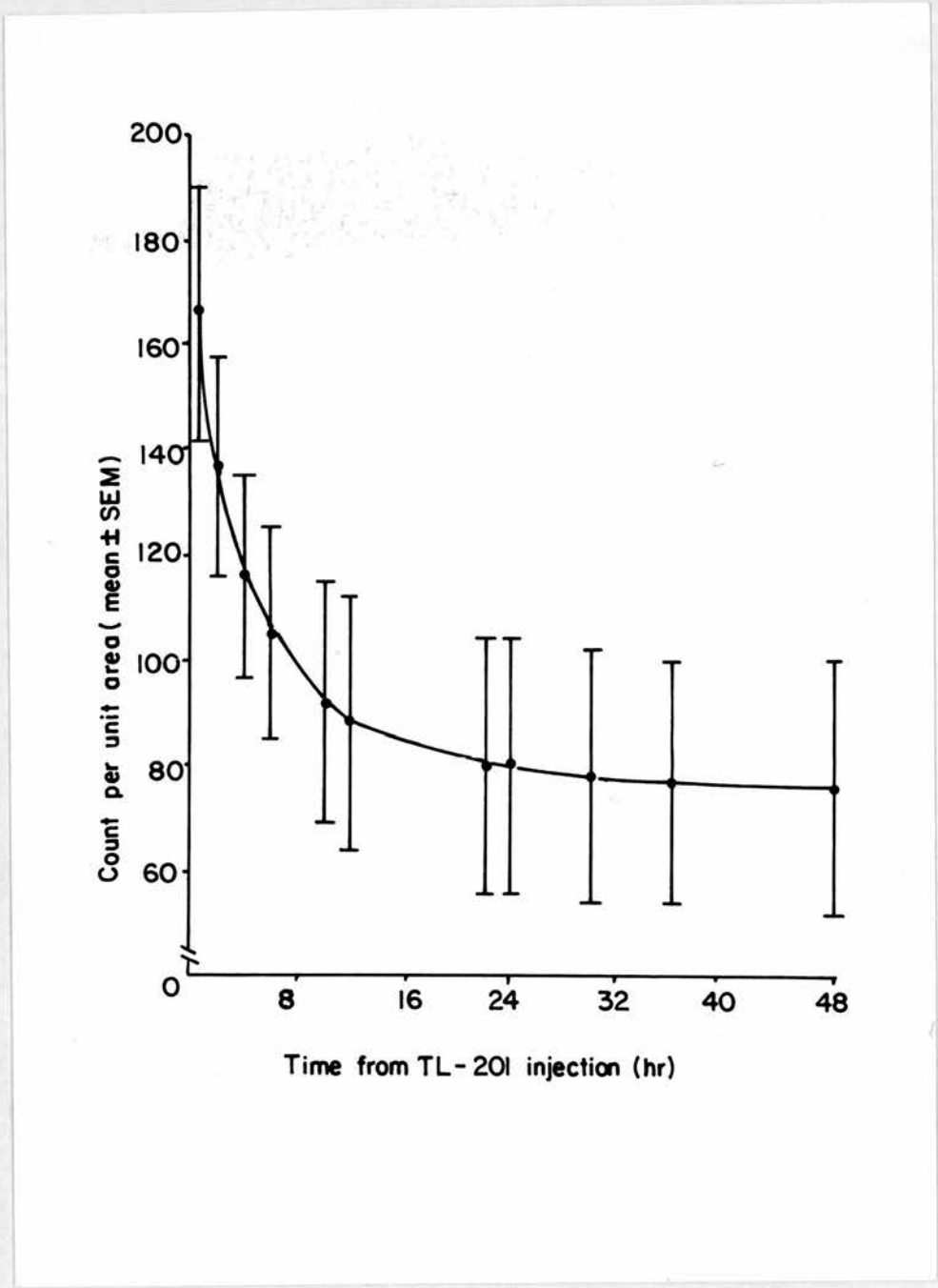

Fig. 2(6) Biological decay curve of Tl-201.

Results

The mean myocardial count/unit area ± SEM is shown in Fig. 2(6) for 48 hr after Tl-201 injection in 8 patients. Myocardial activity decays exponentially, with the slope of the curve being zero for the period 22-24 hr.

Conclusion

The decay curve suggests that if redistribution scans are performed at 22-24 hr, followed immediately by rest scans, biological decay would be an insignificant cause of change in redistribution counts from the time the redistribution scans were acquired till the completion of rest scans.

Problems such as detector non-uniformity and detector drift could certainly have influenced the recorded count density. A uniformity correction was performed to minimise such effects. Another major factor is likely to have been the large biological variation between patients; the error bars on Fig 2 (6) confirm this. Notwithstanding these problems, the study suggested that the biological decay curve became acceptably flat by 22-24 hr. The reproducibility of redistribution scans performed 24 hr after Tl-201 injection was further assessed in section 2.6.

2.4 Optimal time for imaging following Tl-201 injection

The same 8 patients were studied as for the biological decay curve experiments. Tl-201 was injected either at rest (n=4) or on exercise (n=4). Scanning was begun 2 min after injection and serial 300 sec frames were recorded in the LAO projection for 40 min.

With the light pen, ROI's were created to obtain counts per unit area on each frame for (1) myocardial and (2) background activity. The areas of the background and myocardial ROI's were comparable. The background ROI was drawn posterior to myocardial activity, mid-way between the edge of the scan and activity from the posterior left ventricular wall. A myocardial-to-background ratio was then calculated for each frame for injection at rest and on exercise; the ratio (mean $\pm$ SEM) is shown in Fig. 2(7).

Fig 2(7)

MYOCARDIAL – TO – BACKGROUND RATIO (Mean ± SEM)
PLOTTED AGAINST TIME FOR INJECTION AT REST & ON EXERCISE

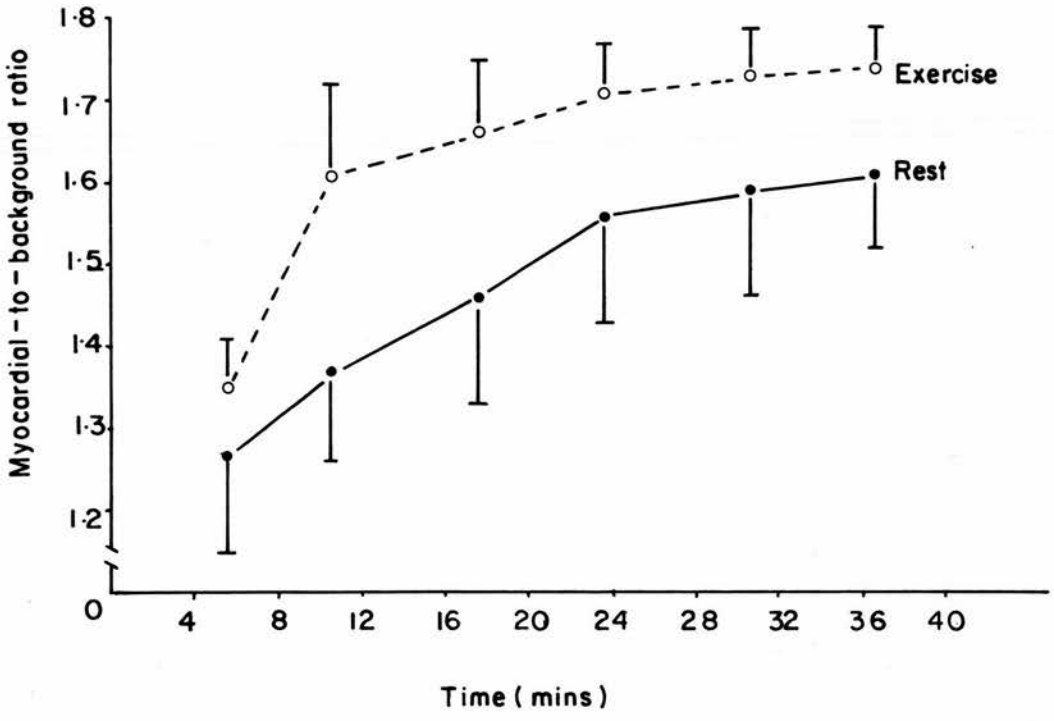

Results

In the post-exercise scans, myocardial-to-background ratio was at its lowest in the first frame (2-7 min) and rose in each subsequent period. While there was a 19% rise in the ratio from the first to the second frame (8-13 min) subsequent changes were small (< 3.1%). Myocardial-to-background ratios after injection at rest showed a steady rise during the observation period (Fig. 2(7)).

Discussion

Post-exercise ratios suggested that scanning should begin 8 min after Tl-201 injection; earlier scanning would make identification of the myocardial outline difficult because of high background (especially lung) activity, and later scanning might lead to unacceptable redistribution of Tl-201 activity before scanning was completed.

Redistribution of Tl-201 activity begins very soon after relief of myocardial ischaemia, as early as 5 min after experimental occlusion and reperfusion of the circumflex coronary artery in the pig[62]. The problem is emphasised by Maseri et al[148] who pointed out that only the initial distribution of Tl-201 appears to reflect regional flow at the time of injection. Therefore no matter how soon after exercise scanning is begun, significant redistribution will have taken place by the time all views are acquired. The advantage of beginning scanning at a set time after exercise and acquiring views in the

same order is to standardise the degree of redistribution that takes place. Beginning scanning 8 min after exercise is an acceptable compromise.

The optimal starting time for scanning after Tl-201 injection at rest is not clearly defined by this study. Myocardial-to-background ratio continued to rise during the observation period, although the rate of rise decreased after about 24 min. In the 30-40 min after injection at rest, Tl-201 redistribution is thought to be negligible, unless the patient has myocardial ischaemia at the time of injection[141,142]. However, for the purposes of this thesis it was advisable to have redistribution and rest scans close together to limit changes in redistribution counts from their acquisition till the completion of rest scans. The contribution of redistribution counts to the rest scan could then be determined from the preceding redistribution scan. It was therefore decided that rest imaging would begin 20 min after Tl-201 injection.

2.5 Determination of the optimal number of ROI's per myocardial image

A myocardial image has to be subdivided to assess regional change in Tl-201 activity. The number of ROI's into which the image is divided should be large enough to allow changing activity in small areas of myocardium to be detected, but not so large that counts within each region become so small that a large sampling error is introduced from Poisson statistics.

A visual analysis of abnormal Tl-201 scans obtained in our department, in conjunction with reports of the correlation of perfusion defects with the site of coronary artery disease[73], suggested that for any stenosed major coronary artery the pattern of perfusion defect would depend on whether the stenosis was proximal or distal, before or after any large branches. For instance, a left anterior descending lesion proximal to the origin of major diagonal branches would result in a perfusion defect involving the whole of the anterior left ventricular wall, whereas a stenosis distal to diagonal branches would leave perfusion to some of the anterior wall uncompromised and result in perfusion defects involving only part of the anterior wall. Similarly, proximal lesions of the right coronary artery and left circumflex artery would cause perfusion defects involving the whole of the inferior and postero-lateral left ventricular walls respectively, whereas

more distal lesions would result in more localised perfusion defects. Therefore the expected patterns of perfusion defect suggested that the anterior, septal, inferior and postero-lateral wall images should each be divided into two ROI's, one proximal and one distal. Furthermore, because of the normal finding of reduced Tl-201 activity at the left ventricular apex, this segment should be included in a separate ROI. Therefore five appeared to be the optimal number of ROI's into which the myocardial image should be divided in each of the three standard views.

The count density and its statistical error from a division of each myocardial image into five ROI's was assessed in four patients undergoing a full Tl-201 study (exercise scintigraphy, redistribution imaging at 24 hr followed by repeat imaging after Tl-201 injection at rest).

Each anterior myocardial image was divided into five ROI's so that two encompassed the anterior left ventricular wall, two the inferior and one the apex. Count density for each region was obtained for exercise, redistribution and rest images. The left anterior oblique view was analysed similarly, the left ventricular image being divided into two regions over the septum, two over the postero-lateral wall and one over the apex. The division of the lateral image was into two ROI's over the anterior wall, two over the inferior and one at the apex.

Results

Recorded counts (mean ± SEM) for exercise, redistribution and rest scans in five ROI's on anterior, LAO and lateral views are shown in Fig. 2(8). The large SEM for counts in all regions reflects inter-patient variation in the dose of Tl-201 administered and/or taken up by the myocardium. Counts recorded during rest scans were higher than those on exercise scans, which were in turn higher than those on redistribution scans. Although myocardial uptake is greater when Tl-201 is injected on exercise than at rest, rest counts were higher in this study as they represented the sum of redistribution counts and counts attributable to the injection at rest.

Table 2 (1) shows the standard deviation (SD) for each of the mean counts for each ROI, the SD being a measure of the error from counting statistics. When expressed as a percentage of the mean count for each view, the SD has a value of 1.0, 1.4 and 0.8% on the exercise, redistribution and rest scans respectively. These values confirm that the subdivision of myocardial images into five ROI's does not result in an unacceptable error from counting statistics. The largest error would be expected on redistribution scans but further studies (vide infra) established that there was no significant difference in regional counts between two sets of redistribution scans performed immediately after one another.

It was concluded that myocardial images would be divided into five ROI's to enable small changes in regional Tl-201 activity to be detected without introducing a significant Poisson error.

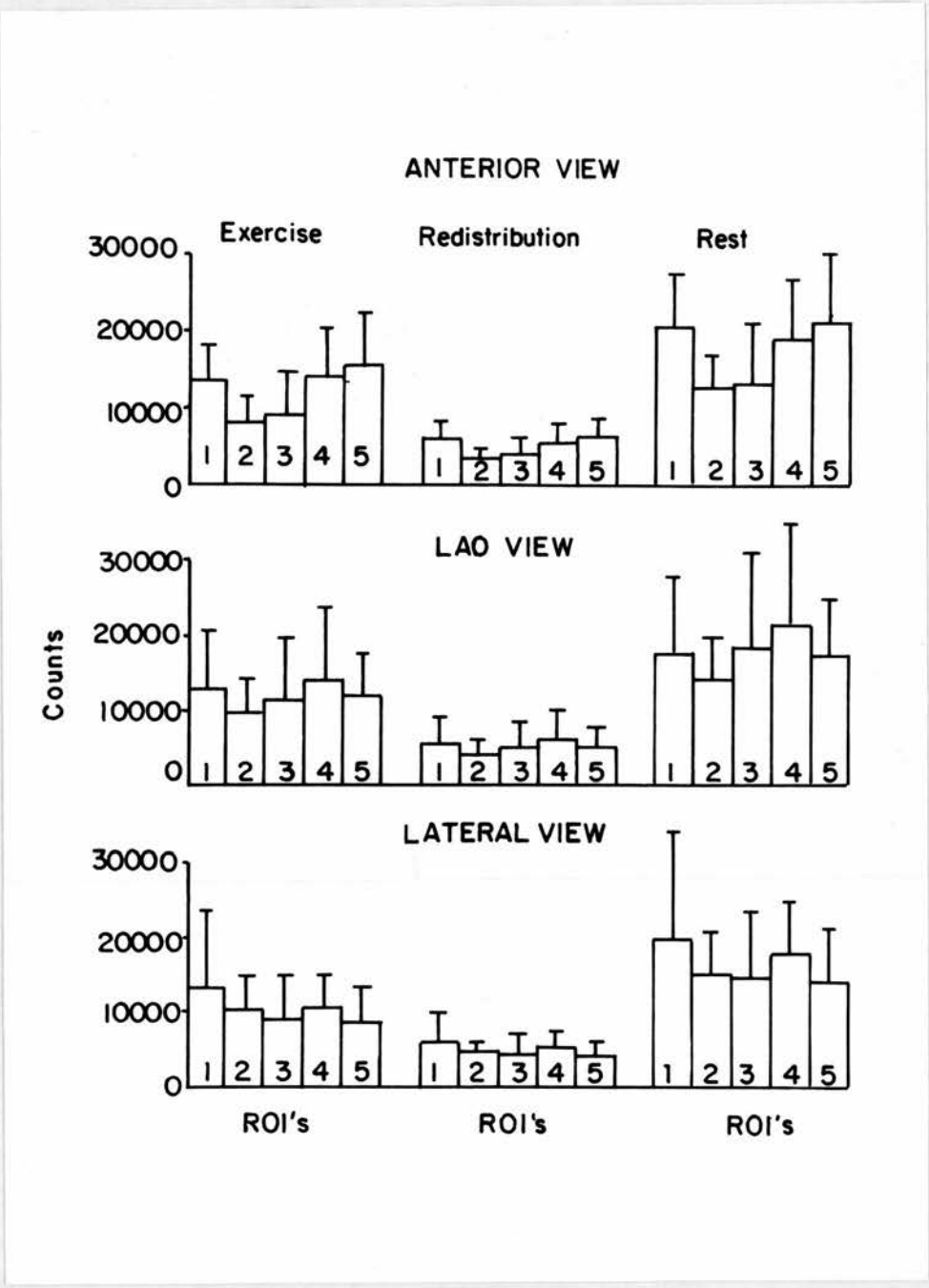

Fig. 2(8). Counts per ROI (mean ± SEM) with exercise, redistribution and rest scans divided into 5 ROI's per view.

(a) Anterior View

ROI	Exercise	SD	Redistribution	SD	Rest	SD
1	13753	117	5921	77	20746	144
2	8005	89	3532	59	12386	111
3	8968	95	3727	61	13184	115
4	14053	119	5557	75	19010	138
5	15519	125	6295	79	21260	146
Mean	12060	110	5006	71	17317	132

((b) LAO view

ROI	Exercise	SD	Redistribution	SD	Rest	SD
1	12871	113	5650	75	17749	133
2	9634	98	4137	64	14172	119
3	11467	107	5114	72	18264	135
4	13924	118	6121	78	21449	146
5	12080	110	5181	72	16993	130
Mean	9678	98	5241	72	17725	133

(c) Lateral view

ROI	Exercise	SD	Redistribution	SD	Rest	SD
1	13325	115	5882	77	19432	139
2	10416	102	4581	68	14835	122
3	9067	95	4303	66	14301	120
4	10642	103	5190	72	17409	132
5	8637	93	4050	64	13746	117
Mean	10417	102	4801	69	15945	126

Table 2(1) : Count density and standard deviation with myocardial images divided into five regions (see text).

2.6 Reproducibility of redistribution scans

The biological decay curve for Tl-201 (section 2.3) showed that if redistribution scans were performed at 24 hr and followed by rest scans, biological decay would not alter redistribution counts from their acquisition until the completion of rest scans. In the previous section (2.5), it was shown that the redistribution scans would be affected more than exercise and rest scans by count fluctuation from counting statistics. The following study was therefore undertaken to consider the reproducibility of redistribution scans and thence to decide whether redistribution counts could be subtracted accurately from the ensuing rest scans. The alternative approach (delaying rest scans until residual Tl-201 activity from injection on exercise becomes negligible), would mean that exercise and rest scans would have to be separated by at least a week, as the physical half-life of Tl-201 is 73.5 hr.

Method

In three normal subjects and three patients with coronary disease, exercise scans were acquired in the usual fashion. 24 hr later, scanning was repeated in the standard views (first redistribution scans) and followed by repeat imaging (second redistribution scans) without further injection of Tl-201. The second series of redistribution images were completed within 40 min of the first. Computer analysis was

then undertaken.

In each view of the first redistribution scans, the left ventricular image was divided into five ROI's using the light pen. Counts per unit area for each ROI were recorded and the ROI's stored. The second redistribution scans were then displayed and the stored ROI's were recalled and manipulated on the myocardial image until the best visual fit was obtained; new counts per unit area were recorded for all ROI's in each view. It was therefore possible to compare regional count density on the two sets of redistribution scans.

Results

As no difference was found between patients and normal subjects the results are presented together (n=6).

In each view the mean count per unit area ± SEM was almost identical in the two sets of redistribution scans (Fig. 2(9)). However, an analysis of mean counts could have masked marked fluctuations in individual patients, and so individual differences between the first and second redistribution scans were also analysed (Fig. 2(10)).

Fig. 2 (9)

HISTOGRAMS SHOWING THE SIMILARITY OF COUNTS PER ROI OBTAINED IN TWO SETS OF REDISTRIBUTION SCANS RECORDED IN THREE VIEWS

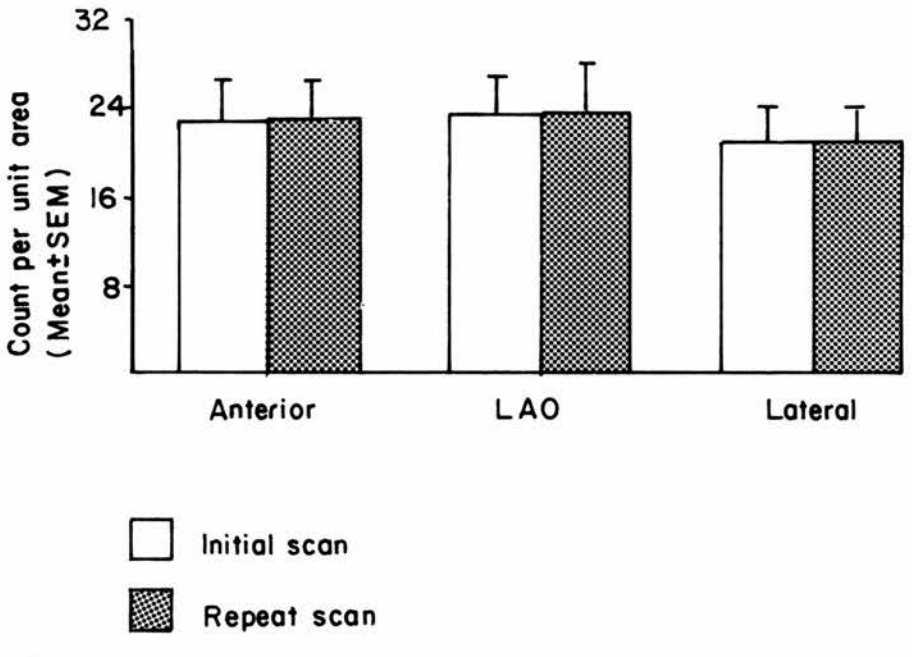

Fig. 2 (10)

A COMPARISON OF COUNT DENSITY IN EACH OF FIVE ROI's ON INITIAL (A) AND REPEAT (B) REDISTRIBUTION SCANS IN THREE VIEWS
(Results for 6 patients)

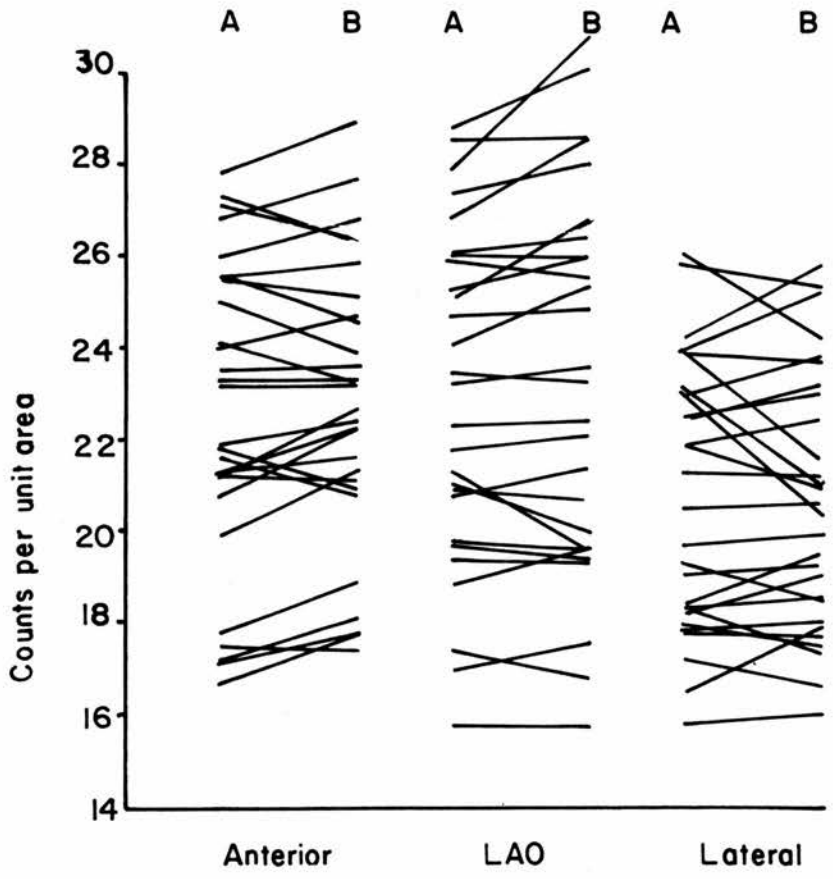

In the anterior view, the maximum change was 6.5%; in 26 of 30 ROI's the difference was < 5%. In the LAO view, one ROI in one patientshowed a 12% difference between the first and second redistribution scan; in the remaining 29 ROI's the difference was < 7%. Figures for the lateral view were similar; one ROI showed a change of 11% whereas 25 of 30 ROI's showed a change of less than 5%.

The results show that there is no significant difference between the mean count densities of the two sets of redistribution scans, and that when individual ROI's are considered, initial and repeat scans show differences which can be attributed to counting statistics. If, therefore, redistribution scans at 24 hr are followed by an injection of Tl-201 at rest and another series of scans obtained, the contribution of redistribution counts to the rest scans can be subtracted; the error involved can be calculated from Poisson statistics.

2.7 Accuracy of drawing ROI's on exercise images and superimposing them on redistribution and rest scans

To compare changes in regional Tl-201 activity at exercise and rest, count density must be measured from the same myocardial segments on exercise and resting scans. If ROI's are drawn on exercise images, stored and then recalled and superimposed on redistribution and rest scans, counts from the same myocardial areas can be compared. The Dycom system, interfaced with the Elscint gamma camera, allows for storage and retrieval of light pen generated ROI's whose position can be altered in horizontal and vertical planes independently. Rotational differences between scans could impair the accuracy with which ROI's could be superimposed; a method using plumb-lines was devised to ensure a constant relationship between gamma camera and patient for any given view.

Methods

The patient remained supine for all views. Before the acquisition of exercise scans in the anterior and LAO view, three plumb-lines were suspended from marked points on the gamma camera head. As the camera was brought towards the patient the point of contact of each plumb-line on the patient's chest was marked; thus three points were marked on the chest for the anterior and LAO views. While the patient remained still the camera was rotated to obtain lateral views. When anterior and LAO

redistribution and rest scans were performed, the plumb lines and points marked on the chest were matched, ensuring that the patient-camera orientation was identical to that for the exercise scans. Keeping the patient supine while the camera was rotated ensured that comparable lateral views were obtained.

Reproducibility of superimposing stored ROI's was tested in three patients. Routine exercise, redistribution and rest scans were obtained using the plumb line system. On the exercise scans the myocardial image was divided into five ROI's in each view (the position of the ROI's is described in section 2.5), the count density was recorded for each region and the ROI's were stored. The redistribution scans and the appropriate ROI's for each view were then displayed; the ROI's were moved relative to the myocardial image until the best visual fit of the ROI's on the myocardial image was obtained. Count densities for the ROI's on the redistribution scans were recorded and the process repeated for rest scans. Count densities on exercise, redistribution and rest scans for the same ROI's were thus obtained. The process of superimposing ROI's on redistribution and rest scans was repeated twice for each view in three patients, count densities being recorded each time.

Results

Results are shown in table 2 (2). For each view

(anterior, LAO and lateral) the count density (mean ± SEM) is shown for each of five ROI's. Very low values were obtained for SEM (all values < 4% of the mean count, 68% of readings < 1%).

Conclusion

These results confirm that the proposed protocol allows for highly reproducible assessment of regional count density in equivalent segments of redistribution and rest scans after ROI's are drawn on exercise images.

(a) Redistribution

ROI		Patient 1	Patient 2	Patient 3
Ant	1	21.6±0.7	24.7±0.4	19.5±0.1
	2	23.4±0.1	26.3±0.6	19.2±0
	3	21.4±0.4	23.7±0.6	19.6±0.1
	4	21.3±0.3	25.9±0.1	20.9±0.1
	5	20.2±0.6	25.5±0.2	18.4±0.1
LAO	1	23.6±0.2	24.2±0.4	18.6±0.2
	2	23.2±0.2	25.9±0.2	19.0±0
	3	22.3±0.1	27.3±0.1	20.2±0.2
	4	21.8±0.1	25.2±0.1	19.5±0
	5	19.8±0.1	24.8±0.1	19.4±0
Lat	1	20.5±0	25.8±0	15.7±0.3
	2	20.0±0.5	24.2±0	16.2±0.3
	3	18.3±0	21.9±0	15.5±0.6
	4	19.1±0.3	22.4±0	16.0±0.1
	5	18.8±0.5	23.9±0	16.9±0

Table 2(2) Count densities (mean ± SEM) obtained on repeated superimposition of ROI's on (a) redistribution and (b) rest scans. Consistently low values for the SEM indicate that superimposition is highly reproducible.

(b) Rest

ROI		Patient 1	Patient 2	Patient 3
Ant	1	84.2±1.0	86.7±0.7	70.6±0.4
	2	90.1±0.6	91.8±0.5	69.8±0.2
	3	82.1±1.5	80.6±1.2	67.3±0.3
	4	83.1±0.5	83.9±0.5	70.2±0.6
	5	81.3±0.6	84.2±0.3	63.8±0.4
LAO	1	86.8±0	80.4±0.1	63.1±0.2
	2	91.3±0	86.5±0.2	65.4±1.4
	3	83.9±0	100.3±0.1	70.5±0.3
	4	83.9±0	88.3±0.4	67.0±0.5
	5	74.9±0	82.2±0.2	64.0±0.5
Lat	1	78.4±1.4	90.1±0	56.1±0.5
	2	78.3±0.7	90.5±0	57.9±0.4
	3	68.7±2.8	76.2±0	57.6±0.2
	4	70.9±1.5	73.9±0	55.9±0.4
	5	70.6±0.9	74.0±0	55.6±0.6

Table 2(2) continued

2.8 Variability arising from operator-dependent division of myocardial images into ROI's

The purpose of subdividing the myocardial image into ROI's was so that regional changes in myocardial counts (and therefore perfusion) could be measured. The method chosen allowed the operator to determine the exact site and size of the five ROI's per view. The intention was to make the count density in each ROI as homogeneous as the myocardial image would allow, thus giving maximum contrast between perfusion defects and areas of normal perfusion.

Inter- and intra-observer variability are recognised drawbacks of non-automated scintigraphic analysis, and have been shown to affect visual analysis of Tl-201 scans[70]. All studies in this thesis were analysed by the author; therefore inter-observer variability need not be considered. The following study was performed to assess intra-observer variability in the use of a subjective method for drawing ROI's.

Method

In four normal subjects and four patients with coronary artery disease, ROI's were drawn on the exercise images and count density was recorded for each ROI. In each view, the region with highest count density was designated arbitrarily as having a count density of 1.0; count densities in the other four ROI's were expressed as a proportion.

Two months later, the exercise images of the same nrmal subjects and patients were re-analysed by the same operator, who drew fresh ROI's on each view. Relative

count densities were determined as in the initial analysis.

Results

An example of results is shown below for a patient with coronary artery disease.

Relative count density

ROI	Anterior view		LAO view		Lateral view	
	Initial	Repeat	Initial	Repeat	Initial	Repeat
1	0.66	0.64	0.86	0.88	0.93	0.91
2	0.80	0.81	0.93	0.90	1.0	1.0
3	0.83	0.82	0.89	0.89	0.88	0.89
4	1.0	1.0	1.0	1.0	0.78	0.77
5	0.76	0.77	0.94	0.92	0.80	0.79

The maximal change in relative count density was less than $\pm$5% for all ROI's, and less than $\pm$2% for 90% of ROI's (patients and normal subjects). Paired t-testing showed that there was no significant difference between the relative count densities recorded on the initial and repeated analysis.

Discussion

The results of this study suggest that there is little intra-observer variability in choosing ROI's. This is very likely due to the guidelines used for subdividing the myocardial image (five ROI's for each view; count density in each ROI to be as homogeneous as the image allowed).

2.9 Background studies

Because of the relatively low myocardial-to-background ratio with Tl-201 imaging, a background correction has been advocated in quantitative studies but there is no generally accepted method (section 1.7). In this study a method of background correction was derived from phantom and cadaver heart studies.

Method

A torso and heart phantom were constructed from a perspex resin. The heart phantom was suspended within the torso, which was filled with a solution of Tl-201 (30 MBq) in saline. Tl-201 imaging was carried out in the standard views. Imaging was repeated with a fresh cadaver heart suspended in the anatomical position within the torso.

In each view the myocardial image appeared as a cold area (negative image) compared to background. The image was divided into five ROI's and a sixth periventricular region was drawn over the background; counts per unit area were obtained for all six regions in each view.

One series of observations were made for the cadaver and phantom hearts. Any variation in these measurements would have been primarily due to counting statistics; therefore enough counts were taken to ensure that such variation was small.

Results

The results for the phantom and cadaver heart are shown in table 2 (3). Counts per unit area in each ROI were measured but as the difference between myocardial ROI's could be accounted for by Poisson statistics alone, the counts from all regions were grouped to give a myocardial count density for each view.

a) Phantom heart

Counts per unit area (mean ± SEM)

	Anterior	LAO	Lateral
Myocardium	90.6±4.9	99.5±3.1	105.6±2.2
Background	118.4	118.8	118.9
M/B Ratio	0.77	0.84	0.89

b) Cadaver heart

Counts per unit area (mean ± SEM)

	Anterior	LAO	Lateral
Myocardium	109.0±2.6	110.0±2.9	112.4±1.7
Background	133.3	143.8	150.6
M/B Ratio	0.82	0.77	0.75

Table 2(3) Background studies with phantom and cadaver heart

The reduced counts from the myocardial ROI's compared to those from background represented the

net effect of scatter and attenuation by the heart. The difference beween the results with the phantom and cadaver heart is easily explicable by their obviously different structures; the heart phantom was a hollow perspex shell moulded into an external cardiac shape but no attempt had been made to obtain a representation of muscle mass and separate cardiac chambers. The heart phantom was therefore useful as a model for investigating background correction but the results with the cadaver heart were felt to be more representative of the in vivo situation.

Therefore, if during the measurement of myocardial count density, background activity was also recorded a correction factor could be applied for scatter and attenuation affects (0.82, 0.77 and 0.75 of the background count density for anterior, LAO and lateral views respectively). These results are in agreement with those of Narahara et al[133], who suggested that simple thresholding (not exceeding 20-30% of maximal myocardial counts) was appropriate for background correction.

2.10 Effect of photon absorption by chest wall and breast tissue

Low energy photons are heavily absorbed even in relatively low density media such as breast tissue and water which have a similar total attenuation coefficient ($0.19cm^{-1}$ and $0.18cm^{-1}$ respectively) for 80 keV photons (80 keV being the photopeak of the X-rays used for Tl-201 imaging). The importance of photon absorption producing false positive Tl-201 scans was suspected clinically[67] and the following studies were undertaken to assess the effect.

The penetration of Tl-201 photons through 5,10 and 15cm of water predicted by the total attenuation coefficient is 40, 16 and 6% respectively if "narrow beam" conditions apply. To show that these figures were applicable to our gamma camera system, a small Tl-201 source was imaged through air and then through 10cm of water. The penetration through water was found to be 19.7% of that through air; the difference from the predicted value (16%) could be attributed to scattering effects and the emission by Tl-201 of X-rays with energies between 65 and 87 keV, as well as higher energy gamma rays of low abundance.

Serial scanning and measurement of count density demands that the problem of photon absorption, if unavoidable, should be kept constant. To a certain extent this could be done by keeping constant the camera-patient orientation for serial scans; the plumb line system as described in section 2.7 serves

this purpose. However, it could be predicted that in myocardial imaging in women, breast tissue of 5-10cm thickness could cause the attenuation of myocardial counts to background levels (false positive perfusion defects). In quantitative studies such attenuation effects would introduce a random error which was avoided by confining subsequent studies to male patients.

Chapter 3 MATERIALS AND METHODS

3.1 Patients and normal subjects

60 patients with coronary artery disease (mean age 54, age range 38-67 years) underwent exercise, redistribution and rest Tl-201 imaging. All were male, females having been excluded to eliminate the possible error from photon absorption by breast tissue. Patients were selected for study from those entering hospital for investigation (including cardiac catheterisation and coronary angiography) of angina refractory to medical treatment. Patients with associated valvular heart disease were excluded. All gave a typical history of chronic, stable, effort-induced angina; 18 had a past history of one or more myocardial infarctions; 29 of the 42 who had had an exercise test showed diagnostic changes of myocardial ischaemia (> 1mm planar ST segment depression during exercise-induced chest pain). All were on anti-anginal treatment which consisted of beta-adrenoreceptor blockade and sublingual nitrates (45 patients), beta-adrenoreceptor blockade, nitrates and nifedipine (10), or nifedipine and nitrates (5). Treatment had been constant for at least four weeks and was not altered for the purposes of the study. Coronary angiography showed disease involving one (14 patients), two (26) or three vessels (20). Tl-201 scans were performed between two and three weeks after cardiac catheterisation; patients were excluded from the study if any symptomatic or electrocardiographic changes had occurred since

catheterisation.

15 non-smoking subjects (mean age 51, age range 35-64 years) were selected from patients admitted for elective non-cardiac surgery (herniorrhaphy in 7, varicose vein procedures in 5, cholecystectomy in 2 and vagotomy and pyloroplasty in one). Evidence of cardiovascular disease was sought from the history, physical examination and resting electrocardiogram; if none was present, an exercise test was performed and the patient was excluded if there were any changes (diagnostic or equivocal) of myocardial ischaemia. Three patients were on regular medication (antacids) but none were taking cardio-active drugs.

3.2 Exercise and imaging protocols

Patients and control subjects performed upright exercise on a bicycle ergometer with a mechanical braking system which allowed the workload to be adjusted in 25 watt steps. All performed one and sometimes two preliminary tests so that exercise tolerance and the time to Tl-201 injection could be assessed. The starting workload and increments were adjusted so that exercise duration was 3-12 min. All exercise studies took place in the afternoon; no medication or food was taken after 08.00 on the day of the study. An indwelling, intravenous cannula was inserted in the arm about 1 hr before exercise and kept patent with heparinised saline.

A single lead electrocardiogram was monitored continuously during and for 3 min after exercise (vide infra); electrodes were then removed prior to scanning. Patients pedalled at a constant rate (50 rpm) against the pre-determined starting workload which was increased by 25 watts every 3 min until the time for Tl-201 injection was reached. The end point of exercise was either moderately severe angina (48 patients with coronary disease) or dyspnoea and/or exhaustion (12 patients with coronary disease and all 15 normal controls). Heart rate (from the R-R interval on the electrocardiogram) and systolic blood pressure (by sphygmomanometer) were noted at that time and Tl-201 was injected (45-60MBq) via the indwelling cannula followed by a flushing injection

of 5-10 ml normal saline. Patients and normal subjects were encouraged to keep exercising for a further minute. At the end of exercise, which took place in the gamma camera room, the study subject was transferred to the scanning couch (supine position). The gamma camera was positioned for the anterior view, using the plumb-line system as described previously (section 2.7). Myocardial imaging, beginning 8 min after injection of Tl-201, was carried out in anterior, LAO and lateral views recorded for 300 sec each.

22-24 hr after the exercise study, redistribution scans were performed in anterior, LAO and lateral views, 300 sec per frame. The plumb lines were used to ensure constant patient-camera orientation. A further 45-60 MBq of Tl-201 was then injected via an indwelling cannula and followed by a saline flush. 20 min later (see section 2.4) repeat scanning (rest scans) was performed in three views, 300 sec per frame, using the plumb lines for patient positioning.

All imaging was performed with an Elscint gamma camera with a 30 cm field of view and 37 photomultiplier tubes of 6cm diameter and a low energy, medium resolution collimator (CCL4). A 40 keV energy window was centred on the 80 keV X-ray peak and all images were stored in a 128 X 128 matrix on magnetic disc. Tl-201 was supplied by Phillips-Duphar cyclotron and isotope laboratories, Petten, Holland and used on

the supplier's reference day for the radionuclide.

3.3 Electrocardiographic monitoring

A single lead electrocardiogram (modified V_5) was observed throughout exercise and for 3 min post-exercise and recorded for 8-10 beats at every minute. ST segment shift at the time of Tl-201 injection was measured (to the nearest 0.5 mm) 80 msec past the J point and the slope of the ST segment noted (horizontal, downsloping or upsloping). It was not the intention of the study to compare exercise electrocardiography and Tl-201 scans as indicators of myocardial ischaemia; however, the electrocardiogram could be used as one parameter to determine whether comparable ischaemia was produced by exercise in those patients who had two Tl-201 studies (see section 3.9).

3.4 Quantitative analysis of Tl-201 scans

In each projection, the post-exercise myocardial image was magnified x4 and divided into five ROI's determined by the operator; pilot studies which decided the number and position of ROI's are described in section 2.5. ROI's were drawn so that count density in each region was as homogeneous as the myocardial image would allow. As well as five ROI's encompassing the myocardial image a sixth region was drawn outside the myocardial image for assessment of background. Counts and areas were noted for all six regions in each projection; the ROI's were then stored on magnetic disc.

The redistribution scans were then recalled, together with the six ROI's drawn on the exercise scan of the same projection. The redistribution myocardial image was magnified X4 and the ROI's were moved in a horizontal and/or vertical direction until the best visual fit of the ROI's on the myocardial image was obtained. Magnification allowed more accurate positioning of the ROI's. Counts for each ROI were noted (the areas were obviously the same as the for the exercise scans). The process of obtaining the best fit of the ROI's on the myocardial image was performed three times for each view and an average count obtained. A similar analysis was performed on the rest scans, obtaining the new average counts in each of five myocardial and one background ROI.

The data from exercise, redistribution and rest scans from a single projection could then be represented

thus :

Exercise scan	Redistribution scan	Rest scan	Area
CE (1)	CL (1)	CR (1)	A (1)
CE (2)	CL (2)	CR (2)	A (2)
CE (3)	CL (3)	CR (3)	A (3)
CE (4)	CL (4)	CR (4)	A (4)
CE (5)	CL (5)	CR (5)	A (5)
BE	BL	BR	
ABE	ABL	ABR	
Z	Z	Z	

where Cx (1 - 5) represents counts in five myocardial ROI's on exercise (CE), redistribution (CL) and rest (CR) scans; BE, BL and BR represent background counts and ABE, ABL and ABR background areas for the exercise, redistribution and rest scans respectively; Z the myocardial-to-background ratio for the particular projection, and A (1 - 5) the areas of the five myocardial ROI's. As the same ROI's were used for each view on exercise, redistribution and rest scans, A (1 - 5) was the same for any one view. Z was determined from preliminary studies (section 2.8).

The first step in the analysis is to correct the rest counts for the contribution of redistribution counts and the rest and exercise counts for background activity. Thus corrected rest counts for any region, R (n), are given by :

$$R(n) = CR(n) - BR \times Z \times \frac{A(n)}{ABR} - \left[CL(n) - BL \times Z \times \frac{A(n)}{ABL}\right]$$

where $n = 1 - 5$,

$BR \times Z \times \frac{A(n)}{ABR}$ = background correction,

and $CL(n) - BL \times Z \times \frac{A(n)}{ABL}$ = redistribution count - background correction.

Assuming a Poisson error for each count, the standard deviation, SR(n), for the corrected rest count is given by :

$$SR(n) = \left[CR(n) + BR\left(Z \times \frac{A(n)}{ABR}\right)^2 + CL(n) + BL\left(Z \times \frac{A(n)}{ABL}\right)^2\right]^{1/2}$$

By a similar process, corrected exercise counts E(n) and the standard deviation SE(n) are given by :

$$E(n) = CE(n) - BE \times Z \times \frac{A(n)}{ABE}$$

and $$SE(n) = \left[CE(n) + BE\left(Z \times \frac{A(n)}{ABE}\right)^2\right]^{1/2}$$

We now have two sets of counts with their standard deviations :

Corrected rest counts;	SD	Corrected exercise counts;	SD
R(1)	SR(1)	E(1)	SE(1)
R(2)	SR(2)	E(2)	SE(2)
R(3)	SR(3)	E(3)	SE(3)
R(4)	SR(4)	E(4)	SE(4)
R(5)	SR(5)	E(5)	SE(5)

By summing the rest and exercise counts and taking the ratio, a factor is obtained which represents the difference in total myocardial uptake as a result of the difference in dosage of Tl-201 and total myocardial perfusion at rest and on exercise.

$$D = \frac{\sum_{n=1}^{n=5} E(n)}{\sum_{n=1}^{n=5} R(n)} = \frac{\text{Sum E}}{\text{Sum R}}$$

The standard deviation of D, DE, is given by :

$$DE = D \left[\left\{ \frac{E \text{ Sum } E}{\text{Sum E}} \right\}^2 + \left\{ \frac{E \text{ Sum } R}{\text{Sum R}} \right\}^2 \right]^{1/2}$$

where E sum E $= \left[\sum_{n=1}^{n=5} SE(n)^2 \right]^{1/2}$

and E sum R $= \left[\sum_{n=1}^{n=5} SR(n)^2 \right]^{1/2}$

If there is no change in Tl-201 distribution within the myocardium from exercise to rest scans,

$$\frac{E(1)}{R(1)} = \frac{E(2)}{R(2)} = \frac{E(3)}{R(3)} = \frac{E(4)}{R(4)} = \frac{E(5)}{R(5)} = D$$

Therefore $\frac{E(n)}{R(n) \times D}$ should equal unity, apart from Poisson statistical errors. Taking logarithms,

$F(n) = \log_e \frac{E(n)}{R(n) \times D}$ should be equal to zero.

Values less than zero indicate a count (and therefore perfusion) deficit on the exercise scan. F(n) is an index of the change of perfusion from exercise to rest in each of the five ROI's.

When a term w is converted to a logarithmic scale,

$$\text{var log } w \simeq \frac{d}{dw} (\log w)^2 . \text{ var } w \quad \text{(reference 149)}$$

The standard deviation (SD) of log w,

$$\text{SD log } w = \frac{d}{dw} \log w . \text{ SD}(w)$$

Now $\frac{d}{dw} \log w = \frac{1}{w}$

$$\therefore \text{SD log } w = \frac{\text{SD } (w)}{w}$$

If $w = \frac{a}{bxc}$

$$\log w = \log a - \log b - \log c$$

$$\therefore \text{SD log } w = [\text{SD } (\log a)^2 + \text{SD } (\log b)^2 + \text{SD } (\log c)^2]^{1/2}$$

(equation 1)

In our case, a = E (n), b = R (n), c = D and w = F (n); the standard deviation of E (n) = SE (n), the standard deviation of R (n) = SR (n) and the standard deviation of D = DE.

With appropriate substitution in equation 1, the standard deviation of F (n), SF (n), is given by :

$$SF(n) = \left[\left\{ \frac{SE(n)}{E(n)} \right\}^2 + \left\{ \frac{SR(n)}{R(n)} \right\}^2 + \left\{ \frac{DE}{D} \right\}^2 \right]^{1/2}$$

The ratio $\frac{F(n)}{SF(n)}$ is a measure of the deviation of F(n)

from zero in terms of numbers of standard deviations. To generate an index of overall change in count distribution from exercise to rest we may take the root mean square of $\frac{F(n)}{SF(n)}$; we call this index the perfusion variation index (PVI).

$$PVI = \left[\frac{1}{5} \sum_{n=1}^{n=5} \left\{\frac{F(n)}{SF(n)}\right\}^2\right]^{1/2}$$

This index takes into account Poisson variations in the original counts. We would expect the PVI to be low in cases of normal myocardial perfusion on exercise and at rest, and high when exercise-induced myocardial ischaemia results in a change in myocardial perfusion from exercise to rest.

For each patient, in each of three views, the PVI was derived as described above from the raw counts recorded in operator-generated myocardial and background ROI's.

3.5 PVI and its reproducibility

To assess the reproducibility of PVI, 20 patients with coronary disease were randomly selected for repeat Tl-201 studies and recalculation of PVI.

The repeat study was performed four weeks after the first; patients were excluded if there had been any symptomatic, clinical or electrocardiographic changes in the interim. The exercise protocol of the repeat study was planned to be identical to the first in workload and duration to induce an equivalent degree of myocardial ischaemia. If the end-point of exercise was being approached and the patient felt that an equivalent degree of angina had not been reached, the exercise duration was increased. Heart rate, blood pressure and electrocardiographic recording was as for the first study. Myocardial scanning was begun at exactly the same time after the Tl-201 injection as for the initial study. The protocol for the redistribution and rest scans in the first study was repeated.

Analysis of the repeat Tl-201 scans was performed by drawing new ROI's, although regions were similar to the first study. Counts in each ROI (five myocardial and one background region per view) were obtained for the exercise, redistribution and rest scans and the PVI was derived as previously described.

3.6 Statistical analysis

Results were analysed using Student's t test for paired and unpaired data, the Mann-Whitney test for non-parametric analysis and analysis of variance for the comparison of several variables.

Chapter 4 RESULTS

4.1 Exercise data (table 4 (1))

All patients and normal subjects began exercise at a workload of 50 watts. The duration of exercise in patients with coronary disease (7.3 ± 3.2 min, mean ± SEM) was less than for normal subjects (9.6 ± 2.5 min); the latter as expected developed significantly less ST segment depression ($p<.01$) on exercise. The maximal exercise heart rate and systolic blood pressure (and therefore the double product, HR x BP) was greater in normal subjects compared to patients with coronary disease, reflecting the effect of beta-adrenoreceptor blockade in the latter.

Paired t-testing showed no difference between heart rate, systolic blood pressure, double product, ST segment depression and exercise duration recorded in the two exercise tests for those patients with coronary disease who had two Tl-201 studies to assess the reproducibility of PVI. There was no significant difference in terms of age and extent of coronary disease between those patients who were chosen for re-study and those who were not.

	HR	BP	DP	Ex duration	ST↓
n=60	143±14	150±17	215±40	7.3±3.2	1.6±0.7
n=15	162±11	182±17	295±41	9.6±2.5	0.3±0.3
n=20(A)	145±10	152±15	220±44	7.2±3.2	1.8±0.8
n=20(B)	150±13	147±14	221±37	7.0±3.2	1.7±0.6

Table 4(1). Exercise data

n=60 : patients with coronary disease

n=15 : normal controls

n=20 (A) : data for the first study in 20 patients who had two studies

n=20 (B) : data for the second study in 20 patients who had two studies

HR : heart rate at maximal exercise (beats/min, mean ± SEM)

BP : systolic blood pressure (mm Hg) at maximal exercise (mean ± SEM)

DP : double product, HR x BP (beats/min x mm Hg x 10^{-2}, mean ± SEM)

Ex duration : duration of exercise (min) to Tl-201 injection (mean ± SEM)

ST↓ : ST segment depression (mm, mean ± SEM)

4.2 Exercise, residue and rest counts

Considering patients and controls together, the maximum count density on the exercise scans was 21.4 ± 7.7 (mean ± SEM) with a wide range (10.7 - 42.2) which reflected the dose of Tl-201 administered.

Lowest count densities were on redistribution scans, where the mean of maximal counts per unit area was 6.8 ± 1.7, range 4.3 - 9.1. As the rest counts were the sum of redistribution counts and further counts from Tl-201 injection at rest, rest scans showed the highest count density (32.7 ± 8.4, range 17.5 - 47.9 counts per unit area).

Maximal myocardial-to-background ratios (maximal myocardial count density : background count density) for the exercise, redistribution and rest scans were 2.8, 1.5 and 2.3 respectively.

4.3 Perfusion variation index (PVI)

Raw counts from exercise, redistribution and rest scans from which the PVI was derived were tabulated as shown in the example of results (tables 4 (2), 4 (3) and 4 (4)). Myocardial : background ratio and magnification factor were also noted for each view.

F(n), SF(n) and thence PVI were calculated according to the formulae in section 3.5 and tabulated. Each patient had three values for PVI, one for each projection, and 20 patients who had repeat studies each had a further three values.

Tables 4 (5) - 4 (7) show values for PVI in 40 patients with coronary disease who had a single study, in 15 normal subjects and in 20 patients who underwent two studies to test for the reproducibility of PVI; for the sake of clarity, the decimal point is omitted so that actual PVI is 10^{-2} that shown in the tables.

Patient WM Anterior view

ROI	Rest counts	Redistribution counts	Exercise counts	Area
1	118506	29232	63100	646
2	71275	18354	41648	368
3	92926	24504	59619	489
4	119630	30805	82188	559
5	124917	33817	80680	718
B.G.	38636	12791	20017	658

Myocardial : Background ratio = 0.82

Magnification x 4

ROI	F(n)	SF(n)
1	-0.2218	0.0179
2	-0.08032	0.02098
3	0.04954	0.01855
4	0.1175	0.01572
5	0.07487	0.01730

PVI = 7.07

Table 4(2) An example of results (anterior view)

B.G. = background. Other abbreviations as in text.

Patient WM. LAO view

ROI	Rest counts	Redistribution counts	Exercise counts	Area
1	133663	35283	82817	721
2	72847	18332	46287	369
3	139781	34898	79191	665
4	159459	41369	97949	729
5	113501	30360	74509	592
B.G.	68055	17930	34120	658

Myocardial : Background ratio = 0.77

Magnification x 4

ROI	F(n)	SF(n)
1	0.03927	0.02154
2	0.03598	0.02515
3	0.1468	0.0195
4	-0.01289	0.01778
5	-0.1259	0.02193

$$\underline{PVI} = \underline{4.37}$$

Table 4(3) An example of results (LAO view)

B.G. = background. Other abbreviations as in text.

Patient WM. Lateral view

ROI	Rest counts	Redistribution counts	Exercise counts	Area
1	159673	41021	99836	780
2	90523	23264	62192	452
3	106851	26690	63330	523
4	107601	26770	57180	534
5	93783	23819	53850	491
B.G.	80122	21554	40176	658

Myocardial : Background ratio = 0.75

Magnification x 4

ROI	F(n)	SF(n)
1	0.06303	0.02035
2	0.2126	0.02469
3	-0.03781	0.02372
4	-0.2208	0.02522
5	-0.06917	0.02704

$$\underline{PVI} = \underline{5.82}$$

Table 4(4) An example of results (lateral view)

B.G. = background. Other abbrevations as in text.

Patient Number	Anterior view	LAO view	Lateral view
1	419	242	275
2	71	194	164
3	1438	218	309
4	448	306	365
5	182	270	160
6	243	413	299
7	268	130	172
8	291	144	111
9	361	198	92
10	136	42	135
11	294	223	141
12	286	340	286
13	418	154	164
14	79	282	397
15	350	153	501
16	195	227	354
17	255	372	123
18	207	122	394
19	426	114	219
20	179	112	368
21	239	291	138
22	271	280	332
23	152	104	242
24	358	266	426
25	377	459	438
26	480	236	394
27	74	64	292
28	427	741	430
29	64	137	169
30	181	269	157
31	74	103	130
32	292	134	121
33	163	104	129
34	274	49	292
35	207	121	142
36	375	186	274
37	451	293	365
38	289	151	120
39	217	230	106
40	163	102	101

Table 4(5) : PVI (decimal point omitted) for patients with coronary disease (40 patients having a single study)

Patient Number	Anterior view	LAO view	Lateral view
a)			
41	109	248	109
42	376	193	261
43	441	666	441
44	267	396	424
45	212	227	98
46	442	499	144
47	183	284	195
48	709	528	148
49	288	71	74
50	173	90	86
51	538	405	251
52	76	56	231
53	222	194	153
54	335	686	445
55	134	284	339
56	214	232	104
57	742	531	139
58	326	149	474
59	491	327	217
60	165	104	96
b)			
41	219	149	158
42	388	227	139
43	707	437	582
44	166	311	449
45	61	151	167
46	635	190	210
47	212	119	301
48	214	196	315
49	170	155	127
50	251	21	202
51	281	120	44
52	65	184	378
53	69	144	111
54	486	239	376
55	205	196	192
56	172	404	323
57	324	141	426
58	291	236	194
59	340	624	409
60	291	84	174

Table 4(6). PVI (decimal point omitted) in (a) the first and (b) the second study in 20 patients with coronary disease who had two Tl-201 studies.

Patient Number	Anterior view	LAO view	Lateral view
61	101	84	121
62	124	86	79
63	142	104	83
64	94	120	114
65	114	74	96
66	130	87	94
67	80	104	117
68	140	84	114
69	123	101	94
70	110	74	84
71	139	97	105
72	137	86	84
73	192	132	131
74	174	88	101
75	126	79	66

Table 4(7) PVI (decimal point omitted) in 15 control subjects.

Table 4(8) lists the mean and standard deviation of the PVI for each view in patients with coronary disease and in normal subjects. For each projection, the range in normals is contained within, and is very much lower than, that in patients with coronary disease. Therefore no transformation is possible to make both groups of comparable standard deviation. A transformation was sought for within-groups analyses, but between-groups analyses had to be non-parametric (Mann-Whitney test).

Transformation of the PVI data by the factor $\log(x + 1)$, where x = the numerical value of PVI, produced a normal distribution to a good approximation. The values for the PVI (mean and standard deviation) for the data thus transformed are given in Table 4(9), and show that acceptably similar standard deviations are obtained for the patients with coronary disease (CAD(a) and CAD(b)). The standard deviations for the controls are also acceptably similar but unavoidably much less than those for patients with coronary disease.

In patients with coronary disease having duplicate studies, the values for the PVI in the repeat and original studies were compared by paired t-tests for each view. In all projections, the value for PVI was similar in the two studies ($p>0.05$).

A comparison of views by paired t-test in patients with coronary disease (n=60) showed that

the PVI was higher for the anterior view compared to the oblique ($p<0.01$) and to the lateral ($p<0.03$) whereas there was no significant difference between the oblique compared to the lateral view. Similar statistical analysis of the PVI in normal subjects gave similar results (anterior > oblique, $p<0.01$; anterior > lateral, $p<0.01$ and no significant difference between oblique and lateral views).

The PVI in equivalent views in patients with coronary disease (n=60) and normal subjects (n=15) were compared by the Mann-Whitney test which showed significantly higher values in the former in all three projections (anterior, $p<0.001$; oblique, $p<0.001$; lateral, $p<0.001$). A similar analysis comparing the repeat and original values for PVI in patients having duplicate studies showed no statistical difference between the two studies in any of the three views.

Finally, a two-way analysis of variance was performed on the PVI (untransformed and log transformed data) to compare the three views in patients with coronary disease and also in normal subjects. This analysis confirmed the results of paired t-testing and showed that in patients and controls the anterior view was significantly different from the oblique and lateral views and that the PVI in the oblique and lateral views was statistically similar.

a) Anterior view

		PVI	
Group		Mean	S.D.
CAD(a)	n=60	3.0195	2.0898
Controls	n=15	1.2840	0.2867
CAD(b)	n=20	2.7735	1.7210

(b) LAO view

Group	Mean	S.D.
CAD(a)	2.4577	1.5838
Controls	0.9333	0.1650
CAD(b)	2.1640	1.3775

(c) Lateral view

Group	Mean	S.D.
CAD(a)	2.3760	1.2369
Controls	0.9887	0.1808
CAD(b)	2.6385	1.3906

Table 4(8). PVI (mean and standard deviation) for patients with coronary disease (CAD(a)), control subjects and in the second study of patients with coronary disease having duplicate studies (CAD(b)).

PVI

Group	n	View	Mean	S.D.
CAD(a)	60	anterior	0.56206	0.186
CAD(a)	60	LAO	0.49927	0.184
CAD(a)	60	lateral	0.50017	0.157
CAD(b)	20	anterior	0.53665	0.192
CAD(b)	20	LAO	0.46688	0.171
CAD(b)	20	lateral	0.53018	0.170
Control	15	anterior	0.35557	0.0537
Control	15	LAO	0.28490	0.0358
Control	15	Lateral	0.29688	0.0397

Table 4(9). Data for PVI (mean and standard deviation) after transformation by the factor log (x + 1) for groups as in table 4(8).

4.4 Correlation of the PVI with the presence of coronary artery disease

In each view, the normal range for PVI was defined from the mean ± 2SD for the group of 15 normal subjects. Thus the normal range was 0.71 - 1.86 (anterior view), 0.60 - 1.26 (LAO) and 0.63 - 1.35 (lateral). In control subjects, if the PVI in any view fell above these ranges a false positive result was assumed. In patients with coronary disease, a false negative result was assumed if the PVI remained in the normal range for all views. With these criteria, one of the normal subjects had a false positive result. 5 of 60 patients with coronary disease had a false negative result, although one of these 5 had a repeat study in which the PVI was abnormal.

Sensitivity and specificity for the PVI in the detection of coronary artery disease was therefore 92% and 93% respectively.

Chapter 5 DISCUSSION

Quantitative assessment of myocardial ischaemia by determining the PVI produced figures for sensitivity (92%) and specificity (93%) of Tl-201 for the detection of coronary disease which compare favourably with reports in the literature. However, this does not imply that the quantitative methods in this study are better than those previously reported; as has been mentioned previously, figures for sensitivity and specificity can be improved merely by careful patient selection.

This is an expression of Bayes' theorem of conditional probability, first proposed as a possible basis for medical diagnosis in 1959 by Ledley and Lusted[150]. Bayes' theorem highlights the fact that while sensitivity and specificity define the quality of a test, the result cannot be interpreted satisfactorily without additional knowledge of the prevalence of disease in a given population. The probability that a patient with a given syndrome has a particular disease is directly proportional to the probability of occurrence of his syndrome in that disease multiplied by the a priori prevalence of that disease and inversely proportional to the probability of occurrence of his syndrome in all diseases times the prevalence of those diseases.

In this study, normal subjects had no historical or clinical evidence of myocardial disease and were chosen so that they would be expected to have a less than 1% chance of having coronary disease. Conversely, patients

with coronary disease all had severe, typical symptoms which warranted their consideration for coronary artery bypass grafting for the relief of their angina. These selection criteria for patients and normal subjects would be expected to produce good figures for the predictive capacity of a measure of myocardial ischaemia. Nevertheless it is encouraging that an empirical method derived to quantify regional myocardial ischaemia was successful in differentiating between normal and abnormal myocardial perfusion.

In patients with coronary disease, the PVI showed a very wide range (0.21 - 14.38), offering the possibility that the index might differentiate between varying degrees of ischaemia. However, whether the value for PVI correlated with the severity of myocardial ischaemia cannot be answered directly by this study as there was no reliable independent method of assessing ischaemia. Electrocardiographic changes on exercise are qualitative rather than quantitative particularly when only a single lead is monitored as in this study. Exercise time to the onset of angina can be an indirect assessment of the severity of ischaemia but other factors may influence exercise duration. In patients with coronary disease in this study, there was no correlation between the exercise time and the severity of coronary disease defined angiographically into one, two and three vessel disease. A recent study has demonstrated the lack of correlation between assessments of coronary stenosis on coronary angiograms and more

objectively determined indices of ischaemia[151].

In experimental situations, regional Tl-201 myocardial uptake has been shown to correlate with regional myocardial perfusion assessed by microspheres[49]. In the clinical context there is no adequate assessment of myocardial perfusion with which Tl-201 myocardial uptake can be compared quantitatively. Methods such as coronary infusion of Krypton-81m, measurements of coronary sinus flow or myocardial lactate production all have significant drawbacks.

A comparison of the mean PVI in initial and repeat thallium studies in 20 patients with coronary disease showed that there was no statistical difference between the two values. This suggests superficially that the PVI is a reproducible measure of myocardial ischaemia which should therefore lend itself to the monitoring of changes in perfusion induced by such interventions as coronary artery bypass surgery or drug treatment of myocardial ischaemia.

A closer examination of the results casts doubt on the value of the PVI for quantifying myocardial ischaemia. In 60% of readings, the PVI varied by more than 1.00 from the first to the repeat study; in 25% of cases, it varied by more than 2.00; in only 16.7% of results did the PVI alter by less than 0.50. This variation in PVI occurred despite the fact that there was no significant difference between the two studies in exercise duration, maximum heart rate, systolic blood pressure, double product and ST segment depression.

These parameters are, however, an indirect assessment of myocardial ischaemia and it could be postulated that an equivalent degree of ischaemia was not produced in the two exercise thallium studies and that the variation in PVI was real rather than a reflection of the lack of reproducibility of the measurement. Studies of the events which precede and accompany myocardial ischaemia have emphasised the difficulty in deciding by what method ischaemia should be assessed. Monitoring of coronary sinus oxygen saturation has shown that there is a decrease in regional coronary blood flow in the affected segment of myocardium before the onset of anginal pain[2]. There is evidence that in anginal patients the function of an affected myocardial segment may remain disturbed for much longer than the duration of pain or the electrocardiographic signs of ischaemia[152,153]; both contractile function and key respiratory enzymes in mitochondria can be disturbed for hours after an ischaemic episode lasting only five to ten minutes.

Serial myocardial imaging with positron tomography has shown that episodes of myocardial ischaemia can take place without chest pain or electrocardiographic changes, that angina accompanies the more severe episodes of reduced perfusion and that patients who have frequent attacks of angina might have disturbed myocardial function for long periods because of the long time course of recovery from each episode of transient ischaemia[154].

The implication of these studies is that exercise-induced myocardial ischaemia could well be on a background of disturbed myocardial function at rest from previous ischaemic episodes. Furthermore, awareness of anginal pain does not correlate with myocardial ischaemia and is influenced by the nervous system's processing of signals from afferent pathways. It therefore follows that quite differing degrees of myocardial ischaemia could be induced by apparently similar stress such as exercise. A variable degree of myocardial ischaemia could also be present at rest when Tl-201 is injected; the absence of symptoms and electrocardiographic evidence cannot be taken to indicate the absence of ischaemia. Redistribution of thallium activity after injection at rest in patients with both stable and unstable angina probably indicates the presence of resting ischaemia, as shown by Berger et al[142].

Epicardial coronary arteries constrict and relax under the influence of autonomic innervation and a variety of humoral agents. When the arteries are already narrowed by atherosclerosis, changes in vasomotor tone may upset the critical balance between vessel diameter and flow, thus triggering ischaemia which could vary from moment to moment[155]. Patients with coronary disease in this study had moderately severe symptoms with critical coronary stenoses; as flow varies with the fourth power of the radius of the coronary artery, minor changes in vasomotor tone could lead to profound changes in the degree of myocardial

ischaemia, either at rest or on exercise.

Angina and myocardial ischaemia cannot therefore be considered to result solely from fixed, or slowly progressive atherosclerosis. Variability of symptoms may be related to transient phenomena in and around the atherosclerotic plaque e.g. plaque dissection, exposure of platelets to collagen, platelet aggregation and sometimes the formation of thrombi. An additional factor, as discussed in section 1.1, is the normal, and sometimes inappropriately high, coronary vasomotor tone which will influence the severity of a stenosis in an epicardial coronary artery.

However, patients with coronary disease who were included in this study were chosen for the presence of moderately severe yet stable, classical angina. Patients in whom angina was unpredictable or in whom angina occurred at rest (possible variant angina) were excluded. Patients underwent one and sometimes two preliminary exercise tests to assess the exercise time to angina; the exercise time to angina in the study itself correlated well with the pre-study exercise tests. Those patients who had two thallium studies showed remarkably consistent exercise data. Therefore it is reasonable to assume that exercise-induced ischaemia in the initial and repeat studies was comparable in those patients in whom the PVI was calculated in two separate studies.

When Tl-201 is injected at rest in experimental animals, initial myocardial uptake correlates well with

regional myocardial perfusion. However, factors which have been alluded to above could mean that, in patients, resting myocardial perfusion could vary with time, and therefore interfere with a study attempting to quantify the reproducibility of an assessment of myocardial ischaemia. Once again, though, the careful selection of patients for this study would have made it unlikely that there would be much variation in resting myocardial perfusion with time. Although repeated occult ischaemia cannot be excluded in these patients, the frequency of symptomatic episodes of myocardial ischaemia was such that they would be unlikely to show evidence of "stunned" myocardium[153]. As the patients knew they were being assessed for myocardial revascularisation, and had a prolonged history of stable angina, they had learned to avoid effort angina and reported at most one or two episodes of angina a day. Therefore those patients having repeat thallium studies would be expected to have comparable regional myocardial perfusion at rest in the two studies.

Can, therefore, the results for the reproducibility of the PVI be taken to indicate that the index is a reliable marker for the presence and severity of ischaemia ? The large variation of the PVI from the initial to the repeat study, even though there was no statistical difference demonstrable in the mean values for the two studies, suggests that the PVI is an adequate measure for the presence, but not for the severity, of myocardial ischaemia.

The question then arises as to whether any intrinsic errors in the method of calculation of the index of variation precluded reproducible results. The fundamental problem of noisy data obtained with a low energy isotope such as Tl-201 could not be avoided as Tl-201 is the best available isotope of its kind. Comparative studies have shown little benefit of seven pin-hole or single-photon emission computed tomography over planar imaging. Current evidence suggests that single photon emission computed tomography with Tl-201 may have advantages in spatial localisation of perfusion defects. Error propagation in reconstruction of images and difficulties in attenuation correction are such that reliable quantitative analysis of tomographic Tl-201 scans is not possible. Therefore the fact that this study did not include tomographic imaging is unlikely to have influenced its outcome.

The exact timing of scanning after Tl-201 injection at rest and exercise may well influence results. Redistribution of Tl-201 activity begins as early as 5 min after initial uptake on exercise; the faster the redistribution occurs the more likely it is that Tl-201 scans will underestimate the degree of exercise-induced ischaemia. Scanning in three views makes it inevitable that some post-exercise redistribution will take place before scanning is completed. In this study protocol, it was hoped to ensure a consistent degree of redistribution by scanning all patients at a fixed time after exercise and resting Tl-201 injections.

Contemporary methods of quantification of Tl-201 scans were reviewed critically (see introduction) to draw up a method likely to achieve the purpose of quantifying myocardial ischaemia. Many previous studies had involved analysis of exercise and redistribution scans, but for reasons mentioned in section 1.8, exercise and rest scans were more appropriate. For the same reason, a background correction was incorporated; simple thresholding was decided upon, as there was no convincing benefit from more complex methods. Background studies with a cadaver heart decided the degree of background subtraction, the results agreeing with those of Narahara et al[133].

Therefore the methods employed in this study appear not to be responsible for the failure to obtain a consistent value for an index in apparently equivalent degrees of myocardial ischaemia. The study suggests that data processing of Tl-201 scans cannot compensate for the basic problems of poor signal-to-noise ratio and statistical count deficiencies. Because of the fairly recent advances in the understanding of the pathogenetic mechanisms of myocardial ischaemia, there is a need for an objective, reproducible assessment of the severity of ischaemia. Such an assessment could provide valuable insight into the relative roles played by the differing mechanisms precipitating angina, myocardial ischaemia and myocardial infarction. The greater awareness of such mechanisms has led to a more physiological approach to the treatment of patients with myocardial ischaemia;

the advantages of such an approach appear inescapable, but documentation remains difficult because of the limitation of available methods of assessing ischaemia. Myocardial perfusion imaging would appear to be the key investigative method, but further advances in radiopharmaceuticals and imaging apparatus will be necessary before reliable, non-invasive quantification of myocardial ischaemia is possible.

Computer development has made possible single photon and positron emission tomography and will permit three-dimensional display of data by holography. Imaging consoles will facilitate the comparison of nuclear with other data from transmission computerised tomography, digital radiography, nuclear magnetic resonance and anatomical drawings. Special collimators such as the seven pinhole and slant hole collimators have been tested but ring or transaxial detectors are more likely to provide an adequate number of views for quantitative imaging.

Studies of regional myocardial blood flow are most accurate with invasive techniques such as radioactive microspheres and the arterial reference sampling method[156]. The procedure involves administration of radioactive microspheres into the left atrium or ventricle, withdrawal of arterial blood and measurement of regional microsphere tissue concentrations in myocardium by in vitro counting of tissue samples. The latter requirement precludes the use of this technique for clinical studies.

Recently, positron-emission computed tomography has provided a means of studying regional myocardial metabolism; in vivo regional myocardial indicator tissue concentrations can now be measured. Free fatty acids (FFA's) and glucose are the major myocardial energy substrates. In the presence of ischaemia, well-recognised metabolic changes occur[157]. In the well-oxygenated heart, glucose enters the cell via a facilitated membrane transport system and is phosphorylated to glucose-6-phosphate. It is then metabolised through anaerobic glycolysis to pyruvate or can be stored in the cell as glycogen. FFA's diffuse across the cell membrane, are activated through an ATP-requiring step to acetyl-CoA, and are transferred via the carnitine shuttle from the outer to the inner mitochondrial membranes or esterified to mainly triglycerides. In the beta-oxidation spiral, acetyl-CoA is cleaved off and represents the common entrance point for glucose and FFA into the oxidative pathway of the Krebs cycle, which results in the production of high-energy phosphates and the breakdown of acetyl-CoA to CO_2 and H_2O. The activity of both beta-oxidation and the citric acid cycle depends on the availability of oxygen and hence on blood flow.

If blood flow (and therefore oxygen delivery) is reduced, the activity of beta-oxidation and the citric acid cycle decreases or even stops. A shift from FFA to glucose metabolism occurs in response, and the production of high-energy phosphates is attempted

through either residual oxidative capacity or anaerobic glycolysis. Although extraction of FFA's by the myocardium may continue, their entrance into the beta-oxidation spiral is impaired. In the presence of alpha glycerophosphate as an intermediate of anaerobic glycolysis, FFA's are esterified or may even remain in unesterified form in the cytosol.

With the above considerations in mind, myocardial FFA metabolism has been studied using C-11 palmitic acid with positron computed tomography[158]. Schon et al[159,160] compared the myocardial extraction fraction and clearance of C-11 palmitate with myocardial oxygen consumption, blood flow and production of C-11 CO_2 as the end product of C-11 palmitate oxidation. They concluded that this tracer could be used for the in vivo study of myocardial FFA metabolism. FFA's are the preferred substrates for myocardial metabolism, but as regional perfusion decreases, there is a proportional decrease in FFA utilisation; images of regional FFA uptake closely resemble images of perfusion.

C-11 palmitic acid selectively traces the uptake and metabolic fate of FFA's, but the kinetics of this tracer in the myocardium may change considerably as substrate availability is altered. It has been shown[158] that with C-11 palmitate and serial imaging in dogs it is possible to examine not only changes in the rate of myocardial oxidative metabolism when substrate availability is constant, but also the ability of the heart to resort to alternative substrates when substrate availability is altered.

The assumed model that describes the kinetics of C-11 palmitate in the myocardium very probably oversimplifies the complexities of FFA fluxes through myocardial cells. For instance, C-11 palmitic acid is incorporated not only into triglycerides but also into other lipids and cell organelles[161]. This illustrates the need to restructure and refine models if conditions can be identified where the model breaks down.

Tracer kinetic models used in brain studies have been adapted for the external quantification of regional metabolic processes in the heart. An example is the use of fluorine-18 2-fluoro 2-deoxyglucose (FDG). In isolated perfused rabbit myocardium[162], in living dog[163] and human myocardium[164], estimates of exogenous glucose utilisation by this method agree with those by the Fick method and direct biochemical tissue assays. In the myocardium, however, the FDG method is not completely specific for the measurement of the myocardial glycolytic rate. It only provides a specific measurement of the utilisation rate of exogenous glucose[165].

N-13 ammonia has also been characterised as a marker of myocardial perfusion. When administered intravenously, it clears rapidly from the blood into the myocardium, where it becomes trapped in proportion to myocardial blood flow. Thus the properties of this tracer resemble those of radioactive microspheres, but N-13 ammonia has the advantage that it can be given intravenously. It is suitable, therefore, for the non-

invasive measurement of regional myocardial blood flow in man. Shah et al[166] suggested that with N-13 ammonia and positron emission tomography it might be possible to provide quantitative estimates (in ml/min/100g) of myocardial blood flow. However, the myocardial extraction fraction of N-13 ammonia is less than 100% and declines with higher flows. Therefore the N-13 ammonia technique consistently underestimates blood flow determined by the microsphere method. The low spatial resolution of some imaging devices is another potential source of error. Tamaki et al[167] constructed a whole-body, multislice positron computed tomography device which they used with N-13 ammonia to obtain further information on tracer kinetics. They validated the applicability of the device for serial dynamic assessment of N-13 ammonia distribution in human myocardium.

In comparison with other more complex methods for measuring myocardial blood flow (e.g. using rubidium-82[168] or oxygen-15 water technique[169]) the N-13 ammonia technique offers the advantage of simplicity. The shortcomings of current instrumentation represent a major limitation to the use of the technique in the human heart in which in vivo determination of ventricular wall thickness (necessary for regional tisssue tracer concentration measurement) in exactly the imaged cross section may be limited or impossible.

The use of positron computed tomography as an in vivo biochemical assay technique is likely to have a major impact on clinical cardiology. Animal and

clinical investigations with positron tomography can determine not only the site and extent of myocardial infarctions but also tissue viability. Further studies may be able to determine whether an ischaemic segment of myocardium is capable of recovery, or is likely to develop into a necrotic infarction. Such information will be of enormous therapeutic importance as pharmacological intervention is developing rapidly in the treatment of myocardial ischaemia and infarction.

Many diagnostic efforts have been devoted to the detection of coronary artery disease. The most definitive approach is with coronary angiography, and yet it is clear that anatomical description of coronary lesions does not predict their functional significance. Techniques such as Tl-201 perfusion imaging have helped to define the functional consequences of coronary stenoses. Positron tomography gives the possibility of detecting mild, and perhaps, pre-clinical coronary disease. What is needed are quantitative methods for measuring tissue perfusion. Until such methods are available, many questions will remain unanswered in the subject of regional metabolism in human myocardium. Clarification of these questions will help to improve the understanding of the pathophysiology of myocardial ischaemia, and lead to rational selection of the most appropriate clinical management. Tl-201 myocardial perfusion imaging has been found to have physical deficiencies which have limited its clinical usefulness. Tl-201 has, however, been invaluable as a pilot isotope

which has encouraged technological development aimed at providing reliable noninvasive assessment of myocardial ischaemia.

REFERENCES

1. Robinson BF. Relation of heart rate and systolic blood pressure to the onset of pain in angina pectoris. Circulation 1967; 35: 1073-1083.

2. Chierchia S, Brunelli C, Simonetti I, Lazzari M, Maseri A. Sequence of events in angina at rest: Primary reduction in coronary flow. Circulation 1980; 61: 759-768.

3. Maseri A, Severi S, De Nes M, L'Abbate A, Chierchia S, Marzilli M, Ballestra AM, Parodi O, Biagini A, Distante A. 'Variant' angina : One aspect of a continuous spectrum of vasospastic myocardial ischaemia. Am J Cardiol 1978; 42: 1019-1035.

4. Schwartz JN, Kong Y, Hackel DB, Bartel AG. Comparison of angiographic and postmortem findings in patients with coronary artery disease. Am J Cardiol 1975; 36: 174-178.

5. Franch RH, King SB, Douglas JS. Techniques of cardiac catheterisation including coronary angiography. In: The Heart. Hurst JW ed. (5th Ed). McGraw-Hill, New York 1982; 1843-1880.

6. Maseri A, Mimmo R, Chierchia S, Marchesi C, Pesola A, L'Abbate A. Coronary artery spasm as a cause of acute myocardial ischaemia in man. Chest 1975; 68: 625-633

7. Gregg DE, Patterson RE. Functional importance of the coronary collaterals. N Engl J Med 1980; 303: 1404-1406.

8. Kolibash AJ, Bush CA, Wepsic RA, Schroeder DP, Tetalman MR, Lewis RP. Coronary collateral vessels: Spectrum of physiologic capabilities with respect to providing rest and stress myocardial perfusion, maintenance of left ventricular function and protection against infarction.
Am J Cardiol 1982; 50: 230-238.

9. Ganz W, Tamura K, Marcus HS, Donoso R, Yoshida S, Swan HJC. Measurement of coronary sinus blood flow by continuous thermodilution in man.
Circulation 1971; 44: 181-195.

10. Ashburn WL, Braunwald E, Simon AL, Peterson KL, Gault JH. Myocardial perfusion imaging with radioactive-labeled particles injected directly into the coronary circulation of patients with coronary artery disease.
Circulation 1971; 44: 851-865.

11. Jansen C, Judkins MP, Grames GM, Gander M, Adams R. Myocardial perfusion color scintigraphy with MAA.
Radiology 1973; 109: 369-380.

12. Harper PV, Ryan JW, Al-Sadir J, Chua KG, Resnekov L, Neirinckx R, Loberg M. Intracoronary use of rubidium-82 (Abstract).
J Nucl Med 1982; 23: P69.

13. L´Abbate A, Maseri A. Xenon studies of myocardial blood flow : theoretical, technical and practical aspects. Semin Nucl Med 1980; 10: 2-15.

14. Selwyn AP, Steiner R, Kivisaari A, Fox KM, Forse G. Krypton-81m in the physiologic assessment of coronary arterial stenosis in man. Am J Cardiol 1979; 43 : 547-553.

15. Borer JS, Brensike JF, Redwood DR, Itscoitz SB, Passamani ER, Stone NJ, Richardson JM, Levy RI, Epstein SE. Limitations of the electrocardiographic response to exercise in predicting coronary artery disease. N Engl J Med 1975; 293 : 367-371.

16. Elamin MS, Mary DASG, Smith DR, Linden RJ. Prediction of severity of coronary artery disease using slope of submaximal ST segment/ heart rate relationship. Cardiovasc Res 1980; 14 : 681-691.

17. Quyyumi AA, Raphael MJ, Wright C, Bealing L, Fox KM. Inability of the ST segment/heart rate slope to predict accurately the severity of coronary artery disease. Br Heart J 1984; 51 : 395-398.

18. Sheffield LT. Exercise stress testing. In: Heart disease. A textbook of cardiovascular medicine. Braunwald E ed. (2nd ed.) W.B. Saunders Philadelphia: 1984; 258-278.

19. Varnauskas E. The ECG and exercise testing. In: Angina pectoris. Julian DG ed. (2nd Ed.) Edinburgh, Churchill Livingston 1985; 96-127.

20. Ellestad MH, Wan MKC. Predictive implications of stress testing. Follow up of 2700 subjects after maximum treadmill stress testing.
Circulation 1975; 51: 363-369.

21. Goldschlager N, Selzer A, Cohn K. Treadmill stress tests as indicators of presence and severity of coronary artery disease.
Ann Intern Med 1976; 85: 277-286.

22. Starling MR, Moody M, Crawford MH, Levi B, O'Rourke RA. Repeat treadmill exercise testing : variability of results in patients with angina pectoris. Am Heart J 1984; 107: 298-303.

23. Feigenbaum H. Echocardiography. 3rd Ed. Lea and Febiger, Philadelphia; 1980.

24. Griffith JM, Henry WL. A sector scanner for real-time two-dimensional echocardiography.
Circulation 1974; 49: 1147-1152.

25. Corya BC, Rasmussen S, Knoebel SB, Feigenbaum H. M-mode echocardiography in evaluating left ventricular function and surgical risk in patients with coronary artery disease.
Chest 1977; 72: 181-185.

26. Horowitz RS, Morganroth J. Immediate detection of early high-risk patients with acute myocardial infarction using two-dimensional echocardiographic evaluation of left ventricular regional wall motion abnormalities.
Am Heart J 1982; 103: 814-822.

27. Daly K, Monaghan M, Jackson G, Jewitt DE. Cross-sectional echocardiography in the early detection of acute myocardial ischaemia and infarction (Abstr). Br Heart J 1981; 45: 610.

28. Goldstein RE, Bennett ED, Leech GL. Effect of glyceryl trinitrate on echocardiographic left ventricular dimensions during exercise in the upright position.
Br Heart J 1979; 42: 245-254.

29. Feigenbaum H. Echocardiography : an overview.
J Am Coll Cardiol 1983; 1: 216-224.

30. Parisi AF, Moynihan PF, Folland ED, Feldman CL. Quantitative detection of regional left ventricular contraction abnormalities by two-dimensional echocardiography. II. Accuracy in coronary artery disease.
Circulation 1981; 63: 761-767.

31. Borer JS, Bacharach SL, Green MV, Kent KM, Epstein SE, Johnston GS. Real time radionuclide cineangiography in the non-invasive evaluation of global and regional left ventricular function at rest and during exercise in patients with coronary artery disease.
N Engl J Med 1977; 296 : 839-844.

32. Okada RD, Boucher CA, Strauss HW, Pohost GM. Exercise radionuclide imaging approaches to coronary artery disease. Am J Cardiol 1980; 46 : 1188-1204.

33. Borer JS, Bacharach SL, Green MV, Kent KM, Henry WL, Rosing DR, Seides SF, Johnston GS, Epstein SE. Exercise-induced left ventricular dysfunction in symptomatic and asymptomatic patients with aortic regurgitation: Assessment with radionuclide cineangiography. Am J Cardiol 1978; 42: 351-357.

34. Borer JS, Bacharach SL, Green MV, Kent KM, Rosing DR, Seides SF, McIntosh CL, Conkle D, Morrow AG, Epstein SE. Left ventricular function in aortic stenosis : Response to exercise and effects of operation (Abstr). Am J Cardiol 1978; 41: 382.

35. Borer JS, Bacharach SL, Green MV, Kent KM, Maron BJ, Rosing DR, Seides SF, Epstein SE. Obstructive vs. non-obstructive asymmetric septal hypertrophy : Differences in left ventricular function with exercise (Abstr). Am J Cardiol 1978; 41: 379.

36. Berger HJ, Davies RA, Batsford WP, Hoffer PB, Gottschalk A, Zaret BL. Beat-to-beat left ventricular performance assessed from the equilibrium cardiac blood pool using a computerised nuclear probe. Circulation 1981; 63: 133-142.

37. Iskandrian AS, Hakki AH. Thallium-201 myocardial scintigraphy. Am Heart J 1985; 109: 113-129.

38. Phelps ME, Hoffman EJ, Huang SC, Kuhl DE. ECAT : A new computerised tomographic imaging system for positron-emitting radiopharmaceuticals. J Nucl Med 1978; 19: 635-647.

39. Ratner AV, Goldman MR, Pohost GM. Visualisation of myocardial ischemic damage using nuclear magnetic resonance imaging (Abstr). Clin Res 1983; 31: 213a.

40. Kawana M, Krizek H, Porter J, Lathrop A, Charleston D, Harper PV. Use of 199-thallium as a potassium analog in scanning. (Abstr). J Nucl Med 1970; 11 : 333

41. Belgrave E, Lebowitz E. Development of ^{201}Tl for medical use. (Abstr). J Nucl Med 1972; 13: 781

42. Lebowitz E, Greene MW, Fairchild R, Bradley-Moore PR, Atkins HL, Ansari AN, Richards P, Belgrave E. Thallium-201 for medical use: I. J Nucl Med 1975; 16 : 151-155.

43. Bradley-Moore PR, Lebowitz E, Greene MW, Atkins HL, Ansari AN. Thallium-201 for medical use. II: Biological behaviour. J Nucl Med 1975; 16 : 156-160.

44. Zaret BL, Strauss HW, Martin ND, Wells HP, Flamm MD. Non-invasive regional myocardial perfusion with radioactive potassium. N Engl J Med 1973; 288 : 809-812.

45. Berman DS, Salel AF, Denardo GL, Mason DT. Non-invasive detection of regional myocardial ischaemia using Rubidium-81 and the scintillation camera. Comparison with stress electrocardiography in patients with arteriographically documented coronary stenosis. Circulation 1975; 52 : 619-626.

46. Martin ND, Zaret BL, McGowan RL, Wells HP, Flamm MD. Rubidium-81 : A new myocardial scanning agent. Radiology 1974; 111 : 651-656.

47. Poe ND. Comparative myocardial uptake and clearance characteristics of potassium and caesium. J Nucl Med 1972; 13 : 557-560.

48. Strauss HW, Pitt B. Thallium-201 as a myocardial imaging agent. Semin Nucl Med 1977; 7: 49-58.

49. Strauss HW, Harrison K, Langan JK et al. Thallium-201 for myocardial imaging : relation of thallium-201 to regional myocardial perfusion. Circulation 1975; 51 : 641-645.

50. Nielsen AP, Morris KG, Murdock R, Bruno FP, Cobb FR. Linear relationship between the distribution of thallium-201 and blood flow in ischaemic and non ischaemic myocardium during exercise. Circulation 1980; 61: 797-801.

51. Weich HF, Strauss HW, Pitt B. The extraction of thallium-201 by the myocardium. Circulation 1977; 56: 188-191.

52. Mullins LJ, Moore RD. The movement of thallium ions in muscle. J Gen Physiol 1960; 43: 759.

53. Conn HL, Robertson JS. Kinetics of potassium transfer in the left ventricle of the intact dog. Am J Physiol 1955; 181: 319-324.

54. Robertson JS. Theory and use of tracers in determining transfer rates in biological systems. Physiol Rev 1957; 37: 133-154.

55. Renkin EM. Transport of potassium-42 from blood to tissue in isolated mammalian skeletal muscles. Am J Physiol 1959; 197: 1205-1210.

56. Sheehan RM, Renkin EM. Capillary, interstitial, and cell membrane barriers to blood-tissue transport of potassium and rubidium in mammalian skeletal muscle. Circ Res 1972; 30: 588-607.

57. Gehring PJ, Hammond PB. The inter-relationship between thallium and potassium in animals. J Pharmacol Exp Ther 1967; 155: 187-201.

58. Gewirtz H, O'Keefe DD, Pohost GM, Strauss HW, McIlduff JB, Daggett WN. The effect of ischaemia on thallium-201 clearance from the myocardium. Circulation 1978; 58: 215-219.

59. Carlin RD, Jan K-M. Mechanism of thallium extraction in pump perfused canine hearts. J Nucl Med 1985; 26: 165-169.

60. Grunwald AM, Watson DD, Holzgrefe HH, Irving JF, Beller GA. Myocardial thallium-201 kinetics in normal and ischaemic myocardium. Circulation 1981; 64 : 610-618.

61. Sapirstein LA. Regional blood flow by fractional distribution of indicators. Am J Physiol 1958; 193: 161-168.

62. Schwartz JS, Ponto R, Carlyle P, Forstrom L, Cohn JN. Early redistribution of thallium-201 after temporary ischaemia. Circulation 1978; 57 : 332-335.

63. Gould KL, Lipscomb K, Hamilton GW. Physiologic basis for assessing critical coronary stenosis. Am J Cardiol 1974; 33 : 87-94.

64. Mueller TM, Marcus ML, Ehrhardt JC, Chandhuri T, Abboud FM. Limitations of thallium-201 myocardial perfusion scintigrams.
Circulation 1976; 54 : 640-646

65. Losse B, Kuhn H, Raffenbuhl D, Kronert IT, Hart W, Feinendegen LE, Loogen E. Thallium-201 myocardial scintigraphy in patients with normal coronary arteries and normal left ventriculogram : Comparison with haemodynamics, metabolic and morphologic findings. Z Kardiol 1980; 69 : 523.

66. Opherk D, Zebe H, Weihe E, Mall G, Durr C, Gravert B, Mehmel HC, Schwartz F, Kubler W. Reduced coronary dilatory capacity and ultrastructural changes in the myocardium in patients with angina pectoris but normal coronary arteriograms.
Circulation 1981; 63 : 817-825.

67. Dunn RF, Wolff L, Wagner S, Botvinick EH. The inconsistent pattern of thallium defects: A clue to the false positive scintigram.
Am J Cardiol 1981; 48 : 224-232.

68. Singh H, Causer DA. The effect of photon absorption by breast tissue in myocardial imaging with thallium -201. Br J Radiol 1981; 54 : 966-968.

69. Wackers FJ, Fetterman RC, Mattera JA, Clements JP. Quantitative planar thallium-201 stress scintigraphy : a critical evaluation of the method.
Semin Nucl Med 1985; 15: 46-66.

70. Trobaugh GB, Wackers FJ, Sokole EB, DeRouen TA, Ritchie JL, Hamilton GW. Thallium -201 myocardial imaging : an interinstitutional study of observer variability. J Nucl Med 1978; 19: 359-363.

71. Pohost GM, Okada RD, O'Keefe DD, Gewirtz H, Beller G, Strauss HW, Chaffin JS, Leppo J, Daggett WM. Thallium-201 redistribution in dogs with severe coronary artery stenosis of fixed caliber. Circ Res 1981; 48: 439-466.

72. Okada RD, Jacobs ML, Daggett WM, Leppo J, Strauss HW, Newell JB, Moore R, Boucher CA, O'Keefe D, Pohost GM. Thallium-201 kinetics in nonischaemic canine myocardium. Circulation 1982; 65: 70-77.

73. Lenaers A, Block P, van Thiel E, Lebedelle M, Beccquevort P, Erbsmann F, Ermanns AM. Segmental analysis of Tl-201 stress myocardial scintigraphy. J Nucl Med 1977; 18 : 509-516.

74. McKillop JH, Murray RG, Turner JG, Bessent RG, Lorimer AR, Grieg WR. Can the extent of coronary artery disease be predicted from thallium-201 myocardial images ? J Nucl Med 1979; 20 : 715-719.

75. Massie BM, Botvinick EH, Brundage BH. Correlation of thallium-201 scintigrams with coronary anatomy : factors affecting region by region sensitivity. Am J Cardiol 1979; 44 : 616-622.

76. Rigo P, Bailey IA, Griffith LSC, Pitt B, Wagner HN, Becker LC. Stress thallium-201 myocardial scintigraphy for the detection of individual coronary arterial lesions in patients with and without previous myocardial infarction.
Am J Cardiol 1981; 48 : 209-216.

77. Rozanski A, Berman DS, Gray R, Levy R, Raymond M, Maddahi J, Pantaleo N, Waxman AD, Swan HJC, Matloff J. Use of thallium-201 redistribution scintigraphy in the preoperative differentiation of reversible and non-reversible myocardial asynergy.
Circulation 1981; 64 : 936-944.

78. Iskandrian AS, Lichtenberg R, Segal BL, Mintz GS, Mundth ED, Hakki AH, Kimbiris D, Bemis CE, Croll MN, Kane SA. Assessment of jeopardised myocardium in patients with one-vessel disease.
Circulation 1982; 65 : 242-247.

79. Brown KA, Osbakken M, Boucher CA, Strauss HW, Pohost GM, Okada RD. Positive exercise thallium-201 test responses in patients with less than 50% maximal coronary stenosis : angiographic and clinical predictors.
Am J Cardiol 1985; 55: 54-57.

80. Uhl GS, Kay TN, Hickman JR Jr. Computer-enhanced thallium scintigrams in asymptomatic men with abnormal exercise tests.
Am J Cardiol 1981; 48 : 1037-1043.

81. Faris JV, Burt RW, Graham MC, Knoebel SB. Thallium-201 myocardial scintigraphy : improved sensitivity, specificity and predictive accuracy by application of a statistical image analysis algorithm. Am J Cardiol 1982; 49 : 733-742.

82. De Coster PM, Melin JA, Detry JR, Brasseur LA, Beckers C, Col J. Coronary artery reperfusion in acute myocardial infarction : assessment by pre- and post-intervention thallium-201 myocardial perfusion imaging. Am J Cardiol 1985; 55: 889-895.

83. Meade RC, Bamrah VS, Horgan JD, Ruetz PP, Kronenwetter C, Yeh EL. Quantitative methods in the evaluation of thallium-201 myocardial perfusion images. J Nucl Med 1978; 19: 1175-1178.

84. Burow RD, Pond M, Schafer AW, Becker L. "Circumferential profiles" : a new method for computer analysis of thallium-201 myocardial perfusion images. J Nucl Med 1979; 20 : 771-777.

85. Llaurado JG, Horgan JD, Bamrah VS, Kronenwetter CM, Ruetz PP. Improved computerised quantitation of Tl-201 myocardial scintigrams by combining two views. Clin Nucl Med 1982; 7: 253-264.

86. Watson DD, Campbell NP, Read EK, Gibson RS, Teates CD, Beller GA. Spatial and temporal quantitation of planar thallium myocardial images. J Nucl Med 1981; 22 : 577-584.

87. Berger BC, Watson DD, Taylor GJ, Craddock GB, Martin RP, Teates CD, Beller GA. Quantitative thallium-201 exercise scintigraphy for detection of coronary artery disease. J Nucl Med 1981; 22 : 585-593.

88. Becker LC, Rogers WJ, Edwards AC. Limitations of thallium washout rate measurements after exercise for detection of coronary artery stenosis. (Abstr). Circulation 1980; 62 (Suppl III) : III - 231,

89. Garcia E, Maddahi J, Berman D, Waxman A. Space/time quantitation of thallium-201 myocardial scintigraphy. J Nucl Med 1981; 22 : 309-317.

90. Maddahi J, Garcia EV, Berman DS, Waxman A, Swan HJC, Forrester J. Improved non-invasive assessment of coronary artery disease by quantitative analysis of regional stress myocardial distribution and washout of thallium-201. Circulation 1981; 64 : 924-935.

91. Reduto LA, Freund GC, Gaeta JM, Smalling RW, Lewis BL, Gould KL. Coronary artery reperfusion in acute myocardial infarction : beneficial effects of intracoronary streptokinase on left ventricular salvage and performance.
Am Heart J 1981; 102 : 1168-1177.

92. Sisson JC. What promise the preliminary tests of coronary artery disease?
J Nucl Med 1981; 22 : 303-308.

93. Hamilton GW, Trobaugh GB, Ritchie JL, Gould KL, DeRouen TA, Williams DL. Myocardial imaging with ^{201} thallium : an analysis of clinical usefulness based on Bayes' theorem.
Semin Nucl Med 1978; 8 : 358-364.

94. Fletcher JW, Walter KE, Witztum KF, Daly JL, Herbig FK, Mueller HS, Donati RM. Diagnosis of coronary artery disease with ^{201}TL. Computer analysis of myocardial perfusion images. Radiology 1978; 128 : 423-427.

95. Verani MS, Jhingran S, Attar M, Rizk A, Quinones MA, Miller RR. Poststress redistribution of thallium-201 in patients with coronary artery disease, with and without prior myocardial infarction. Am J Cardiol 1979; 43 : 1114-1122.

96. Leppo J, Rosenkrantz J, Rosenthal R, Bontemps R, Yipintsoi T. Quantitative thallium-201 redistribution with a fixed coronary stenosis in dogs. Circulation 1981; 63 : 632-639.

97. Laughlin JS, Kenny PJ, Weber DA et al. Methods and applications of quantitative computer-analysed scanning. Medical radio-isotope scintigraphy, Vol. 1, Proceedings of the International Energy Agency, Vienna, 1969; 633-651.

98. Nishiyama H, Adolph RJ, Gabel M, Lukes SJ, Franklin D, Williams CC. Effect of coronary blood flow on thallium-201 uptake and washout. Circulation 1982; 65 : 534-542.

99. Nichols AB, Weiss MB, Sciacca RR, Cannon PJ, Blood DK. Relationship between segmental thallium-201 uptake and regional myocardial blood flow in patients with coronary artery disease. Circulation 1983; 68: 310-320.

100. Okada RD, Pohost GM. The use of preintervention and postintervention thallium imaging for assessing the early and late effects of experimental coronary arterial reperfusion in dogs. Circulation 1984; 69 : 1153-1160.

101. Okada RD, Boucher CA, Kirshenbaum HK, Kushner FG, Strauss HW, Block PC, McKusisk KA, Pohost GM. Improved diagnostic accuracy of thallium-201 stress test using multiple observers and criteria derived from inter-observer analysis of variance. Am J Cardiol 1980; 46: 619-624.

102. Goris ML, Daspit SG, McLaughlin P, Kriss JP. Interpolative background subtraction. J Nucl Med 1976; 17 : 744-747.

103. Read ME, Watson DD, Read EK, Leidholtz E. A method for automatic overlapping of sequential scintiphoto images. (Abstr). J Nucl Med 1980; 21 : P61.

104. Gibson RS, Taylor GJ, Watson DD, Stebbins PT, Martin RP, Crompton RS, Beller GA. Predicting the extent and location of coronary artery disease during the early postinfarction period by quantitative thallium-201 scintigraphy. Am J Cardiol 1981; 47 : 1010-1017.

105. Vogel RA, Kirch DL, LeFree MT, Ramivates JO, Jensen DP, Steele PP. Thallium-201 myocardial perfusion scintigraphy : results of standard and multi-pinhole tomographic techniques. Am J Cardiol 1979; 43 : 787-793.

106. Bateman T, Garcia E, Maddahi J, Rozanski A, Pantaleo N, Staniloff H, Freeman M, Waxman A, Berman D. Clinical evaluation of seven-pinhole tomography for the detection and localisation of coronary artery disease : comparison with planar imaging using quantitative analysis of myocardial thallium-201 distribution and washout after exercise. Am Heart J 1983; 106 : 263-271.

107. Gibson RS, Watson DD, Taylor GJ, Crosby IK, Wellons HL, Holt ND, Beller GA. Prospective assessment of regional myocardial perfusion before and after coronary revascularisation surgery by quantitative thallium-201 scintigraphy. J Am Coll Cardiol 1983; 1: 804-815.

108. Bateman TM, Maddahi J, Gray RJ, Murphy FL, Garcia EV, Conklin CM, Raymond MJ, Stewart ME, Swan HJC, Berman DS. Diffuse slow washout of myocardial thallium-201 : a new scintigraphic indicator of extensive coronary artery disease. J Am Coll Cardiol 1984; 4: 55-64.

109. Lim YL, Okada RD, Chesler DA, Block PC, Boucher CA, Pohost GM. A new approach to quantitation of exercise thallium-201 scintigraphy before and after an intervention : application to define the impact of coronary angioplasty on regional myocardial perfusion. Am Heart J 1984; 108: 917-925.

110. Okada RD, Boucher CA, Pohost GM. Quantitative split dose thallium-201 imaging with exercise : a technique for obtaining rest and exercise perfusion images in one sitting and markedly reducing the study time.
J Am Coll Cardiol 1985; 5: 70-77.

111. Okada RD, Lim YL, Boucher CA, Pohost GM, Chesler DA, Block PC. Clinical, angiographic, haemodynamic, perfusional and functional changes after one-vessel left anterior descending coronary angioplasty. Am J Cardiol 1985; 55: 347-356.

112. Madeira SW, Bodenheimer MM, Banka VS, Agarwal JB, Weintraub WS, Helfant RH. Quantitative thallium-201 imaging : limitations in detecting pathophysiologically significant obstructive coronary artery disease.
Am Heart J 1984; 108: 1448-1454.

113. Abdulla A, Maddahi J, Garcia E, Rozanski A, Swan HJC, Berman DS. Slow regional clearance of myocardial thallium-201 in the absence of perfusion defect : contribution to detection of individual coronary artery stenoses and mechanism for occurrence. Circulation 1985; 71: 72-79.

114. Pamelia FX, Gibson RS, Watson DD, Craddock GB, Sirowatka J, Beller GA. Prognosis with chest pain and normal thallium-201 exercise scintigrams.
Am J Cardiol 1985; 55: 920-926.

115. Wackers FJ Th, Russo DJ, Russo D, Clements JP. Prognostic significance of normal quantitative planar thallium-201 stress scintigraphy in patients with chest pain. J Am Coll Cardiol 1985; 6: 27-30.

116. Vogel RA, Kirch D, LeFree M, Steele P. A new method of multiplanar emission tomography using a seven pinhole collimator and an Anger scintillation camera. J Nucl Med 1978; 19: 648-654.

117. Williams DL, Ritchie JL, Harp GD, Caldwell JH, Hamilton GW. In vivo simulation of thallium-201 myocardial scintigraphy by seven-pinhole emission tomography. J Nucl Med 1980; 21 : 821-828.

118. Brady TJ, O'Keefe DD, Okada RD, Jacocks MA, Johnson RG, Geffin GA, Merrill D, Strauss HW, Daggett WM, Pohost GM. Inability of seven-pinhole myocardial tomography to obtain accurate ^{201}Tl kinetic data.
Eur J Nucl Med 1983; 8: 425-430.

119. Vogel RA, Kirch DL, LeFree MT, Rainwater JO, Jensen DP, Steele PP. Thallium-201 myocardial scintigraphy : results of standard and multi-pinhole tomographic techniques.
Am J Cardiol 1979; 43: 787-793.

120. Ritchie JL, Williams DL, Caldwell JH, Stratton JR, Harp GD, Vogel RA, Hamilton GW. Seven-pinhole emission tomography with thallium-201 in patients with prior myocardial infarction.
J Nucl Med 1981; 22: 107-112.

121. Port SC, Oshima M, Ray G, McNamee P, Schmidt DH. Assessment of single vessel coronary artery disease : results of exercise electrocardiography, thallium-201 myocardial perfusion imaging and radionuclide angiography.
J Am Coll Cardiol 1985; 6: 75-83.

122. Massie BM, Wisneski JA, Hollenberg M, Gertz EW, Henderson S. Quantitative analysis of seven-pinhole tomographic thallium-201 scintigrams : improved sensitivity and estimation of the extent of coronary involvement by evaluation of radiotracer uptake and clearance.
J Am Coll Cardiol 1984; 3: 1178-1186.

123. Brooks RA, Di Chiro G. Principles of computer assisted tomography (CAT) in radiographic and radioisotopic imaging.
Phys Med Biol 1976; 21: 689-732.

124. Budinger TF, Gullberg GT, Huesman RH. Emission computed tomography. In : Topics in applied physics, Vol 32 : Image reconstruction from projections; implementation and applications. Herman GT, ed. Berlin : Springer-Verlag, 1979; 147-246.

125. Prigent FM, Maddahi J, Garcia E, Friedman J, Van Train K, Bietendorf J, Swan HJC, Berman DS. Thallium-201 stress-redistribution myocardial rotational tomography: development of criteria for visual interpretation.
Am Heart J 1985; 109: 274-281.

126. Garcia EV, Van Train K, Maddahi J, Prigent F, Friedman J, Areeda J, Waxman A, Berman DS. Quantification of rotational myocardial tomography. J Nucl Med 1985; 26: 17-26.

127. Caldwell JH, Williams DL, Hamilton GW, Ritchie JL, Harp GD, Eisner RL, Gullberg GT, Nowak DJ. Regional distribution of myocardial blood flow measured by single-photon tomography : comparison with in vitro counting. J Nucl Med 1982; 23: 490-495.

128. Tamaki N, Yonekura Y, Mukai T, Fujita T, Nohara R, Kadota K, Kambara H, Kawai C, Torizuka K, Ishii Y. Segmental analysis of stress thallium myocardial emission tomography for localisation of coronary artery disease. Eur J Nucl Med 1984; 9: 99-105.

129. Nohara R, Kambara H, Suzuki Y, Tamaki S, Kadota K, Kawai C, Tamaki N, Torizuka K. Stress scintigraphy using single-photon emission computed tomography in the evaluation of coronary artery disease. Am J Cardiol 1984; 53: 1250-1254.

130. Tamaki N, Yonekura Y, Mukai T, Kodama S, Kadota K, Kambara H, Kawai C, Torizuka K. Stress thallium-201 transaxial emission computed tomography : quantitative versus qualitative analysis for evaluation of coronary artery disease. J Am Coll Cardiol 1984; 4: 1213-1221.

131. Go RT, MacIntyre WJ, Houser TS, Pantoja M, O'Donnell JK, Feiglin DH, Sufka BJ, Underwood DA, Meaney TF. Clinical evaluation of 360° and 180° data sampling techniques for transaxial SPECT thallium-201 myocardial perfusion imaging. J Nucl Med 1985; 26: 695-706.

132. Goris ML. Nontarget activities : can we correct for them ? J Nucl Med 1979; 20 : 1312-1314.

133. Narahara KA, Hamilton GW, Williams DL, Gould KL. Myocardial imaging with thallium-201 : an experimental model for analysis of the true myocardial and background image components. J Nucl Med 1977; 18 : 781-786.

134. Beck JW, Tatum JL, Cobb FR, Harris CC, Goodrich JK. Myocardial perfusion imaging using thallium-201 : a new algorithm for calculation of background activity. J Nucl Med 1979; 20 : 1294-1300.

135. Steingart RM, Bontemps R, Scheuer J, Yipintsoi T. Gamma camera quantitation of thallium-201 redistribution at rest in a dog model. Circulation 1982; 65 : 542-550.

136. Bailey IK, Griffith LSC, Rouleau J, Strauss HW, Pitt B. Thallium-201 myocardial perfusion imaging at rest and during exercise. Comparative sensitivity to electrocardiography in coronary artery disease. Circulation 1977; 55 : 79-87.

137. Ritchie JL, Trobaugh GB, Hamilton GW, Gould KL, Narahara KA, Murray JA, Williams DL. Myocardial imaging with thallium-201 at rest and during exercise. Comparison with coronary arteriography and resting and stress electrocardiography. Circulation 1977; 56 : 66-71.

138. Pohost GM, Zir LM, Moore RH, McKusick KA, Guiney TE, Beller GA. Differentiation of transiently ischaemic from infarcted myocardium by serial imaging after a single dose of thallium-201. Circulation 1977; 55 : 294-302.

139. Ritchie JL, Albro PC, Caldwell JH, Trobaugh GB, Hamilton GW. Thallium-201 myocardial imaging : a comparison of the redistribution and rest images. J Nucl Med 1979; 20 : 477-483.

140. Hamilton GW, Trobaugh GB, Ritchie JL, Williams DL, Weaver WD, Gould KL. Myocardial imaging with intravenously injected thallium-201 in patients with suspected coronary artery disease. Analysis of technique and correlation with electrocardiographic, coronary anatomic and ventriculographic findings. Am J Cardiol 1977; 39 : 347-354.

141. Wackers FJ, Lie KI, Liem KL, Sokole EB, Samson G, Schoot JB, Durrer D. Thallium-201 scintigraphy in unstable angina pectoris. Circulation 1978; 57 : 738-742.

142. Berger BC, Watson DD, Burwell LR, Crosby IK, Wellons HA, Teates CD, Beller GA. Redistribution of thallium at rest in patients with stable and unstable angina and the effect of coronary artery bypass surgery. Circulation 1979; 60 : 1114-1125.

143. Helfant RH, Pine R, Meister SG, Feldman MS, Trout RG, Banka VS. Nitroglycerin to unmask reversible asynergy : correlation with post coronary bypass ventriculography. Circulation 1974; 50 : 108-113.

144. Brown KA, Okada RD, Boucher CA, Phillips HR, Strauss HW, Pohost GM. Serial thallium-201 imaging at rest in patients with unstable and stable angina pectoris : relationsip of myocardial perfusion at rest to presenting clinical syndrome. Am Heart J 1983; 106 : 70-77.

145. Groch MW, Lewis GK. Thallium-201 scintillation camera imaging considerations. J Nucl Med 1977; 17 : 142-145.

146. Causer DA, Singh H. The effect of gate width on thallium-201 scintigraphy of the myocardium. Br J Radiol 1980; 53 : 142-146.

147. Beck RN, Harper PV. Criteria for evaluating radioisotope imaging systems. Fundamental problems in scanning. Illinois : C.C. Thomas. 1968.

148. Maseri A, Parodi O, Severi S, Pesola A. Transient transmural reduction of myocardial blood flow, demonstrated by thallium-201 scintigraphy, as a cause of variant angina. Circulation 1976; 54: 280-288.

149. Armitage P. Statistical methods in medical research. Oxford : Blackwell; 1971: 97.

150. Ledley RS, Lusted LB. Reasoning foundations of medical diagnosis. Science 1959; 130 : 9-21.

151. White CW, Wright CB, Doty DB, Hiratza LF, Eastham CL, Harrison DG, Marcus ML. Does visual interpretation of the coronary arteriogram predict the physiologic importance of a coronary stenosis ?
N Engl J Med 1984; 310 : 819-824,

152. Selwyn AP, Allan RM, Fox KM, Horlock P, O´Brien HA, Maseri A. Prolonged myocardial ischaemia in angina. (Abstr). Circulation 1981; 64 (Suppl IV): 296

153. Braunwald E, Kloner RA. The stunned myocardium : prolonged postischaemic ventricular dysfunction. Circulation 1982; 66 : 1146-1149.

154. Selwyn AP, Allan RM, L´Abbate A, Horlock P, Camici P, Clark J, O´Brien HA and Grant PM. The relationship between regional myocardial uptake of rubidium-82 and perfusion : Absolute reduction of cation uptake in ischaemia.
Am J Cardiol 1982; 50 : 112-121.

155. Mehta J, Mehta P. Role of blood platelets and prostaglandins in coronary artery disease.
Am J Cardiol 1981; 48 : 366-373.

156. Heymann MA, Payne BD, Hoffman JIE, Rudolph AN. Blood flow measurements with radionuclide labelled particles. Prog Cardiovasc Dis 1977; 20: 55-79.

157. Neely JR, Morgan HE. Relationship between carbohydrate and lipid metabolism and the energy balance of the heart muscle.
Ann Rev Physiol 1974; 36: 413-459.

158. Schelbert HR, Henze E, Schon HR, Keen R, Hansen H, Selin C, Huang S-C, Barrio JR, Phelps ME. C-11 palmitate for the noninvasive evaluation of regional myocardial fatty acid metabolism with positron computed tomography. III. In vivo demonstration of the effects of substrate availability on myocardial metabolism.
Am Heart J 1983; 105: 492-504.

159. Schon HR, Schelbert HR, Najafi A, Robinson G, Huang SC, Barrio J, Phelps ME. C-11 labeled palmitic acid for the noninvasive evaluation of regional myocardial fatty acid metabolism with positron computed tomography. I. Kinetics of C-11 palmitic acid in normal myocardium.
Am Heart J 1982; 103: 532-547.

160. Schon HR, Schelbert HR, Najafi A, Hansen H, Robinson GR, Huang SC, Barrio J, Phelps ME. C-11 labeled palmitic acid for the nonivasive evaluation of regional myocardial fatty acid metabolism with positron computed tomography. II. Kinetics of C-11 palmitic acid in acutely ischaemic myocardium.
Am Heart J 1982; 103: 548-561.

161. Stein O, Stein J. Lipid synthesis, intracellular transport and storage.
J Cell Biol 1968; 36: 63-77.

162. Krivokapich J, Huang S-C, Phelps ME, Barrio JR, Watanabe CR, Selin C, Shine KI. Estimation of myocardial metabolic rate for glucose using ^{18}F-2-fluoro-2-deoxyglucose.
Am J Physiol 1982; 243: H884-H895.

163. Ratib O, Phelps ME, Huang S-C, Henze E, Selin C, Schelbert HR. Positron tomography with deoxyglucose for estimating local myocardial glucose metabolism. J Nucl Med 1982; 23: 557-586.

164. Schwaiger M, Huang S-C, Krivokapich J, Phelps ME, Henze E, Schelbert HR. Myocardial glucose utilisation measured noninvasively in man by positron tomography. (Abstr).
J Am Coll Cardiol 1983; 1: 688.

165. Schelbert HR, Phelps ME. Positron computed tomography for the in vivo assessment of regional myocardial function.
J Mol Cell Cardiol 1984; 16: 683-693.

166. Shah A, Schelbert HR, Schwaiger M, Henze E, Hansen H, Selin C, Huang S-C. Measurement of regional myocardial blood flow with N-13 ammonia and positron-emission tomography in intact dogs.
J Am Coll Cardiol 1985; 5: 92-100.

167. Tamaki N, Senda M, Yonekura Y, Saji H, Kodama S, Konishi Y, Ban T, Kambara H, Kawai C, Torizuka K. Dynamic positron computed tomography of the heart with a high sensitivity positron camera and nitrogen-13 ammonia.
J Nucl Med 1985; 26: 567-575.

168. Mullani NA, Goldstein RA, Gould KL, Marani SK, Fisher DJ, O'Brien HA Jr, Loberg MD. Myocardial perfusion with rubidium-82. I. Measurement of extraction fraction and flow with external detectors. J Nucl Med 1983; 24: 898-906.

169. Huang S-C, Schwaigere M, Carson RE, Carson J, Hansen H, Selin C, Hoffman EJ, MacDonald N, Schelbert HR, Phelps ME. Quantitative measurement of myocardial blood flow with oxygen-15 water and positron computed tomography : an assessment of potential and problems.
J Nucl Med 1985; 26: 616-625.